Synthesis, characterization and electrochemical studies of osmocenyl alcohols with biomedical applications

A dissertation submitted in accordance with the requirements for the degree

Magister Scientiae

in the

Department of Chemistry
Faculty of Natural and Agricultural Sciences

at the

University of the Free State

by

Maheshini Govender

Supervisor

Prof. J. C. Swarts

Co-supervisor

Dr. E. Müller

January 2015

To my dad, Visvanathan Govender

(1 July 1950 – 31 December 2014)

If I could write a story
It would be the greatest ever told
Of a kind and loving father
Who had a heart of gold

If I could write a million pages
But still be unable to say, just how
Much I love and miss him
Every single day

I will remember all he taught me
I'm hurt but won't be sad
Because he'll send me down the answers
And he'll always be MY DAD

- Leah Hendrie

Acknowledgements

I would like to thank my family, friends and colleagues for their support, friendship and guidance throughout this period of my studies. Special thanks must be made to the following people:

My supervisor, Prof. J. C. Swarts, for his excellent guidance, leadership and kindness throughout the course of this study. Also, my co-supervisor, Dr. E. Müller, for her excellent guidance, leadership and kindness throughout the course of this study. It has been a privilege to be your student. Thank you for giving me the opportunity to be able to work with a great research group.

My immediate family, my mom (Rani Govender) and my brothers (Thavashan and Kavantheran Govender). Your love, guidance and support over the years are the reason I am here today. If not for you, I would not have had this opportunity.

To my loving boyfriend, Jan van der Linde, thank you for all the love, support and encouragement through the course of this study. You have been my rock for the last 8 years and I would not have been able to come this far had it not been for you.

To my boyfriend's family, his parents (Jan and Zelda van der Linde), thank you for all your love, support and guidance throughout this trying time. To his brother, Ian van der Linde, thank you for your support and introducing me to Zotero (which saved me a lot of time during this write-up).

To the Physical Chemistry group, thank you *ALL* for your support and guidance throughout this study, and for always helping me whenever I needed it. Also, thank you for all the laughter and fun throughout my time with the group. To my gaming buddies (you know who you are) thank you for the times we have shared gaming, it has helped me stay sane during this trying time.

I would like to acknowledge the Chemistry department at UFS for the available facilities.

I would like to acknowledge Dr. M. Landman from the University of Pretoria for the data collection and refinement of the crystal structures.

A special thank you to the National Research Foundation and the University of the Free State for the financial support.

Abstract

A series of osmocene-containing carboxylic acids, $Oc(CH_2)_mCOOH$ where m = 1, 2 and 3, and osmocene-containing alcohols, $Oc(CH_2)_nOH$ where n = 1, 2, 3 and 4, were obtained in multiple synthetic steps and characterised with the aid of infrared spectroscopy, ^1H nuclear magnetic resonance spectroscopy, elemental analysis and melting point measurements. New methods were developed for the synthesis of these osmocene-containing carboxylic acids and alcohols.

The structures of 2-osmocenylacetonitrile (monoclinic, $P2_1/c$, Z = 4, R = 0.057) and 2-osmocenylethanol (trigonal, P-3, Z = 18, R = 0.092) were determined by single crystal X-ray crystallography. The alcohol, 2-osmocenylethanol, showed an extensive hydrogen bonding network involving the OH functionalities of six neighbouring molecules, arranged in a hexagonal pattern.

Electrochemical studies, utilising cyclic voltammetry, were performed on all compounds synthesised, including precursor compounds. Electrochemical experiments were conducted in DCM and 0.1 M $[NBu_4][B(C_6F_5)_4]$ as supporting electrolyte. A trend was observed between the number of $–CH_2–$ spacers and the formal reduction potentials (E°′) for both the carboxylic acids and alcohols. The formal reduction potentials for both the carboxylic acids and the alcohols were found to decrease as the number of $–CH_2–$ spacers increased. Dimerisation of the osmocenyl moiety, similar to the known dimerisation of ruthenocene, was observed. It was found that the degree of dimerisation diminishes as the number of $–CH_2–$ groups increases for both the osmocene-containing carboxylic acids and alcohols. The formal reduction potentials for 2-osmocenylethanoic acid, 3-osmocenylpropanoic acid and 4-osmocenylbutanoic acid are 418 mV, 357 mV and 317 mV, respectively. The formal reduction potentials for osmocenylmethanol, 2-osmocenylethanol, 3-osmocenylpropanol, and 4-osmocenylbutanol, are 410 mV, 340 mV, 313 mV and 321 mV, respectively. Dimerisation was observed electrochemically for 2-osmocenylethanoic acid, 3-osmocenylpropanoic acid, 2-osmocenylethanol and 3-osmocenylpropanol. No dimerisation was observed electrochemically for 4-osmocenylbutanoic acid and 4-osmocenylbutanol.

Keywords: osmocene, alcohols, carboxylic acids, electrochemistry, dimerisation.

Opsomming

'n Reeks osmoseenbevattende karboksielsure, $Oc(CH_2)_mCOOH$ met m = 1, 2 en 3, sowel as osmoseenbevattende alkohole, $Oc(CH_2)_nOH$ met n = 1, 2, 3 en 4, is in veelvuldige stappe gesintetiseer en gekarakteriseer deur gebruik te maak van infrarooi spektroskopie, ^1H kernmagnetiese resonansspektroskopie, elementele analise en smeltpunt bepalings. Nuwe metodes vir die sintese van hierdie osmoseenbevattende karboksielsure en alkohole is ontwikkel.

Die strukture van $Oc(CH_2)CN$ (monoklinies, $P\ 2_1/c$, Z = 4, R = 0.057) en $OcCH_2CH_2OH$ (trigonaal, P-3, Z = 6, R = 0.092) is met behulp van enkelkristal X—straalkristallografie bepaal. Die alkohol vertoon ‘n uitgebreide waterstofbindingnetwerk bestaande uit die OH funksionele groepe van ses naasliggende molekule gerangskik in ‘n heksagonale patroon.

‘n Elektrochemiese studie, wat gebruik maak van sikliese voltammetrie, van alle gesintetiseerde verbindings is uitgevoer. Elektrochemie is uitgevoer in DCM en 0.1 M $[NBu_4][B(C_6F_5)_4]$ as hulp elektroliet. 'n Tendens is gevind tussen die aantal $-CH_2-$ eenhede en die formele reduksiepotensiaal ($E^{\circ\prime}$) vir beide die karboksielsure en alkohole. Die formele reduksiepotensiaal vir beide die karboksielsure en alkohole neem af soos die aantal $-CH_2-$ groepe toeneem. Die graad van dimerisasie van die osmoseniel groep is soortgelyk gevind aan die van die rutenoseniel groep. Dit is gevind dat dimerisasie afneem namate die aantal $-CH_2-$ groepe toeneem, vir beide die karboksielsure en alkohole. Die formele reduksiepotensiaal van 2-osmoseniel asynsuur, 3-osmoseniel etanoësuur en 4-osmoseniel propanoësuur is 418 mV, 357 mV en 317 mV onderskeidelik. Die formele reduksiepotensiaal vir osmosenielmetanol, 2-osmosenieletanol, 3-osmosenielpropanol, en 4-osmosenielbutanol, is 410 mV, 340 mV, 313 mV en 321 mV onderskeidelik. Dimerisasie is elektrochemies waargeneem vir 2-osmoseniel asynsuur, 3-osmoseniel etanoësuur, 2-osmosenieletanol en 3-osmosenielpropanol. Geen dimerisasie is elektrochemies waargeneem vir 4-osmoseniel propanoësuur of 4-osmosenielbutanol nie.

Table of contents

List of Structures

M = Fe, Ru

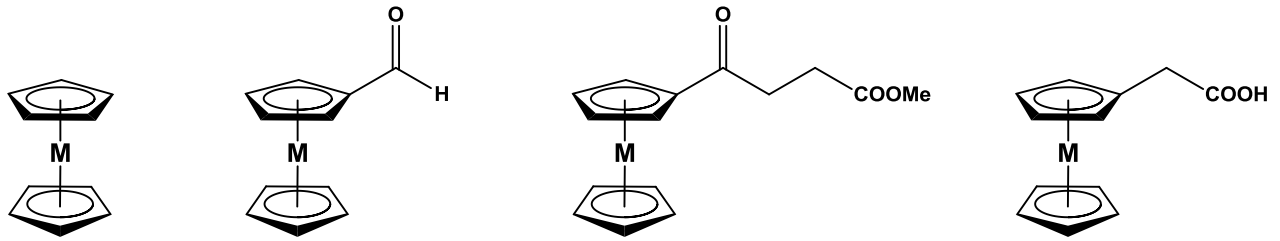

1 **2** **3** **4**

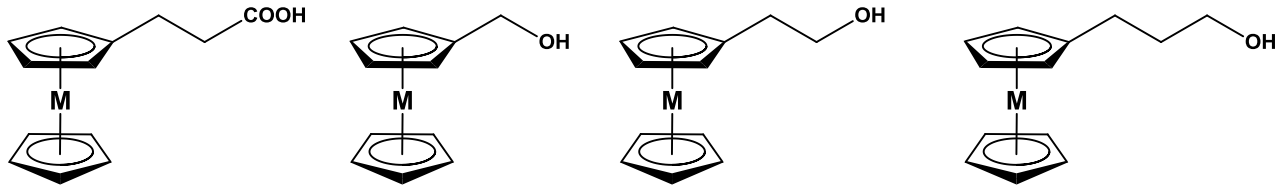

5 **6** **7** **8**

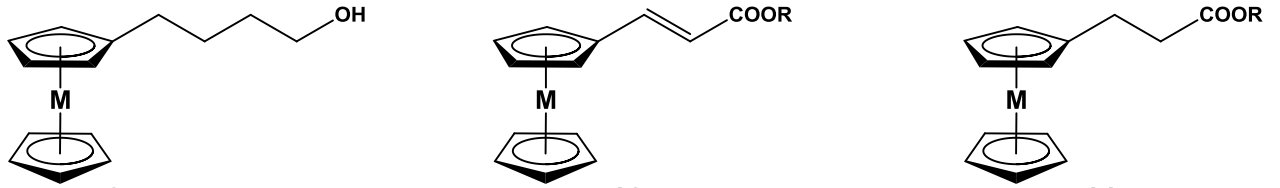

9 **10** **11**

R = H - Method A
R = Et - Method B

R = H, Et

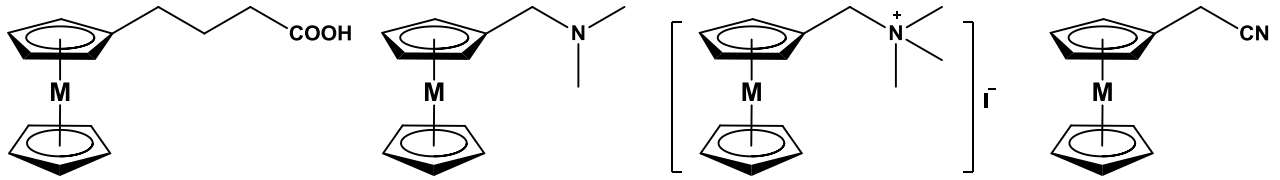

12 **13** **14** **15**

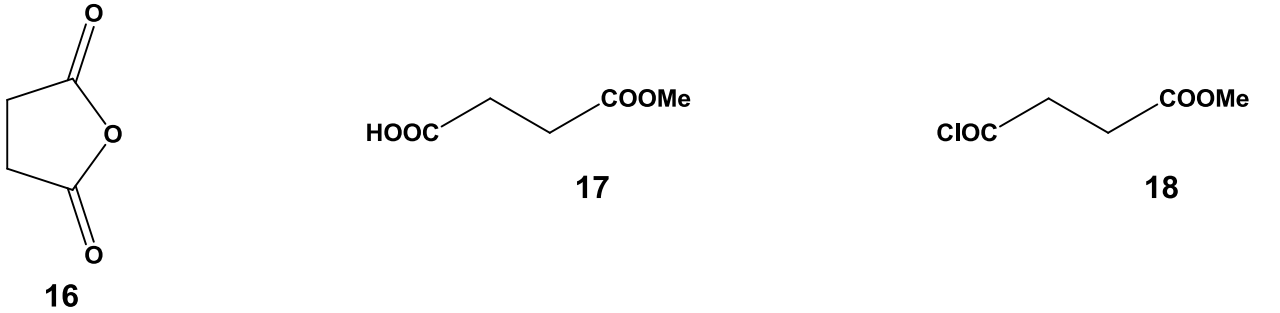

16 **17** **18**

List of Structures

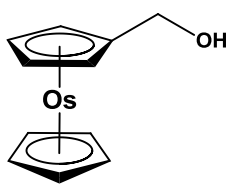

19

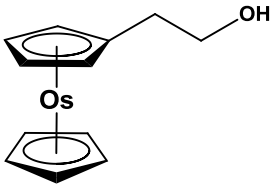

20

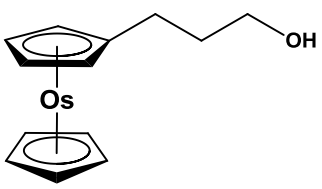

21

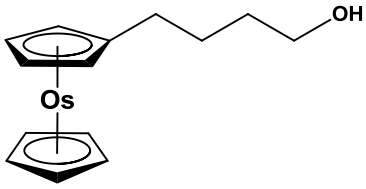

22

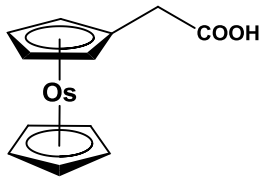

23

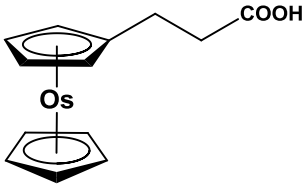

24

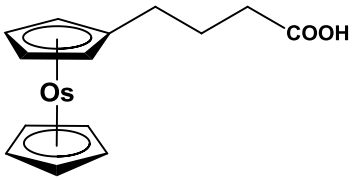

25

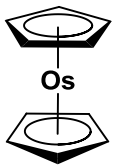

26

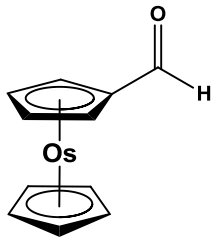

27

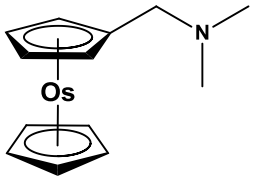

28

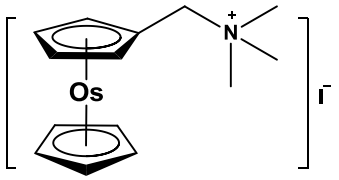

29

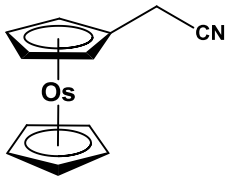

30

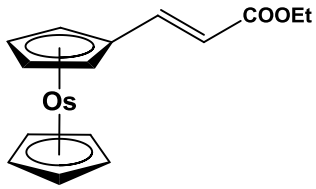

31

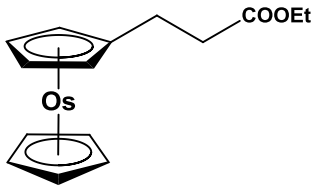

32

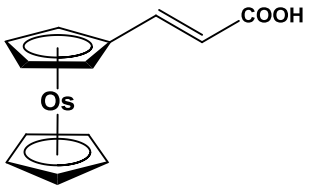

33

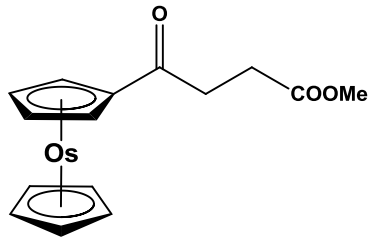

34

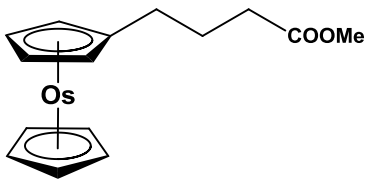

35

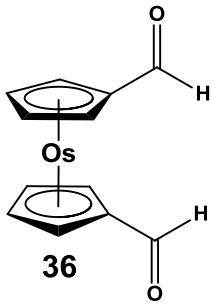

36

Abbreviations

^{1}H NMR	proton nuclear magnetic resonance
Å	Ångström
cm^3	cubic centimetres
CV	cyclic voltammetry/cyclic voltammogram
DCM	dichloromethane
DME	dropping mercury electrode
DMF	*N,N*-dimethylformamide
DNA	deoxyribonucleic acid
E°´	formal reduction potential
E_{pa}	peak anodic potential
E_{pc}	peak cathodic potential
Fc^*	decamethylferrocene
FcH	ferrocene
IC_{50}	drug dosage necessary for 50% cell death
i_{pa}	peak anodic current
i_{pc}	peak cathodic current
IR	infra-red
LSV	linear sweep voltammetry
M	molar
m.p.	melting point
mg	milligram
mM	millimolar
mmol	millimole
mV	millivolts
mV/s	millivolts per second
n-BuLi	n-butyllithium

Abbreviations

ORTEP	Oak Ridge Thermal Ellipsoid Plot
PTA	1,3,5-triaza-7-phosphaadamantane
RAPTA	Ruthenium(II) PTA complex
SW	square-wave
t-BuLi	*tert*-butyllithium
THF	tetrahydrofuran
ΔE_p	separation of forward and reverse peak potentials

1 Introduction and Aims of study

1.1 Introduction

Cancer, a disease characterised by the uncontrolled proliferation of abnormal cells and ability to invade healthy tissue, was found to cause more deaths than HIV/AIDS, tuberculosis and malaria combined.[1,2] In 2008 alone there was an estimated 12.7 million cancer cases and 7.6 million cancer related deaths; these figures are on a growing trend.[3,4] Cis-diamminedichloroplatinum(II), commonly referred to as Cisplatin, is the most recognized metal-containing drug used in the treatment of cancer. This is due to its effectiveness in testicular and ovarian cancer and its high general toxicity, and is still used to treat approximately 70% of cancer patients.[1,5] However, this powerful anticancer drug is known to relapse in tumour treatment and have harsh side-effects on patients, including neurotoxicity and nephrotoxicity.[6] Oxaliplatin is another platinum-containing chemotherapeutic agent used to treat colorectal cancer, however, side effects include acute and chronic sensory neurotoxicity which often causes the treatment to stop at an early stage in chemotherapy.[4] Drug resistance and side effects of most, if not all, anticancer drugs are a serious limitation to chemotherapy. All anticancer drugs are known to lack selectivity towards cancerous cells which are the main cause of side effects.[7] Designing selective anticancer drugs would increase the efficiency of treatment and reduce side effects in the patient.

In terms of metallocenes, titanocene and ferrocene derivatives are among the most extensively studied derivatives that have shown good anticancer activity, whereas ruthenocene studies are limited.[10] Titanocene dichloride is the most popular drug that has reached Phase II clinical trials and ferrocifen shows promise to enter clinical trials.[5] Osmocene derivatives have thus far not been subjected to clinical or pre-clinical anticancer studies, mainly because they are difficult to synthesise.[13] Potential anticancer activity in metallocenes have been estimated by determining the formal reduction potential of these compounds. This approach has been used for ferrocene and ferrocene-containing alcohol and carboxylic acid derivatives.[14] The cytotoxicity of a compound is often inversely related to its formal reduction potential, as determined by electrochemical studies.[15] Since osmium is further down the same group, group 8, as iron and ruthenium, osmocene derivatives have the potential for utilisation in anticancer studies, and these may be based on the electrochemical properties of these new osmocene derivatives.

1.2 Aims of Study

With the information given in the introduction, the following goals were set for this study:

i) The synthesis and characterisation of a series of potentially antineoplastic osmocene-containing carboxylic acids of the form $Oc(CH_2)_mCOOH$, where m = 1, 2, and 3; Oc = Os $(\eta^5 - C_5H_5)(\eta^5 - C_5H_4)$, the osmocenyl group.

ii) The synthesis and characterisation of a series of potentially antineoplastic osmocene-containing alcohols of the form $Oc(CH_2)_nOH$, where n = 1, 2, 3 and 4; Oc = Os $(\eta^5 - C_5H_5)(\eta^5 - C_5H_4)$, the osmocenyl group.

iii) Electrochemical studies of the osmocene-containing carboxylic acids as described in (i) above, to determine redox properties by means of cyclic voltammetry, linear sweep and square wave electrochemistry.

iv) Electrochemical studies of osmocene-containing alcohols as described in (ii) above, to determine redox properties by means of cyclic voltammetry, linear sweep and square wave electrochemistry.

v) Crystallographic determination of the structures of $OcCH_2CH_2OH$ and $Oc(CH_2)CN$, a precursor of $OcCH_2COOH$.

vi) Explanation of the spectroscopic properties of the new compounds synthesised in this study.

Once the synthetic chemistry of osmocene derivatives has been opened up as a result of this study, future studies may evolve to determine the antineoplastic properties of these new compounds.

References

1. M. F. R. Fouda, M. M. Abd-Elzaher, R. A. Abdelsamaia and A. A. Labib, *Appl. Organomet. Chem.*, 2007, **21**, 613–625.
2. American Cancer Society, *Global Cancer Facts and Figures*, Atlanta, 2nd edn., 2011.
3. A. Jemal, F. Bray, M. M. Center, J. Ferlay, E. Ward and D. Forman, *CA. Cancer J. Clin.*, 2011, **61**, 69–90.
4. J. D. Patel, L. Krilov, S. Adams, C. Aghajanian, E. Basch, M. S. Brose, W. L. Carroll, M. de Lima, M. R. Gilbert, M. G. Kris, J. L. Marshall, G. A. Masters, S. J. O'Day, B. Polite, G. K. Schwartz, S. Sharma, I. Thompson, N. J. Vogelzang and B. J. Roth, *J. Clin. Oncol.*, 2013, **32**, 129–161.
5. A. D. Claire S. Allardyce, *Appl. Organomet. Chem.*, 2005, **19**, 1 – 10.
6. M. Agrez, *J. Cancer Ther.*, 2011, **02**, 295–301.
7. C. M. Clavel, E. Păunescu, P. Nowak-Sliwinska and P. J. Dyson, *Chem. Sci.*, 2014, **5**, 1097–1101.
8. L. L. Komane, E. H. Mukaya, E. W. Neuse and C. E. J. van Rensburg, *J. Inorg. Organomet. Polym. Mater.*, 2008, **18**, 111–123.
9. E. W. Neuse, G. Caldwell and A. G. Perlwitz, *Polym. Adv. Technol.*, 1996, **7**, 867–872.
10. A. M. Pizarro, A. Habtemariam and P. J. Sadler, in *Medicinal Organometallic Chemistry*, eds. G. Jaouen and N. Metzler-Nolte, Springer Berlin Heidelberg, 2010, pp. 21–56.
11. E. W. Neuse, *J. Inorg. Organomet. Polym. Mater.*, 2005, **15**, 3–31.
12. C. C. Joubert, M. Sc., University of the Free State, 2011.
13. M. W. Droege, W. D. Harman and H. Taube, *Inorg. Chem.*, 1987, **26**, 1309–1315.
14. W. L. Davis, R. F. Shago, E. H. G. Langner and J. C. Swarts, *Polyhedron*, 2005, **24**, 1611–1616.
15. R. F. Shago, J. C. Swarts, E. Kreft and C. E. J. van Rensburg, *Anticancer Res.*, 2007, **27**, 3431–3433.

2 Literature Survey

2.1 Introduction

A literature review of the synthesis and physical methods relevant to this study is presented in this chapter.

2.2 Metallocenes

Metallocenes are sandwich type organometallic complexes which consist of one or more cyclopentadienyl ligands and a metal ion. There are five different structural types of metallocene compounds (Figure 2.1):[1,2]

i. parallel sandwich complexes
ii. multi-decker sandwich complexes
iii. half-sandwich complexes
iv. bent or tilted sandwich complexes
v. complexes that consist of more than two cyclopentadienyl ligands

Parallel sandwich type metallocenes are organometallic compounds of the type $M(C_5H_5)_2$, where M is a transition metal and $(C_5H_5)^-$ are aromatic cyclopentadienyl ligands wherein all carbon atoms are covalently bonded to the sandwiched metal atom.

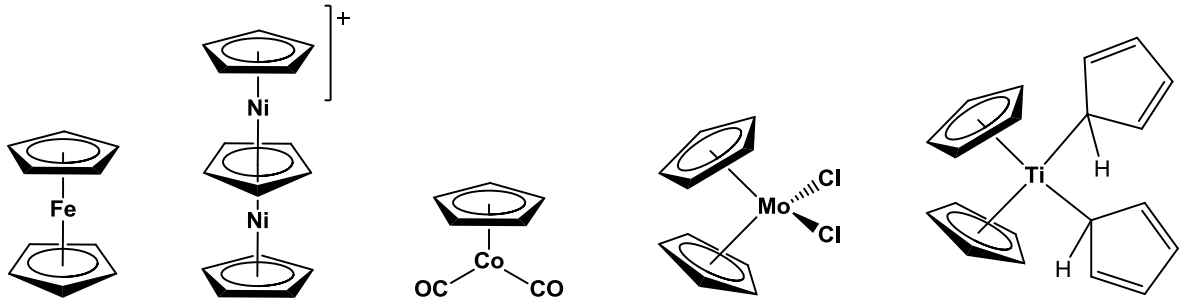

Ferrocene, a parallel sandwich complex

Nickelocene, a multidecker sandwich complex

Cyclopentadienylcobalt-dicarbonyl, a half-sandwich cobalt complex

Molybdocene dichloride, a bent/tilted sandwich complex

Tetra-cyclopentadienyl titanium species, a complex with more than two Cp ligands

Figure 2.1: Some examples of the different structural types of metallocenes[1,3]

Group VIII metallocenes are ferrocene, ruthenocene and osmocene. Ferrocene and ruthenocene, where the sandwiched metal ion is iron(II) and ruthenium(II), respectively, will be discussed due to similar chemical behaviour to the osmium(II)-containing osmocene, which is the focus of this study. The aromatic reactivity of these three metallocenes decreases in the order ferrocene, ruthenocene and then osmocene.[4] As the metal gets larger, the bonding between the cyclopentadienyl ligands and the metal is stronger, thus reducing the π-electron density within the cyclopentadienyl rings.[4] Therefore, the stronger M-Cp bonding is responsible for the decrease in reactivities found in ruthenocene and osmocene, compared to ferrocene.[4] Evidence for stronger M-Cp bonding is illustrated by comparing the infrared spectra of ferrocene, ruthenocene and osmocene.[4,5]

Table 2.1: Infrared frequencies for the C-C and C-H vibrations of ferrocene, ruthenocene and osmocene.[4]

IR Wavenumbers / cm^{-1}			Assignment
Ferrocene	**Ruthenocene**	**Osmocene**	
3083	3078	3095	Symmetrical C-H stretching
1413	1409	1405	Antisymmetrical C-C stretching
1106	1101	1096	Antisymmetrical C-C ring breathing
1002	1001	995	C-H bending
814	806	819	C-H bending

Table 2.1 clearly shows that the antisymmetrical C-C stretching frequencies and the antisymmetrical C-C ring breathing frequencies decrease from ferrocene to ruthenocene and finally to osmocene. In infrared spectroscopy, strong bonds exhibit vibrational energies at higher wavenumbers than weaker bonds.[6] Therefore, the general decrease in wavenumbers shown in Table 2.1 indicate a weakening of the C-C bonds in the cyclopentadienyl ligands, which may be due to stronger M-Cp bonds in the heavier metallocenes.

2.2.1 Group VIII metallocenes

Ferrocene is the first metallocene in the Group VIII metal series and was discovered in 1951; cyclopentadienyl rings on ferrocene undergo organic type reactions like Friedel Crafts alkylation

and acylation, sulphonation reactions and also metallation reactions with *n*-BuLi.[1,4,7] Organometallic chemistry with Group VIII metallocenes largely focuses on ferrocene due to its high reactivity in organic synthesis, high stability and ease of preparation from a cyclopentadienyl anion and ferrous chloride.[1,8] Ruthenocene and osmocene are expensive, have fewer methods of synthesis than ferrocene and preparation gives much lower yields.[9–11] Due to these factors and the reduced reactivities of ruthenocene and osmocene, research on these heavier metallocenes is scarce and limited, with osmocene research being almost completely neglected.

The organic chemistry of ferrocene has flourished since it was first synthesised, with one of the most important discoveries being its ability to undergo Friedel-Crafts acylation reactions. This capability proved its aromatic character.[1] A variety of ferrocene derivatives have been prepared using standard aromatic electrophilic substitution, metallation, nitration and halogenation reactions.[4] Applications for these derivatives vary from catalysts in rocket propellants to a variety of medicinal drugs.[12,13] Examples of medical applications are anticancer agents, antimalarial agents, drugs against HIV infection and DNA detection systems using electrochemical methods.[14] Ferrocifen has shown antiproliferative effects in cancer research and Ferroquine is a drug used as an antimalarial agent and has reached phase I clinical trials.[14]

The chemistry of ruthenocene and osmocene is similar to ferrocene; these metallocenes have also been found to undergo the same organic type reactions as ferrocene, including Friedel-Crafts acylation, lithiation with *n*-BuLi and metallation.[1] However, unlike ferrocene, ruthenocene and osmocene are known to be substantially more thermally stable. Higher thermal stability and reduced interaction between the metal and cyclopentadienyl ligands indicate that ruthenocene and especially osmocene do not undergo organic syntheses as readily as ferrocene.[1,15] The reduced reactivity of these compounds can be seen during Friedel-Crafts acylation. Osmocene only yields a mono-acylated product under relatively strong acylation conditions, utilising acid chlorides.[4] However, ruthenocene yields both mono-acylated and di-acylated products, and under these same conditions for ruthenocene, ferrocene only yields di-acylated products when acid chlorides are employed as acylating reagent.[1,4]

Ruthenocene, although much less researched than ferrocene, is also being used in medical applications with Ruthenocifen being an anticancer drug that has been found to have antitumour

activity.[14] However, there is not much literature on osmocene and applications thereof. The known general chemistry of osmocene is shown in Scheme 2.1.

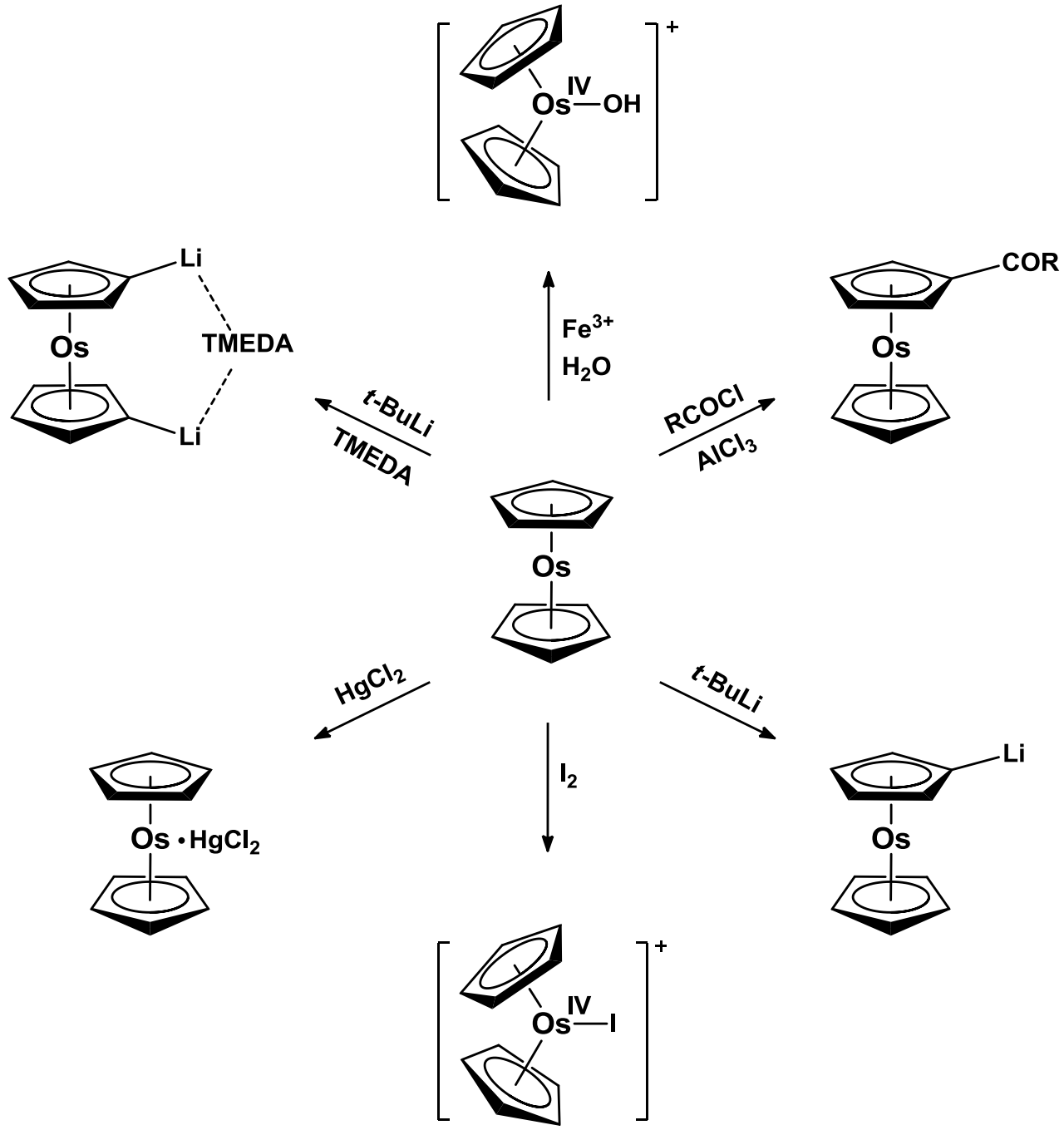

Scheme 2.1: General chemistry of osmocene.[1]

2.3 Synthesis

The synthesis of new alcohols and carboxylic acids containing the osmocenyl moiety was identified as goals (i) and (ii) of this study.

Due to the limited literature on the functionalisation of osmocene, literature on related metallocenes will be discussed. Group VIII metallocenes show similar organic chemistry reactions, however, based on the research of the author, the syntheses with osmocene will react much slower and yield less product due to its reduced reactivity. A series of ferrocene-containing alcohols, $Fc(CH_2)_nOH$, and carboxylic acids, $Fc(CH_2)_mCOOH$ with m = 0,1,2,3 and n = m+1, have previously been described in literature.[12]

The synthetic strategies used for the synthesis of ferrocene-containing alcohols can be seen in Scheme 2.2. For this study, the synthetic techniques shown in Scheme 2.2 were modified and optimised to synthesise the desired osmocenylcarboxylic acids and osmocenylalcohols, as described in goals (i) and (ii) of this study.

2.3.1 Metallocene carboxaldehydes

The preparation of aromatic aldehydes can be achieved by either aromatic formylation or modification of substituents on the aromatic system.[16]

Aromatic formylation of ferrocene has been achieved using the Vilsmeier reaction and results in good yields of formylferrocene, **2** (Scheme 2.2, Method A).[17] It can also be modified to give good yields for formylruthenocene.[18,19] The aldehyde can be obtained by reacting the desired metallocene with phosphoryl chloride and *N*-methylformanilide (71% yield of formylferrocene) or *N,N*-dimethylformamide (23% yield of formylferrocene) as the formylating agent.[16] Vilsmeier formylation is a reliable reaction that can be performed on many aromatic compounds. Osmocenecarboxaldehyde has been prepared in literature (79%) using the Vilsmeier formylation reaction.[20]

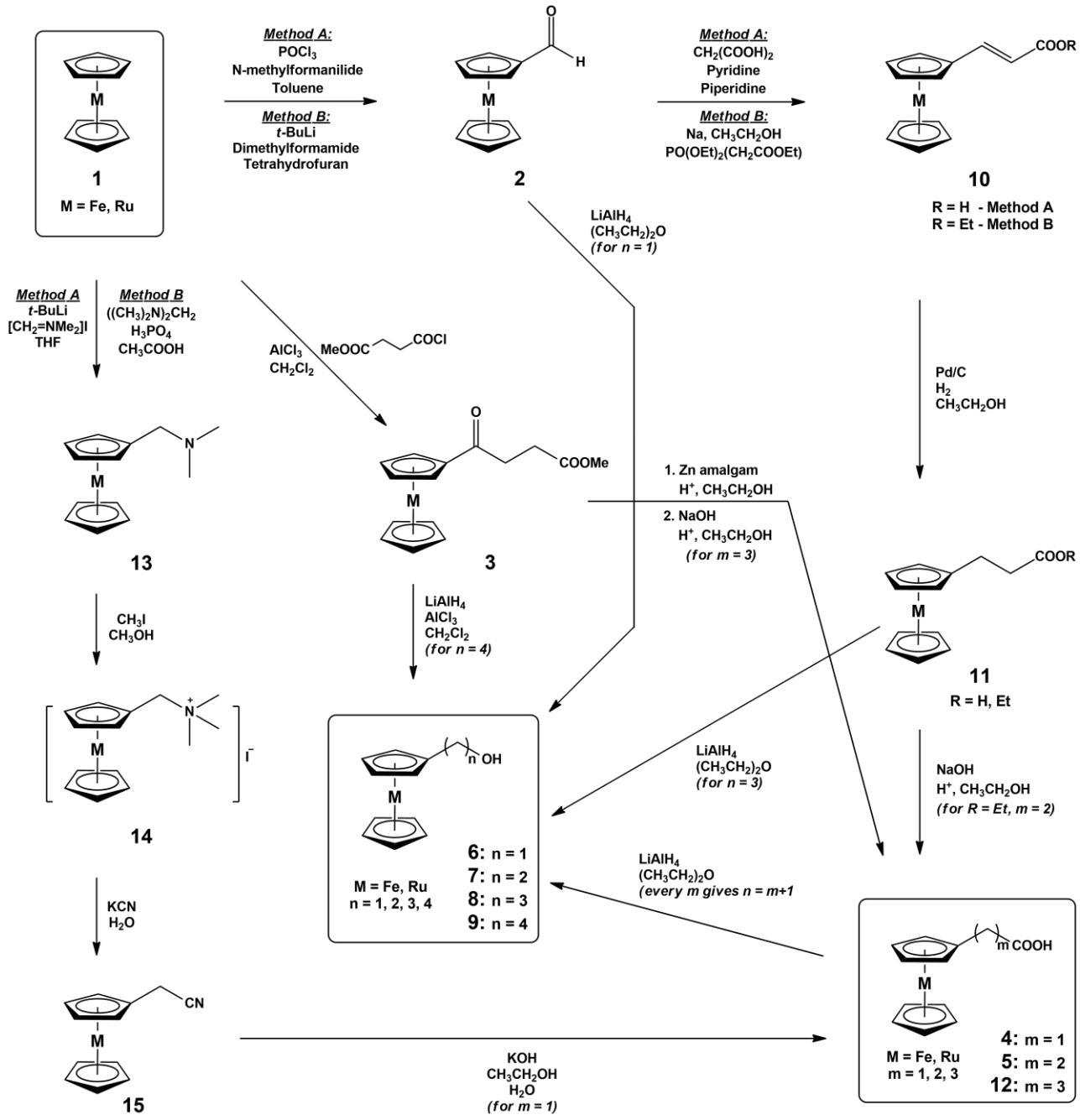

Scheme 2.2: Synthetic strategy for ferrocene-containing alcohols as well as ferrocene- and ruthenocene-containing carboxylic acids. M = Fe, Ru. To the author's knowledge, only (2) with M = Os is known.[12,21]

Formylferrocene, **2**, (Scheme 2.2, Method B) and formylruthenocene have also been prepared in good monosubstituted yields (both in 90.7% yield) via lithiation, using *t*-BuLi as the lithiating agent and *N,N*-dimethylformamide as the formylating agent.[22] The lithiation reaction has a reduced reaction time over the Vilsmeier reaction and gives high mono-substituted yields for ruthenocene. The formylation by lithiation of ruthenocene is more favourable than for ferrocene and yields the same quantity of formylruthenocene as formylferrocene in half the reaction time. It has been observed that lithiated ferrocene is less soluble in tetrahydrofuran than ferrocene. For this reason, a larger quantity of solvent was used to ensure complete dissolution of the starting material.[22]

The Gatterman-Koch reaction can also be used to synthesise aldehydes by reacting an aromatic compound with a mixture of copper(I) chloride and aluminium chloride as a catalyst, and subsequently passing hydrogen chloride and carbon monoxide through the mixture.[16,23] This reaction, however, does not work well with phenols or phenolic ethers due to side reactions with the aluminium chloride. Alternatively, the Gatterman aldehyde synthesis uses hydrogen cyanide and aluminium chloride, and can be used for formylation of phenols and phenolic ethers.[16]

The Reimer-Tiemann reaction is also a popular method used to prepare aromatic aldehydes by reacting the aromatic compound with chloroform and a strong base, usually sodium hydroxide. This reaction works well for phenols, adding the aldehyde functional group in the -*ortho* and -*para* positions to the phenolic OH group.[16,24] This reaction can also be used to formylate naphthols, hydroxyquinolines, pyrroles, indoles, quinoxalines, thiazoles and tropolone.[25]

2.3.2 Metallocene esters

Aromatic esters can be prepared by esterification reactions of carboxylic acids.[16] However, if a long alkyl chain length (e.g. C_6) between ester and aromatic functionality is required, then alkylation or acylation may be required first. Functionalisation of alkyl or acyl substituents onto aromatic systems can be achieved using aromatic electrophilic substitution reactions. In the case of ferrocene, Scheme 2.2 shows that ferrocenylalcohols have been synthesised from appropriate ferrocenylesters or carboxylic acids.

Electrophilic aromatic substitution can be achieved using Friedel-Crafts alkylation or acylation. It has been found that metallocene acylation is more reliable than alkylation due to the following factors:[16,26]

i. Acylation is much more versatile than alkylation since the R-group situated on the acyl chloride can contain almost any functional group without resulting in limitations to the reaction. The alkylation reaction, however, is limited to an R-group that can form a cation for the reaction to proceed.
ii. The side chain of the acylated product deactivates the aromatic system by withdrawing electrons via the acyl group. This reduces the chance of additional (multiple) acylation substitutions.
iii. The alkyl side chain of the alkylated product will activate the aromatic system by electron donation. This will increase the chance of undesired, multiple alkyl substitutions.
iv. The acyl chloride reacts with the Lewis acid catalyst to produce a stable acylium ion, thus reducing the chance of rearrangement of the electrophile.
v. Primary alcohols cannot be used for Friedel-Crafts alkylation due to the possibility of multiple substitutions on the aromatic system. Also, a primary alkyl cation is likely to arrange itself to a more stable secondary or tertiary cation before the reaction can take place.

Ferrocene, in particular, has been found to react in an undesired way during alkylation reactions. Friedel-Crafts alkylation of ferrocene provides poor yields of the desired alkylated product. A variety of multi-alkylated by-products are obtained. Separation of these multi-alkylated compounds becomes labourious.[27,28] In contrast, Friedel-Crafts acylation of ferrocene has been found to be highly successful and it was the first reaction to prove the aromatic nature of the cyclopentadienyl ligands on ferrocene.[1,27] Ferrocene is 10^6 times more reactive towards acylation than benzene.[28] This reaction is also highly versatile for the formation of both mono-substituted and di-substituted acylated products which can be achieved by varying the ratios of acid chloride, ferrocene and aluminium chloride, and by also varying the mode of addition of each of these reagents.[27] Mono-acylation of ferrocene is simply achieved by using equimolar quantities of each reagent; the best mode of preparation is the drop-wise addition of the acid chloride-aluminium chloride complex to the dissolved ferrocene solution.[27] The general procedure for the Friedel-Crafts acylation of ferrocene can be seen in Scheme 2.2, during the synthesis of methyl 3-ferrocenylpropanoate, **3**.

When carrying out Friedel-Crafts acylation using aluminium trichloride as the Lewis acid, 1.2 – 2.2 molar equivalents of aluminium chloride is used per carbonyl group on the acylating agent.[16] This is due to aluminium chloride forming a complex with the carbonyl oxygen, thereby limiting the amount of aluminium chloride being used as the catalyst. An excess has to be used to compensate for this complexion and for the reaction to proceed. Friedel-Crafts acylation of ferrocene can also be achieved using milder conditions (85% phosphoric acid and an appropriate acid anhydride), however, it has been shown that a stronger Lewis acid ($AlCl_3$) is required for acylation for the less reactive ruthenocene and osmocene.[18]

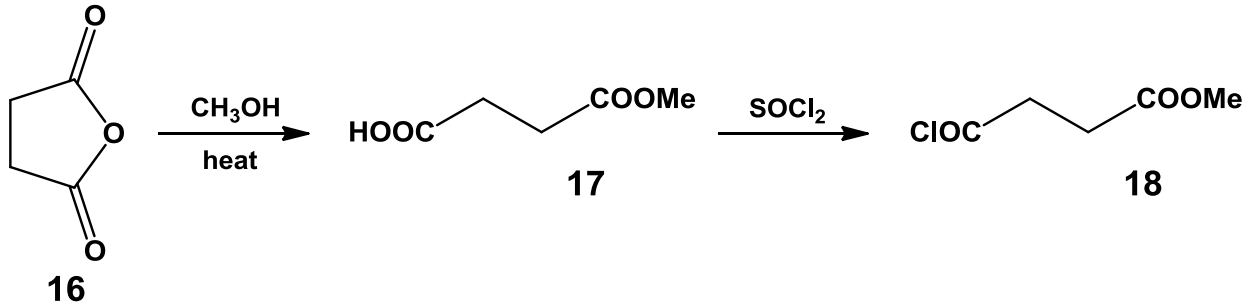

Scheme 2.3: Preparation of 3-carbomethoxypropionyl chloride from succinic anhydride, methanol and thionyl chloride.[29]

In terms of goals (i) and (ii) of this study, 3-carbomethoxypropionyl chloride is a useful acylating agent in Friedel-Crafts acylation (Scheme 2.2, synthesis of **3**). It is prepared from succinic anhydride, **16**, (Scheme 2.3).[29] Succinic anhydride is first heated in a slight excess of methanol to form 3-carbomethoxypropionic acid, **17**. 3-Carbomethoxypropionyl chloride, **18**, is then prepared by the reaction between the isolated acid, **17**, and thionyl chloride. Compound **18** demonstrates the use of a protective group. Here, the methyl ester protects the second carboxylic acid functionality and only a mono-acid chloride is formed.

Reduction of a ketone carbonyl group from the acylated product is required to prepare the alkylated product, such as 4-ferrocenylbutanoic acid, **12**, as shown in Scheme 2.2. The deoxygenation and hydrogenation of ketone carbonyls can be achieved by Clemmensen reduction, which utilises hydrochloric acid and zinc amalgam.[8] Clemmensen reduction has been studied with benzoylferrocene to give benzylferrocene. However, a variety of by-products are formed when the reducing agent, solvent and reaction times are varied.[30,31] The Clemmensen reduction mechanism is thought to be initiated by the action of hydrochloric acid, which produces two free electrons upon

dissolving the zinc metal. These electrons allow for the reduction of the carbonyl oxygen using the protons in the acidic medium.[24,30] Hydrogen gas is evolved during the dissolution of zinc metal; this reaction is also commonly called a dissolving metal reduction reaction. The reaction intermediate is formed by the protonation of the carbonyl group. The formation of dimerised by-products will depend on the stability and/or the concentration of this intermediate in the reaction medium.[32]

An alternative method for the deoxygenation of ketone carbonyl groups is the Wolff-Kishner reduction. In contrast to the Clemmensen reduction, the Wolf-Kishner method utilises an alkaline reaction medium at high temperatures, usually around 200 °C.[33,34] This reduction method reacts the ketone with a hydrazine to form a hydrazone, however the next step in the mechanism requires harsh conditions for the removal of a proton from the NH_2 group.[35] Therefore, a hot solution of concentrated sodium hydroxide is used.[26] The electron in the negatively charged complex can then become delocalised into the carbon of the original ketone, whereby protonation can occur from water in the reaction medium. This step is then repeated for the second protonation of the carbon atom, and nitrogen gas is released.[26,35]

It is clear that the reduction of a carbonyl group to a methylene (CH_2) species requires harsh conditions, but even so, the acylation-reduction method for the preparation of an alkylated aromatic compound is still more favourable than the alkylation of an aromatic compound.[35]

2.3.3 Metallocene alkenes

The formation of an alkene from an aldehyde or ketone can be achieved using the Wittig reaction (Scheme 2.2, synthesis of **10**, Method B). This reaction utilises triphenylphosphine and an alkyl halide for the *in situ* preparation of an alkylidenephosphorane, also known as a phosphonium ylide.[16] The phosphonium ylide is a powerful reagent in the Wittig reaction since the carbanion that is formed *in situ* can readily attack the carbonyl carbon of an aldehyde or ketone, forming an intermediate betaine.[16,26] The carbonyl oxygen then becomes negatively charged and since phosphorus has a strong affinity for oxygen, the phosphorus oxygen bond readily forms a four membered ring complex called oxaphosphetane.[26] The driving force of the Wittig reaction is the formation of the phosphine oxide by-product, which is a very stable compound (bonding energy for the P=O bond is 575 kJ mol^{-1}), and makes the Wittig reaction irreversible.[26] Therefore, the unstable

four membered ring of the oxaphosphetane quickly forms the desired alkene and a phosphine oxide. The preparation of ethyl 3-ferrocenylpropenoate, **10**, (Scheme 2.2, Method B) from ferrocenecarboxaldehyde utilising the Wittig reaction can be seen in Scheme 2.2, where R = Et.[36,37] The Wittig reaction yields **10**, essentially quantitatively.[36]

An alternate route for the formation of an alkene from an aldehyde or ketone (as for **10** in Scheme 2.2, R = H, Method A) is to use the Knoevenagel condensation reaction. This reaction can be achieved using malonic acid and a mixture of pyridine/piperidine which acts as a catalyst.[26] A stable hydrogen-bonded delocalised anion is formed by deprotonation with the basic pyridine/piperidine mixture. The reaction forms an aldol with the malonic anion, then undergoes decarboxylation to yield an alpha-beta conjugated enone system.[16,26,38] The Knoevenagel condensation of ferrocenecarboxaldehyde has been reported to yield 70% of 3-ferrocenylpropenoic acid, **10**, (Scheme 2.2, where R = H).[38]

Hydrogenation of **10** will produce 3-ferrocenylpropanoate or 3-ferrocenylpropanoic acid, **11**, (Scheme 2.2) where R = Et or H respectively. This is a very popular reaction and is easily achieved in near quantitative yields. It utilises hydrogen gas and palladium on carbon as a catalyst (usually 5% palladium).[36]

2.3.4 Metallocene carboxylic acids

Carboxylic acids, such as 2-ferrocenylethanoic acid, **4**, (Scheme 2.2), can be prepared via the hydrolysis of nitriles, using either acid or base as a catalyst. The reaction is initiated by the formation of an amide intermediate, which is then converted to the carboxylic acid using either acid or base.[16] For the base-catalysed hydrolysis of nitriles, the carboxylate anion is formed, which is then acidified to give the desired carboxylic acid. The basic method is preferred as the separation of unreacted nitrile can be achieved by extraction before the reaction mixture is acidified and the carboxylic acid isolated. It also prevents esterification and eliminates equilibria.[39]

Esters can be converted to carboxylic acids via acid- or base-catalysed hydrolysis, as in the synthesis of 3-ferrocenylpropanoic acid, **5**, and 4-ferrocenylbutanoic acid, **12**, (Scheme 2.2). Acid catalysed hydrolysis of esters protonates the carbonyl oxygen of the ester. Water then aids the reaction to proceed and the alkoxide group to leave for the formation of the carboxylic acid. The acid catalyst is then regenerated.[16,26] Alternatively, base-catalysed hydrolysis of esters allows the

partial positive carbonyl carbon to be attacked by the hydroxide group. The carboxylate ion is formed which can be converted to the desired carboxylic acid during an acid work-up.[16,26]

2.3.5 Metallocene amines

Aromatic amines can be synthesised from aromatic nitro compounds, via nitro group reduction. Hydrochloric acid together with tin metal can be used as reducing agents, which forms an amine chlorostannate complex. This complex can then be separated in excess alkaline solution to yield the desired aromatic amine.[16] Alternatively, hydrochloric acid and iron metal can be used; acetic acid instead of hydrochloric acid can be used to reduce the effect of undesirable by-products. For compounds that are sensitive to acidic conditions, Fe(II) sulphate is reacted with the nitro compound in alkaline solution.[16]

A useful tertiary amine in the family of ferrocene amines is dimethylaminomethylferrocene, **13**. The Mannich reaction can be used for aminomethylation of ferrocene. Formaldehyde and acetic acid can be used for preparation of **13** with *N,N,N',N'*-tetramethyldiaminomethane as the aminomethylating agent (Scheme 2.2).[40,41] This reaction works very well for ferrocene (79% yield), however, not so well for ruthenocene (35% yield).[42]

An alternate route for the Mannich product has been explored with ruthenocene, whereby **13** was prepared. This approach utilises lithiation of ruthenocene with *t*-BuLi, followed by reaction with Eschenmoser's salt, ($[CH_2NMe_2]I$), as the aminomethylating agent (Method A, Scheme 2.2).[42] This reaction was optimised for ruthenocene, with yields of 66% for dimethylaminomethylruthenocene and 17% for bis(dimethylaminomethyl)ruthenocene.

The conversion of **13** to *N, N, N*-trimethylaminomethylferrocene iodide, **14**, (Scheme 2.2) can be achieved utilising iodomethane in methanol solution.[39,43] The trimethylammonium group (a good leaving group) is known to be easily displaced by cyanide or hydroxide nucleophiles. [44–46] It has been reported for ferrocene that long reaction times (24 hours) lowers yields and result in small quantities of a by-product, methoxymethylferrocene (14% yield).[43] A much shorter reaction time of four hours yielded 96% of **14**.[39]

2.3.6 Metallocene nitriles

The preparation of 2-ferrocenylacetonitrile, **15**, (Scheme 2.2) can be achieved by displacement of the quaternary ammonium group of **14**, which can readily undergo nucleophilic aromatic substitution. This reaction is performed using sodium/potassium cyanide in an aqueous solvent; **15**, and has been prepared in 76% yield under reflux for 12 hours.[39] Alternatively, **15** has also been prepared in a condensation reaction of ferrocenecarboxaldehyde. This reaction utilises hydroxylamine hydrochloride and NMP (*N*-methyl-2-pyrrolidene) to react with ferrocenecarboxaldehyde at 110°C, resulting in 76% yield of **15**.[47]

2.3.7 Metallocene alcohols

Ferrocenylalcohols of the type $Fc(CH_2)_nOH$ with n = 1(**6**), 2(**7**), 3(**8**) and 4(**9**), (Scheme 2.2) can be synthesised by the reduction of the carbonyl group on aldehyde, ester or acid precursors as shown in Scheme 2.2.

The reduction of aldehydes, ketones, esters and acids can be achieved using sodium metal and absolute ethanol (forming *in situ* sodium ethoxide) solution or zinc dust in aqueous sodium hydroxide. However, these reactions are not selective methods of reduction and are only economical for large scale production.[16] Potassium or sodium borohydride may also be used as a possible reducing agent. They form a borohydride anion with the carbonyl compound. This anionic species is capable of reducing four moles of carbonyl compound with a considerable degree of selectivity.[16] Aluminium alkoxides or aluminium isopropoxide in excess isopropyl alcohol can also be used to selectively reduce aldehydes, ketones and esters to their corresponding alcohols.[16]

Alternatively, lithium aluminium hydride in diethyl ether or tetrahydrofuran solution can also be used; $LiAlH_4$ is the strongest reducing agent that can still reduce selectively. The preparation of 2-ferrocenylethanol, **7**, which utilises lithium aluminium hydride in tetrahydrofuran solvent, results in 75% yield. This reaction is relatively simple and separation of the product is easily achieved using solvent extraction methods.[39]

2.4 Electrochemistry

A short discussion on electroanalytical techniques to be performed in this study is presented. A detailed review on this technique can be found in literature.[48,49]

2.4.1 Voltammetry

Voltammetry is a technique that studies the redox behaviour of a compound by measuring the current as a function of applied potential, at a specific scan rate.[48,49] A typical cyclic voltammogram is shown in Figure 2.2 indicating the positions of peak anodic potential (E_{pa}), peak cathodic potential (E_{pc}), peak anodic current (i_{pa}) and peak cathodic current (i_{pc}).The three voltammetric methods that will be used in this study are cyclic voltammetry (CV), linear-sweep voltammetry (LSV) and square wave voltammetry (SW).

Cyclic voltammetry uses a triangular voltage input which produces both forward and reverse scans, cycling back to the starting potential used.[48,50] The formal reduction potential ($E^{\circ\prime}$, equation [1]) of a redox couple is the average of the forward and reverse peak potentials, known as the peak anodic potential (E_{pa}) and peak cathodic potential (E_{pc}), respectively. However, the formal reduction potential is only accurate when calculated for an electrochemically reversible system.[51] Electrochemical reversibility can be determined from the separation of the forward and reverse peak potentials (ΔE_p, equation [2]).

$$E^{\circ\prime} = (E_{pa} + E_{pc})/2 \quad [1]$$

$$\Delta E_p = E_{pa} - E_{pc} = 59/n \quad [2]$$

$$i_{pc}/i_{pa} = 1 \text{ (denominator is current from forward scan)} \quad [3]$$

$$E = E^{\circ\prime} + \frac{RT}{nF} \ln\left(\frac{[oxidation]}{[reduction]}\right) \quad [4]$$

A system is said to have electrochemical reversibility if the value for ΔE_p is 59/n mV, where n is the number of electrons transferred. This is, however, a theoretical value and in practice, values equal to or lower than 90/n mV are often acceptable, due to cell resistance and over potentials that will always be present in the instrument.[50] Electrochemical reversibility is achieved when the system can maintain the equilibria of oxidised and reduced species, as predicted by the NERNST equation (equation [4]). This requires a fast rate of electron transfer between the substrate and electrode.[50] For systems that have complete electrochemical and chemical reversibility, the ratio of the peak cathodic current (i_{pc}) and the peak anodic current (i_{pa}) is 1 (equation [3]). A system is said to be chemically reversible when both oxidation and reduction are possible quantitatively. When a system has both oxidation and reduction taking place (i.e. $i_{pa}/i_{pc} = 1$), but equation [2] results in ΔEp greater than 59/n mV, then the system is said to be electrochemically quasi-reversible.[52] Due to cell resistance and over potentials, a quasi-reversible system is often identified when equation [2] is experimentally found to be between 90/n mV and 150/n mV.[50]

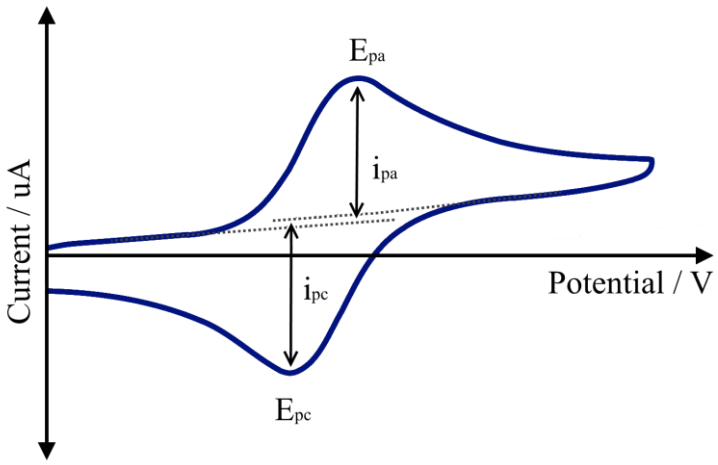

Figure 2.2: A typical cyclic voltammogram.

Linear-sweep voltammetry is similar to cyclic voltammetry, but it only makes use of one forward scan, at a specific scan rate. The scan rate is usually much slower than that used for cyclic voltammetry: 1 or 2 mV/s.[48,50] This voltammetric method is often used for systems where the number of electrons in a transfer process are uncertain. The relative number of electrons transferred in electrochemical processes for the entire system can be determined (by comparison with an internal standard) using a linear-sweep voltammogram.[50]

Square-wave voltammetry is a technique which utilises a pulsed voltage input, in which the complete voltammogram is easily obtained in less than 10 milliseconds.[48,50] The square-wave voltammetric technique offers higher resolution of poorly resolved peaks, which are due to multiple redox peaks in the same potential region.[50] This causes the peaks to overlap with one another. A cyclic voltammogram may not clearly resolve such peaks, but square-wave voltammetry often will.

2.4.2 Ferrocene electrochemistry

Ferrocene oxidises to the ferrocenium ion quantitatively, and the latter is easily reduced back to ferrocene, giving an electrochemically and chemically reversible redox couple.[53] Hence, equations [2] and [3] for electrochemical reversibility are all obeyed for ferrocene. Ferrocene has become an internal standard and reference for electrochemical measurements in non-aqueous solutions, usually referenced at 0 Volts.[53] Internal standards are required due to potential variations caused by fluctuations in the liquid junction potentials that occur between the reference electrode and the solution.[54] For compounds that may overlap with ferrocene, decamethylferrocene can also be used as an internal standard.[54,55] In such cases, decamethylferrocene is referenced against ferrocene in a separate experiment, under the same conditions used in the study.

Ferrocene derivatives such as the alcohols and carboxylic acids in Scheme 2.2, **6 – 9** and **4, 5** and **12** respectively, have been studied and their formal reduction potentials determined (Figure 2.3).[12,56] The electrochemistry of many ferrocene derivatives also exhibit electrochemical reversible behaviour, and those of the carboxylic acids and alcohols have been found to obey equations [2] and [3] as well.[12,56]

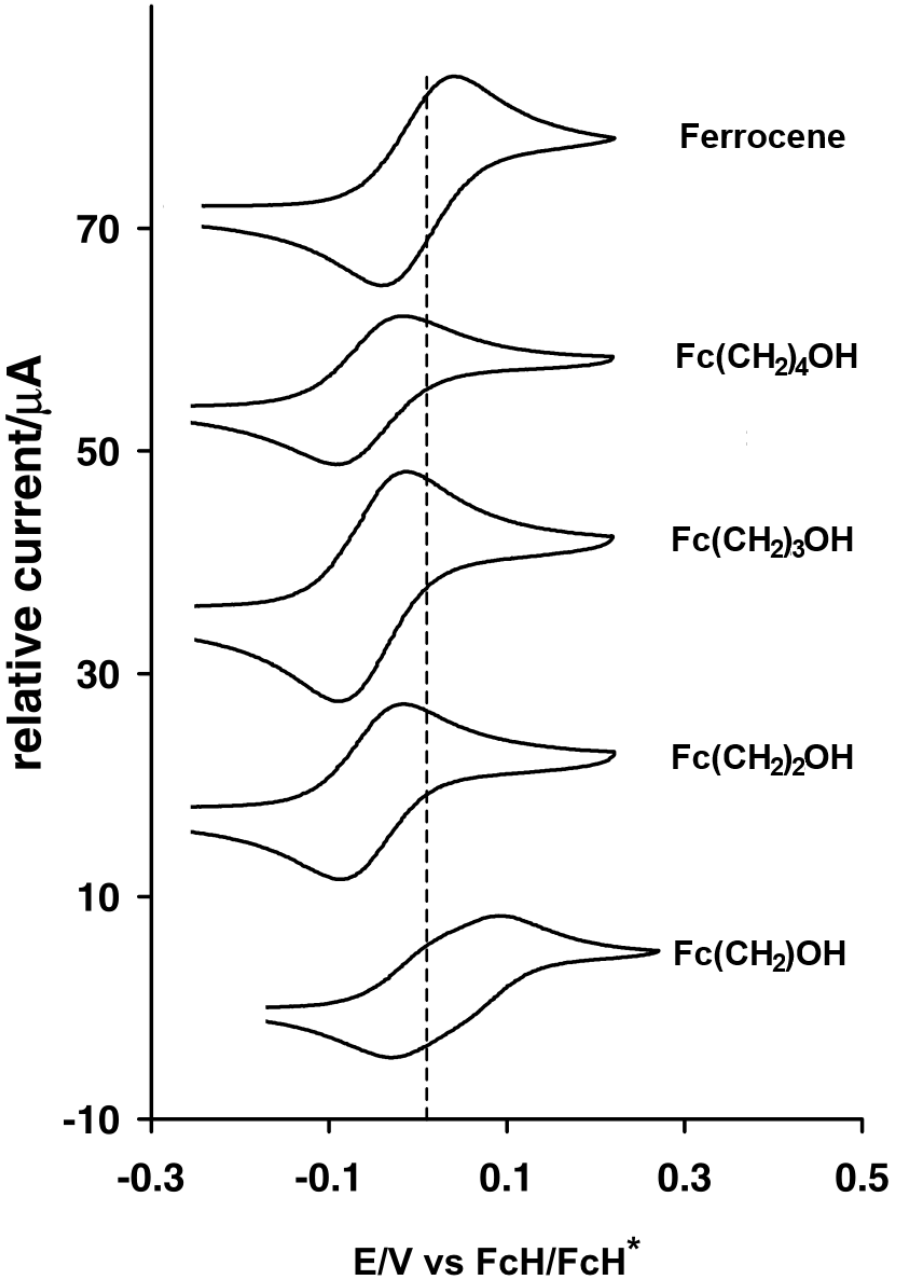

Figure 2.3: Cyclic voltammograms of ferrocene and ferrocenylalcohols $Fc(CH_2)_nOH$ where n = 1, 2, 3 and 4, compounds 6 – 9 (Scheme 2.2). Diagram was reproduced from reference 12.

2.4.3 Osmocene and Ruthenocene electrochemistry

The electrochemical behaviour of osmocene indicates both chemical and electrochemical reversibility in dichloromethane solution, versus aqueous AgCl/Ag in 1.0M KCl.[57] Osmocene oxidation and osmocenium reduction also proceeds as a one-electron, reversible process upon using a dropping mercury electrode (DME), but proceeds as two consecutive, irreversible one-electron oxidation processes at a platinum electrode.[52,58]

Table 2.2 presents the electrochemical data of ferrocene, ruthenocene and osmocene under the same conditions, where the electrochemistry of all three metallocenes are chemically and electrochemically reversible. The ease of oxidation increases in the order ruthenocene, osmocene, ferrocene versus AgCl/Ag in 1.0 M KCl.[57,58]

Table 2.2: Electrochemical data for ferrocene, ruthenocene and osmocene (0.5 mM) in 0.1 M $[NBu_4][B(C_6F_5)_4]$ in DCM, versus aqueous AgCl/Ag in 1.0M KCl. Scan rate = 100 mV/s.[57]

Metallocene	E°´ / V	ΔE / V	i_{pc}/i_{pa}
Ferrocene	0.47 (a)	0.085	1.0 ± 0.05
Osmocene	0.83	0.089	1.0 ± 0.05
Ruthenocene	1.03	0.095	1.0 ± 0.10

(a) E°´ of ferrocene obtained using 0.1 M $[NBu_4][PF_6]$ under identical conditions

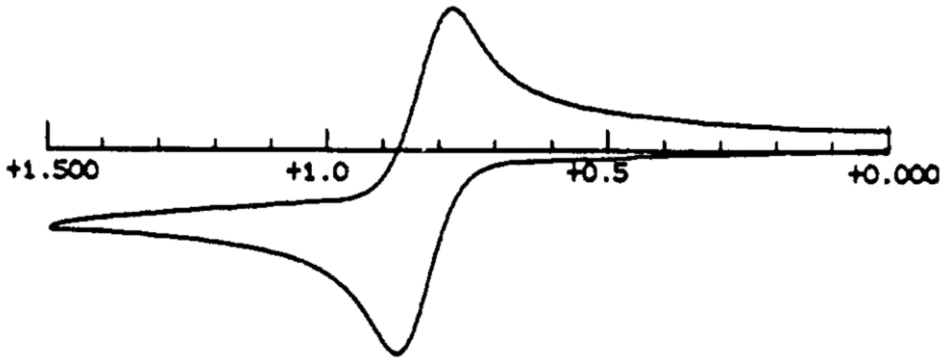

Figure 2.4: Cyclic voltammogram of 0.5 mM osmocene in dichloromethane, 0.1 M $[NBu_4][B(C_6F_5)_4]$. Scan rate = 100 mV/s. Diagram was reproduced from reference 57.

The ruthenocenium cation and osmocenium cation, unlike the ferrocenium cation, have the ability to dimerise if the conditions are favourable.[59,60] The ruthenocenium cation is known to form dimers if it is unable to form an ion pair with the electrolyte.[59] The dimerisation of ruthenocene is illustrated in Figure 2.5. Osmocenium ions have been shown to form dimers of $[(Cp_2Os)_2]^{2+}$ and $[\{Cp(C_5H_4)Os\}_2]^{2+}$ and their crystal structures have been determined by Taube *et al.* (Figure 2.6).[60] The dimerisation of ruthenocenium cations have been observed electrochemically using cyclic voltammetry and was found to be temperature dependent, with different dimeric species dominating at different temperatures. This, however, has not been observed electrochemically for osmocene/osmocenium.[21,59]

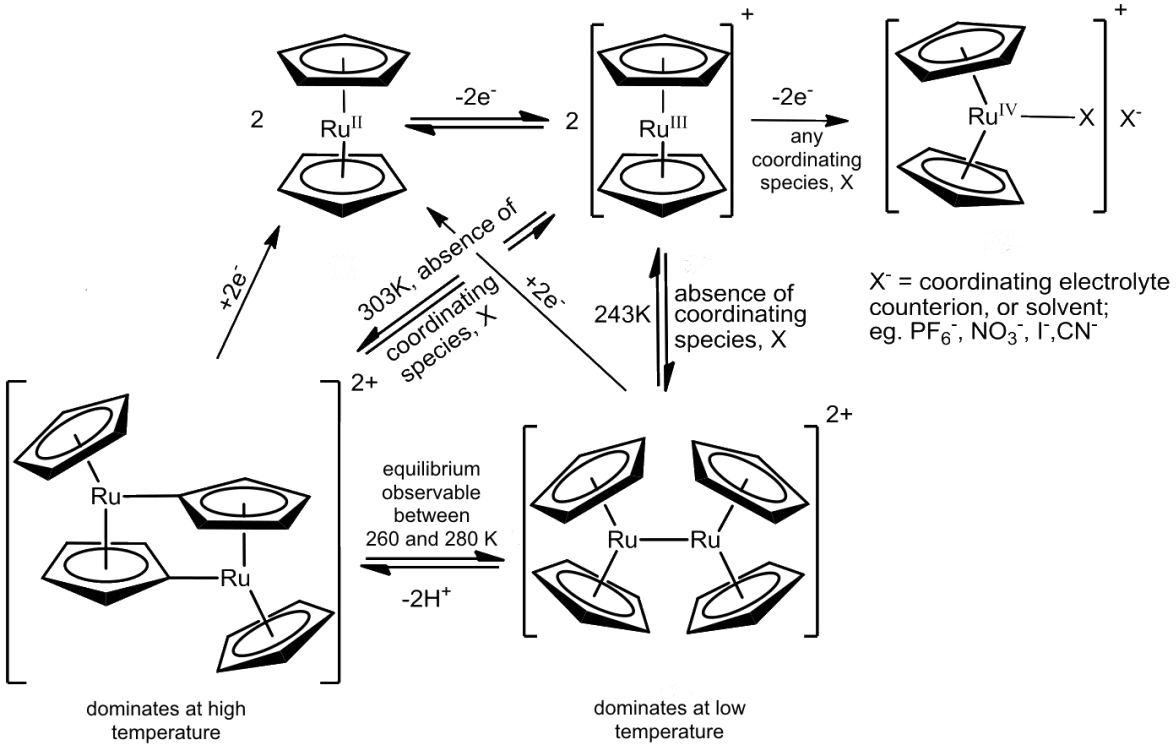

Figure 2.5: The electrochemical oxidation of ruthenocene leads to dimerisation of the ruthenocenium caton, when in the absence of coordinating species. Diagram reproduced from reference 21.

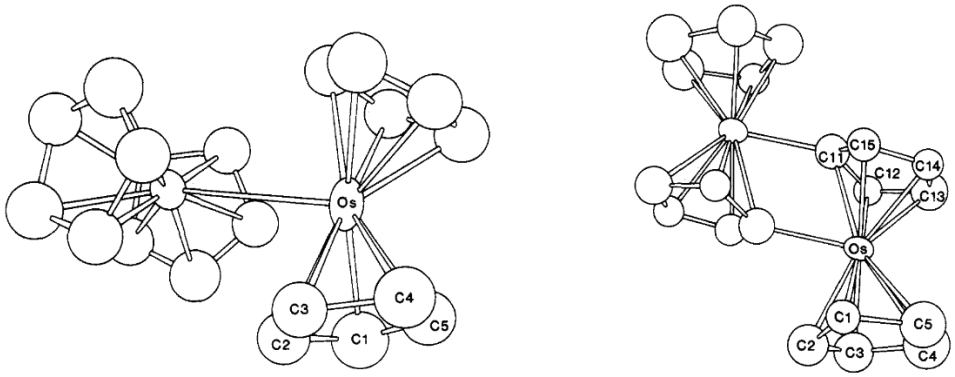

$[(Cp_2Os)_2]^{2+}$ $[\{Cp(C_5H_4)Os\}_2]^{2+}$

Figure 2.6: ORTEP diagrams for the crystal structures of osmocene dimers, $[(Cp_2Os)_2]^{2+}$ (left) and $[\{Cp(C_5H_4)Os\}_2]^{2+}$ (right). Diagram reproduced from reference 60.

2.5 Organometallic anticancer agents

A compound is considered organometallic if it contains at least one direct covalent carbon-metal bond. Organometallic compounds are well known for their applications in homogeneous and heterogeneous catalysis.[61,62] This field of chemistry is also gaining popularity in medicinal chemistry. Carbenes, metallocenes, half-sandwich, carbonyl and π-ligand compounds are continuously finding applications in all fields of medicinal chemistry.[63]

Metallocenes (parallel and bent structural types) with metals comprising of iron, ruthenium, cobalt, titanium, zirconium, vanadium, niobium and molybdenum are all being researched in a medicinal context.[63] Ferroquine is an organometallic drug to have reached phase III clinical trials as an antimalarial agent (Figure 2.7).[63]

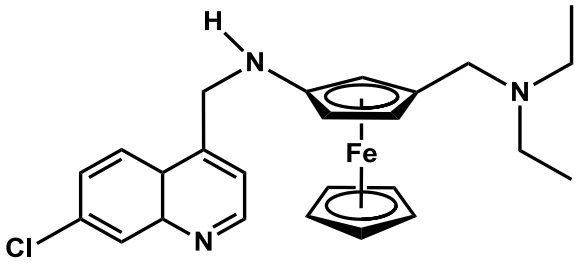

Figure 2.7: Chemical structure of Ferroquine, an organometallic antimalarial agent which has reached phase III clinical trials.[63]

New and more effective chemotherapeutic agents are constantly in demand due to the development of drug resistance and toxicity, which has become a crippling factor in chemotherapy.[63,64]

Ruthenium half-sandwich metallocene derivatives, more specifically ruthenium (η^6-arene) complexes, are a promising class of antiproliferative agents.[65] Ruthenium complexes have been found to not only target deoxyribonucleic acid (DNA), which is similar to the mode of action of current platinum anticancer agents, but also bind strongly to proteins.[63]

The ruthenium(II)-arene ethylenediamine derivative shown in Figure 2.8 has been found to have a similar mode of action as cisplatin, whereby the Ru-Cl bond hydrolyses in the blood to form the active aqua complex, $[(\eta^6\text{-arene})Ru(en)(H_2O)]^{2+}$.[63] In contrast, the ruthenium(II)-arene PTA derivative (also known as a RAPTA complex) has been found to operate differently to that of cisplatin and the ruthenium(II)-arene ethylenediamine derivative. The mode of action is thought to consist of enzymatic binding, however, the complete mechanism is still unknown.[63] RAPTA complexes consist of a PTA ligand (1,3,5-triaza-7-phosphaadamantane) which have good aqueous solubility and two labile chloride ligands.[63,65] These complexes are lower in toxicity than cisplatin and have anti-metastatic and anti-angiogenic properties.[66]

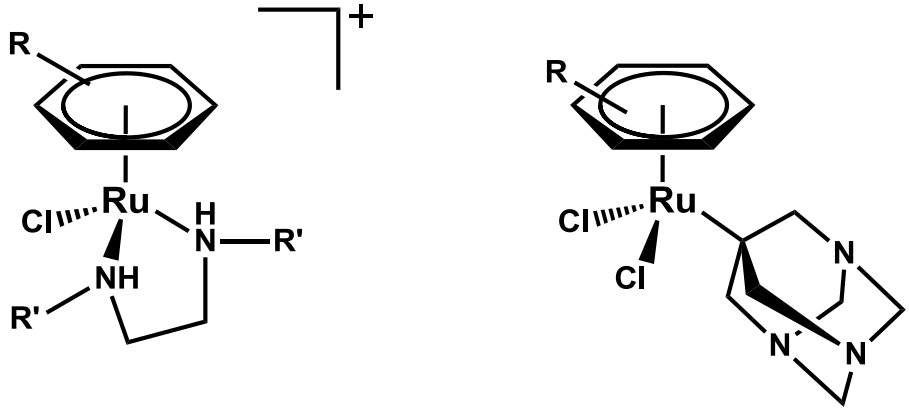

Ruthenium(II)-arene ethylenediamine derivative *Ruthenium(II)-arene PTA derivative*

Figure 2.8: Ruthenium (η^6-arene) PTA derivative and ethylenediamine derivative organometallic anticancer complexes.[63]

2.5.1 Osmium anticancer agents

The anticancer properties of osmium have not been researched as much as ruthenium and platinum. This is due to the high toxicity of osmium tetroxide (OsO_4) and very low substitution reactivity.[63] A nitrodoosmium(VI) Schiff base complex (Figure 2.9) consisting of labile chloro and aqua ligands was tested against human cell lines and compared favourably to cisplatin. The results indicated that the nitrodoosmium(VI) complex was more efficient than cisplatin.[67] Prolonged treatment also displayed higher cancer cell cytotoxicity compared to that of cisplatin.[67]

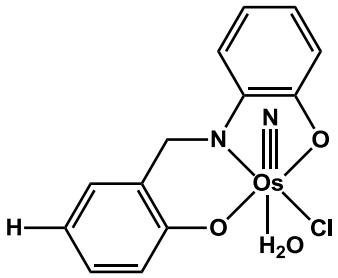

Figure 2.9: Nitrodoosmium(VI) Schiff base complex.[67]

Some osmium(II) arene complexes have also been found to exhibit anticancer activity.[63,65] Both isomers of chiral osmium(II) arene complexes, (S_{Os},S_C)-[Os(η^6-p-cym)(ImpyMe)Cl]PF_6 and (R_{Os},R_C)-[Os(η^6-p-cym)(ImpyMe)Cl]PF_6, exhibit moderate anticancer activity when tested against the A2780 cells (human ovarian cancer cell line). It was found to be more active than cisplatin.[68] The equivalent iodido complexes, (S_{Os},S_C)-[Os(η^6-p-cym)(ImpyMe)I]PF_6 and (R_{Os},R_C)-[Os(η^6-p-cym)(ImpyMe)I]PF_6 exhibited potent anticancer activity against NCI 60-cell-line (National Cancer Institute human tumour cell line) similar to that of cisplatin.[68]

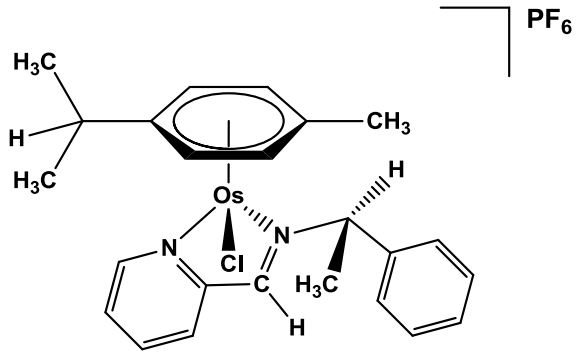

(S_{Os},S_c)-[Os(η^6-*p*-cym)(ImpyMe)Cl]PF_6

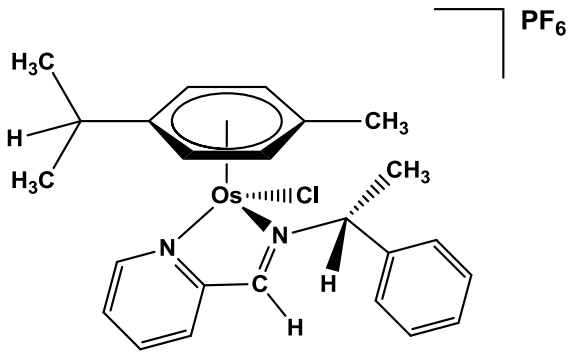

(R_{Os},R_c)-[Os(η^6-*p*-cym)(ImpyMe)Cl]PF_6

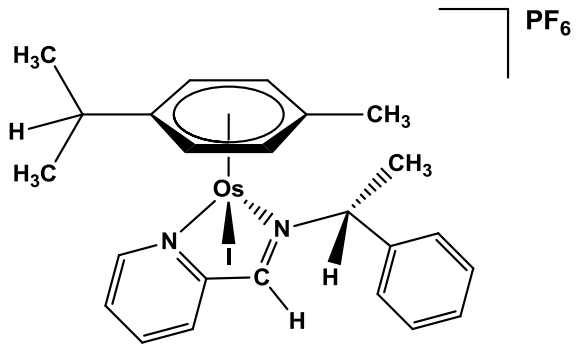

(R_{Os},R_c)-[Os(η^6-*p*-cym)(ImpyMe)Cl]PF_6

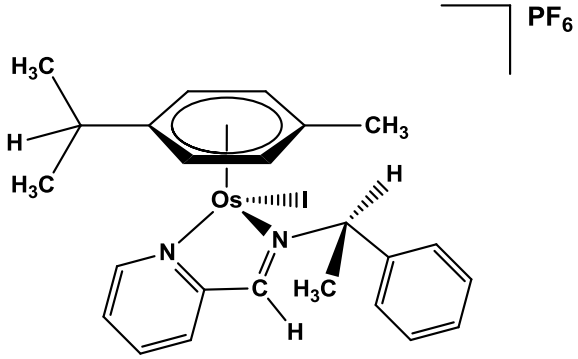

(S_{Os},S_c)-[Os(η^6-*p*-cym)(ImpyMe)Cl]PF_6

Figure 2.10: A series of osmium arene complexes that were found to exhibit anticancer activity. Diagram reproduced from reference 68.

2.5.2 Metallocenes

Metallocene derivatives are of great interest in anticancer research due to their interesting chemical, electronic, spectroscopic and bonding properties. In particular, titanocene, molybdocene, vanadocene and ferrocene have previously exhibited antineoplastic activity due to their cytotoxic activity, with ferrocene and titanocene derivatives being the most studied metallocenes.[69]

Ferrocifen, which is a structural variation of tamoxifen (used as a chemotherapeutic agent in breast cancer) combined with a ferrocenyl moiety, is an anticancer agent that is aimed at combining the cytotoxic effects of ferrocene with the antioestrogenic properties of tamoxifen.[13,14,69,70] Hydroxyferrocifens (Figure 2.11) are ferrocifen derivatives and are also being investigated for their anticancer properties.

Titanocene dichloride [$TiCp_2Cl_2$] displayed antiproliferative properties, however, upon reaching phase I clinical trials the side effects included nephrotoxicity, hypoglycaemia and nausea in humans.[69] Among the various titanocene derivatives being researched, [$Ti\{\eta^5\text{-}C_5H_4(CH_2C_6H_4OCH_3)\}_2Cl_2$] (Figure 2.11) has displayed interesting anticancer properties. It was reported that the titanium ions use a major iron transport protein called transferrin to reach the cells.[69]

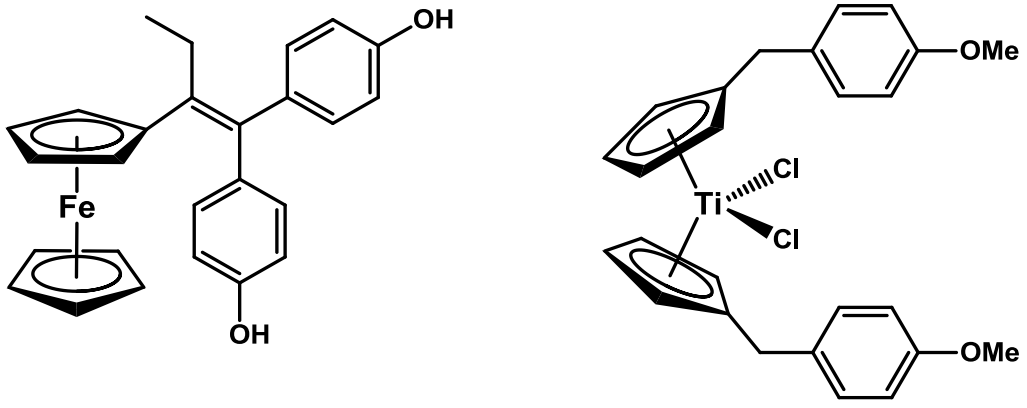

A hydroxyferrocifen derivative *[Ti{η^5-$C_5H_4(CH_2C_6H_4OCH_3)$}$_2Cl_2$]*

Figure 2.11: Ferrocene and titanocene derivatives which exhibit anticancer properties.[69]

Ferrocenylalcohols, **6 – 9** (Scheme 2.2), were tested against the HeLa cancer cell line by the author's UFS laboratory.[71] The results showed that the cytotoxicity of ferrocenylalcohols increased as the alkyl chain length increased. The correlation between a series of ferrocenylalcohols of the type $Fc(CH_2)_nOH$, where n = 1, 2, 3, and 4 (Scheme 2.2), and the IC_{50} values (the dosage necessary for 50% cell death) can be seen in Figure 2.12.[71] Hence, the most active antineoplastic drug in the series of ferrocenylalcohols was 4-ferrocenylbutanol (Figures 2.12).

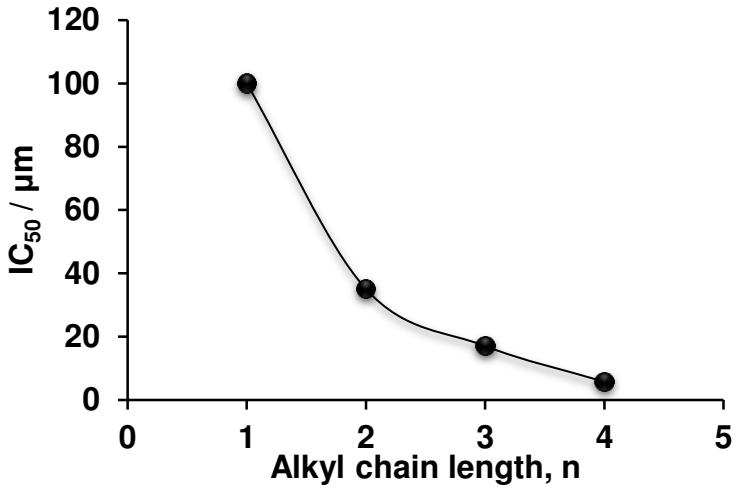

Figure 2.12: Relationship between ferrocenylalcohols ($Fc(CH_2)_nOH$) alkyl chain length, n, and IC_{50} dosages.[71]

The mechanism of antineoplastic action involves first the formation of the ferrocenium ion by a one-electron oxidation of ferrocene. Ferrocenium salts were found to exhibit antiproliferative effects.[63] The correlation between the formal reduction potentials (E°´) of ferrocenylalcohols, $Fc(CH_2)_nOH$ where n = 1, 2, 3, and 4 (Scheme 2.2) and the IC_{50} values is shown in Figure 2.13. The ferrocenylalcohols with increasing chain length displayed decreasing formal reduction potential values. In turn, the IC_{50} values increased as the formal reduction potentials increased, and the ferrocenium ion is more easily formed.

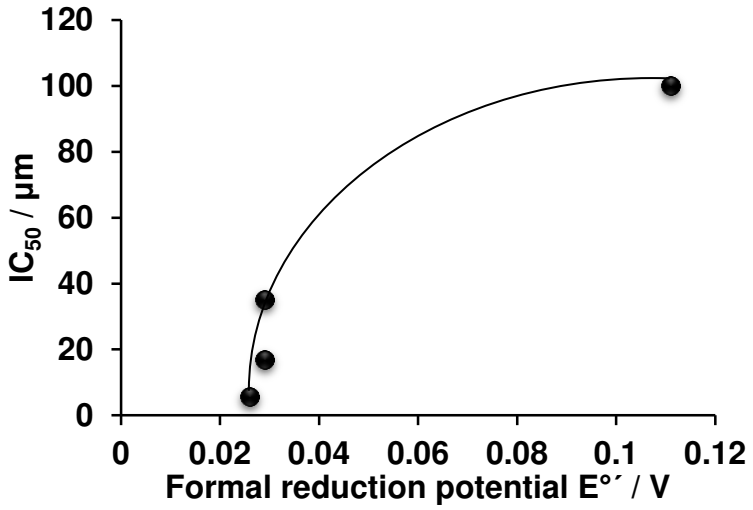

Figure 2.13: Relationship between the formal reduction potentials (E°´) of ferrocenylalcohols, ($Fc(CH_2)_nOH$) where n= 1, 2, 3 and 4, and IC_{50} values.[71]

2.6 Crystallography

Crystallography is a powerful molecular characterisation technique which has become increasingly popular since its discovery.[72] It is a solid-state characterisation technique which is able to provide bond angles between atoms (within hundredths of a degree) and bond lengths (within thousandths on an Ångström).[72] The unit cell of the crystal can also be determined which provides information about the packing/arrangement of the atoms.[73]

2.6.1 Osmocene carboxaldehyde

The crystal structure of osmocenecarboxaldehyde was determined by Swarts *et al*.[20] Structural detail can be seen in Figure 2.14. The two parallel cyclopentadienyl rings deviate from an eclipsed configuration by 10.11°.[20] The cyclopentadienyl rings are separated by a distance of 3.639 Å which is similar to that of the cyclopentadienyl rings in osmocene (3.64 Å).[10,20] The packing of the molecules is anti-parallel.[20] The inter-cyclopentadienyl distance is larger than in substituted ferrocenes (3.339 Å) and ruthenocenes (3.600 Å).[74,75]

This study will present the crystal structure of $OcCH_2CN$ and $OcCH_2CH_2OH$.

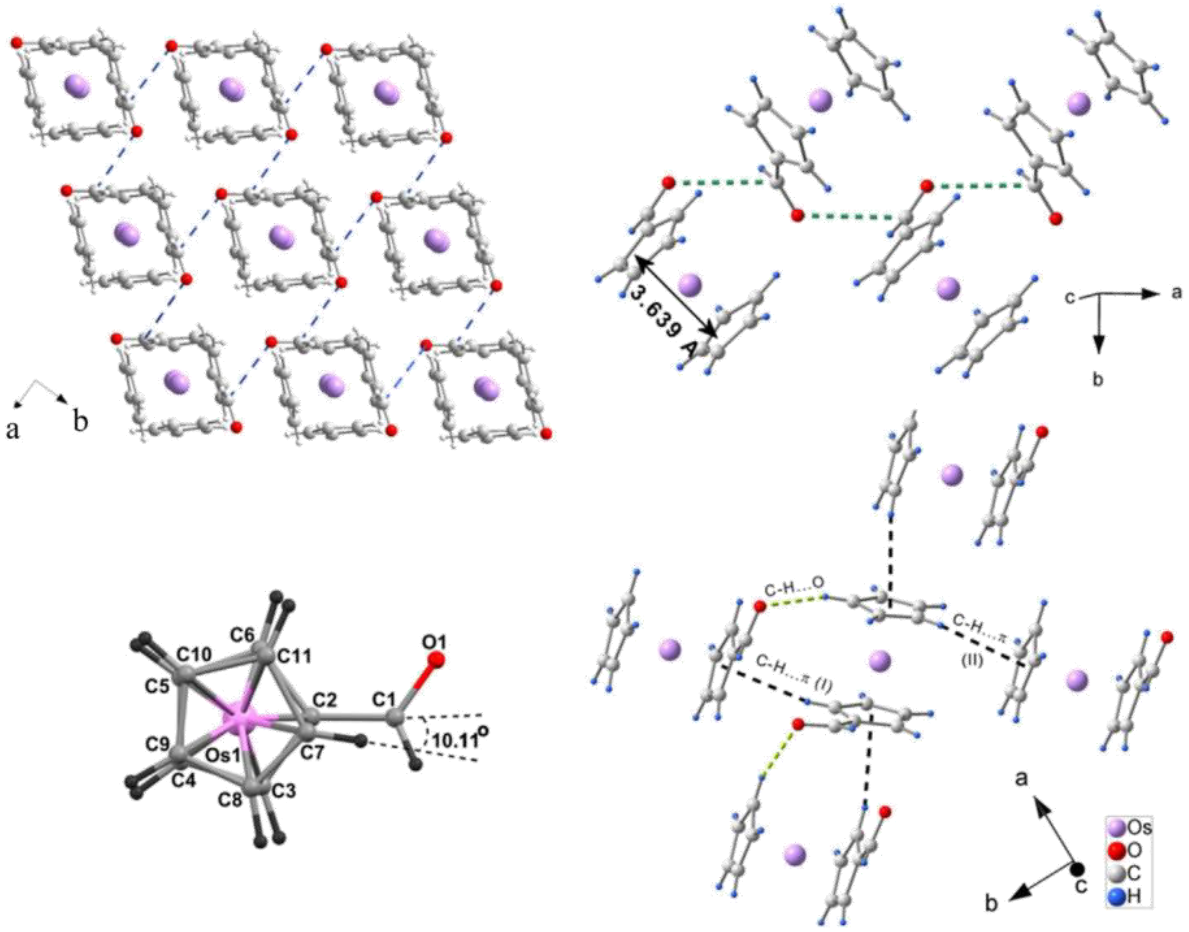

Figure 2.14: Crystallographic data of osmocenecarboxaldehyde. Diagrams were reproduced from reference 20.

This concludes the literature survey of topics the author deemed relevant to her research project. Chapters 3 and 4 will provide details of the author's own research.

References

1. N. J. Long, in *Metallocenes: An Introduction to Sandwiched Complexes*, Wiley-Blackwell, Oxford, USA, 1998, pp. 6–133.
2. D. Astruc, in *Organometallic Chemistry and Catalysis*, Springer Berlin Heidelberg, 2007, pp. 251–288.
3. G. Wilkinson, P. L. Pauson and F. A. Cotton, *J. Am. Chem. Soc.*, 1954, **76**, 1970–1974.
4. M. D. Rausch, E. O. Fischer and H. Grubert, *J. Am. Chem. Soc.*, 1960, **82**, 76–82.
5. S. Barlow and S. R. Marder, *Chem. Commun.*, 2000, 1555–1562.
6. C. Housecroft and A. G. Sharpe, *Inorganic Chemistry*, Prentice Hall, Harlow, England; New York, 3 edition., 2007.
7. M. Rausch, M. Vogel and H. Rosenberg, *J. Org. Chem.*, 1957, **22**, 900–903.
8. M. Rausch, M. Vogel and H. Rosenberg, *J. Chem. Educ.*, 1957, **34**, 268.
9. A. Z. Rubezhov, A. S. Ivanov and A. A. Bezrukova, *Bull. Acad. Sci. USSR Div. Chem. Sci.*, 1979, **28**, 1484–1486.
10. J. C. A. Bobyens, D. C. Levendis, M. I. Bruce and M. L. Williams, *J. Crystallogr. Spectrosc. Res.*, 1986, **16**, 519–524.
11. M. Watanabe and H. Sano, *Bull. Chem. Soc. Jpn.*, 1990, **63**, 1455–1461.
12. W. L. Davis, R. F. Shago, E. H. G. Langner and J. C. Swarts, *Polyhedron*, 2005, **24**, 1611–1616.
13. D. R. van Staveren and N. Metzler-Nolte, *Chem. Rev.*, 2004, **104**, 5931–5986.
14. M. F. R. Fouda, M. M. Abd-Elzaher, R. A. Abdelsamaia and A. A. Labib, *Appl. Organomet. Chem.*, 2007, **21**, 613–625.
15. R. A. S. M. Aslam Siddiqi, *Mater*, 2010, **3**, 1172–1185.
16. A. I. Vogel, A. R. Tatchell, B. S. Furnis, A. J. Hannaford and P. W. G. Smith, *Vogel's Textbook of Practical Organic Chemistry*, Prentice Hall, Harlow, 5th edn., 1996.
17. H. K. Masaru Sato, *Bull. Chem. Soc. Jpn.*, 1968, **41**, 252–252.
18. D. E. Bublitz, W. E. McEwen and J. Kleinberg, *J. Am. Chem. Soc.*, 1962, **84**, 1845–1849.

19. P. J. Graham, R. V. Lindsey, G. W. Parshall, M. L. Peterson and G. M. Whitman, *J. Am. Chem. Soc.*, 1957, **79**, 3416–3420.

20. M. Trzebiatowska-Gusowska, A. Gągor, E. Coetsee, E. Erasmus, H. C. Swart and J. C. Swarts, *J. Organomet. Chem.*, 2013, **745–746**, 393–403.

21. (a) C. C. Joubert, M. Sc. Synthesis and characterisation of ruthenocene-containing complexes with biomedical applications, University of the Free State, 2011.

    (b) J. C. Swarts, A. Nafady, J. H. Roudebush, S. Trupia and W. E. Geiger, *Inorg. Chem.*, 2009, **48**, 2156-2165.

22. R. Sanders and U. T. Mueller-Westerhoff, *J. Organomet. Chem.*, 1996, **512**, 219–224.

23. N. N. Crounse, *J. Am. Chem. Soc.*, 1949, **71**, 1263–1264.

24. J. Hine and J. M. Van Der Veen, *J. Am. Chem. Soc.*, 1959, **81**, 6446–6449.

25. H. Wynberg, *Chem. Rev.*, 1960, **60**, 169–184.

26. J. Clayden, N. Greeves, S. Warren and P. Wothers, *Organic Chemistry*, Oxford University Press, New York, 2001.

27. M. Vogel, M. Rausch and H. Rosenberg, *J. Org. Chem.*, 1957, **22**, 1016–1018.

28. S. Ahn, Y.-S. Song, B. R. Yoo and I. N. Jung, *Organometallics*, 2000, **19**, 2777–2780.

29. J. Cason, *Org. Synth. Coll*, 1945, **3**, 169–171.

30. J. C. Palacios and P. Cintas, *J. Chem. Educ.*, 1998, **75**, 938.

31. M. D. Rausch and D. L. Adams, *J. Org. Chem.*, 1967, **32**, 4144–4145.

32. H. L. Bradlow and C. A. VanderWerf, *J. Am. Chem. Soc.*, 1947, **69**, 1254–1256.

33. H. L. Herzog and E. R. Buchman, *J. Org. Chem.*, 1951, **16**, 99–104.

34. E. Parquet and Q. Lin, *J. Chem. Educ.*, 1997, **74**, 1225.

35. P. Y. Bruice, in *Organic Chemistry*, Prentice Hall, Upper Saddle River, N.J., 5th edn., 2006, pp. 664–813.

36. A.-E. Navarro, N. Spinelli, C. Moustrou, C. Chaix, B. Mandrand and H. Brisset, *Nucleic Acids Res.*, 2004, **32**, 5310–5319.

37. S. C. B. Gnoatto, A. Dassonville-Klimpt, S. Da Nascimento, P. Galéra, K. Boumediene, G. Gosmann, P. Sonnet and S. Moslemi, *Eur. J. Med. Chem.*, 2008, **43**, 1865–1877.

38. D. Naskar, S. K. Das, L. Giribabu, B. G. Maiya and S. Roy, *Organometallics*, 2000, **19**, 1464–1469.

39. M. Ripert, C. Farre and C. Chaix, *Electrochim. Acta*, 2013, **91**, 82–89.

40. O. A. Tarasova, I. V. Tatarinova, T. I. Vakul'skaya, S. S. Khutsishvili, V. I. Smirnov, L. V. Klyba, G. F. Prozorova, A. I. Mikhaleva and B. A. Trofimov, *J. Organomet. Chem.*, 2013, **745–746**, 1–7.

41. J. K. Lindsey and C. R. Hauser, *J. Org. Chem.*, 1957, **22**, 355–358.

42. P. Beagley, M. A. L. Blackie, K. Chibale, C. Clarkson, J. R. Moss and P. J. Smith, *J. Chem. Soc. Dalton Trans.*, 2002, **23**, 4426–4433.

43. G. Grelaud, T. Roisnel, V. Dorcet, M. G. Humphrey, F. Paul and G. Argouarch, *J. Organomet. Chem.*, 2013, **741–742**, 47–58.

44. D. Lednicer and C. R. Hauser, *Org. Synth.*, 1960, **40**, 45.

45. D. Lednicer, T. A. Mashburn and C. R. Hauser, *Org. Synth.*, 1960, **40**, 52.

46. D. Marquarding, H. Klusacek, G. Gokel, P. Hoffmann and I. Ugi, *J. Am. Chem. Soc.*, 1970, **92**, 5389–5393.

47. J. Ma, X. Cui, B. Zhang, M. Song and Y. Wu, *Tetrahedron*, 2007, **63**, 5529–5538.

48. D. A. Skoog, D. M. West, F. J. Holler and S. R. Crouch, *Fundamentals of Analytical Chemistry*, Thomson-Brooks/Cole, 8th edn., 2004.

49. P. T. Kissinger and W. R. Heineman, *J. Chem. Educ.*, 1983, **60**, 702.

50. H. J. Gericke, N. I. Barnard, E. Erasmus, J. C. Swarts, M. J. Cook and M. A. S. Aquino, *Inorganica Chim. Acta*, 2010, **363**, 2222–2232.

51. G. A. Mabbott, *J. Chem. Educ.*, 1983, **60**, 697.

52. Z. S. Ambrose, M. Sc., University of the Free State, 2006.

53. R. R. Gagne, C. A. Koval and G. C. Lisensky, *Inorg. Chem.*, 1980, **19**, 2854–2855.

54. I. Noviandri, K. N. Brown, D. S. Fleming, P. T. Gulyas, P. A. Lay, A. F. Masters and L. Phillips, *J. Phys. Chem. B*, 1999, **103**, 6713–6722.

55. Š. Komorsky-Lovrić, M. Lovrić and F. Scholz, *J. Electroanal. Chem.*, 2001, **508**, 129–137.

56. N. F. Blom, E. W. Neuse and H. G. Thomas, *Transit. Met. Chem.*, 1987, **12**, 301–306.

57. M. G. Hill, W. M. Lamanna and K. R. Mann, *Inorg. Chem.*, 1991, **30**, 4687–4690.

58. S. P. Gubin, S. A. Smirnova, L. I. Denisovich and A. A. Lubovich, *J. Organomet. Chem.*, 1971, **30**, 243–255.

59. E. Fourie, J. M. J. van Rensburg and J. C. Swarts, *J. Organomet. Chem.*, 2014, **754**, 80–87.

60. M. W. Droege, W. D. Harman and H. Taube, *Inorg. Chem.*, 1987, **26**, 1309–1315.

61. K. J. Bennett, *Corp. Environ. Strategy*, 1998, **5**, 42–49.

62. M. P. Conley, C. Copéret and C. Thieuleux, *ACS Catal.*, 2014, **4**, 1458–1469.

63. G. Gasser, I. Ott and N. Metzler-Nolte, *J. Med. Chem.*, 2011, **54**, 3–25.

64. J. D. Patel, L. Krilov, S. Adams, C. Aghajanian, E. Basch, M. S. Brose, W. L. Carroll, M. de Lima, M. R. Gilbert, M. G. Kris, J. L. Marshall, G. A. Masters, S. J. O'Day, B. Polite, G. K. Schwartz, S. Sharma, I. Thompson, N. J. Vogelzang and B. J. Roth, *J. Clin. Oncol.*, 2013, **32**, 129–161.

65. V. B. Arion, A. Dobrov, S. Göschl, M. A. Jakupec, B. K. Keppler and P. Rapta, *Chem. Commun.*, 2012, **48**, 8559–8561.

66. C. M. Clavel, E. Păunescu, P. Nowak-Sliwinska and P. J. Dyson, *Chem. Sci.*, 2014, **5**, 1097–1101.

67. W.-X. Ni, W.-L. Man, M. T.-W. Cheung, R. W.-Y. Sun, Y.-L. Shu, Y.-W. Lam, C.-M. Che and T.-C. Lau, *Chem. Commun.*, 2011, **47**, 2140–2142.

68. Y. Fu, R. Soni, M. J. Romero, A. M. Pizarro, L. Salassa, G. J. Clarkson, J. M. Hearn, A. Habtemariam, M. Wills and P. J. Sadler, *Chem. – Eur. J.*, 2013, **19**, 15199–15209.

69. S. Gómez-Ruiz, D. Maksimović-Ivanić, S. Mijatović and G. Kaluđerović, *Bioinorg. Chem. Appl.*, 2012, **2012**, 1–14.

70. A. D. Claire S. Allardyce, *Appl. Organomet. Chem.*, 2005, **19**, 1 – 10.

71. R. F. Shago, J. C. Swarts, E. Kreft and C. E. J. van Rensburg, *Anticancer Res.*, 2007, **27**, 3431–3433.

72. M. R. Bond and C. J. Carrano, *J. Chem. Educ.*, 1995, **72**, 451.

73. J. P. Glusker, *J. Chem. Educ.*, 1988, **65**, 474.

74. J. D. Dunitz, L. E. Orgel and A. Rich, *Acta Crystallogr.*, 1956, **9**, 373–375.

75. G. L. Hardgrove and D. H. Templeton, *Acta Crystallogr.*, 1959, **12**, 28–32.

3 Results and Discussion

3.1 Introduction

The results obtained by the author, with reference to the goals in chapter 1, are presented in this chapter. A series of mostly new osmocene-containing alcohols and carboxylic acids were synthesised in this study, as shown in Figure 3.1. The series of alcohols that have been synthesised are osmocenylmethanol, **19**, 2-osmocenylethanol, **20**, 3-osmocenylpropanol, **21**, and 4-osmocenylbutanol, **22**. The series of carboxylic acids that have been synthesised are 2-osmocenylethanoic acid, **23**, 3-osmocenylpropanoic acid, **24**, and 4-osmocenylbutanoic acid, **25**.

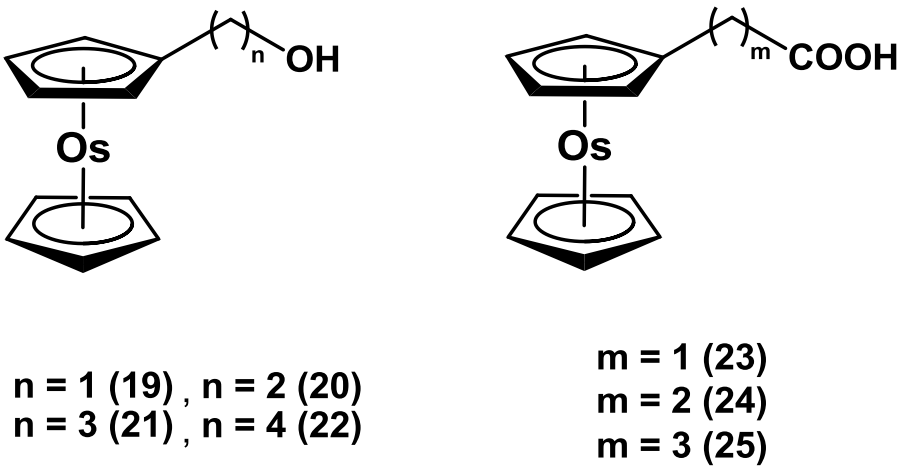

Figure 3.1: Chemical structures of osmocene-containing alcohols and carboxylic acids that were synthesised in this study.

The compounds were characterised using nuclear magnetic resonance spectroscopy (^{1}H and ^{13}C NMR) and infra-red spectroscopy (IR). The compounds were also analysed using electrochemical methods (cyclic voltammetry, square wave voltammetry and linear sweep voltammetry). Crystal structures of selected compounds were determined in this study.

3.2 Synthesis

3.2.1 Osmocenylmethanol

Osmocenylmethanol,**19**, the first alcohol in the series with $1 \leq n \leq 4$ (Figure 3.1) was synthesised in two steps, according to Scheme 3.1.

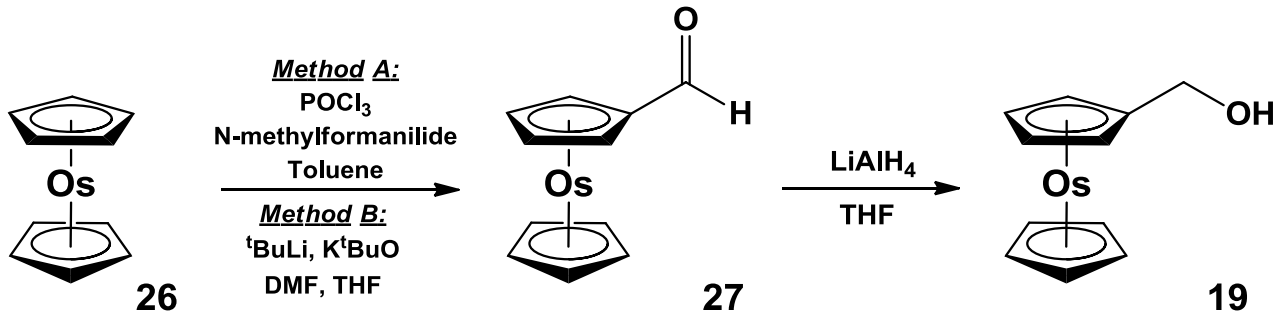

Scheme 3.1: Synthesis of osmocenylmethanol, 19.

Osmocenecarboxaldehyde, **27**, was used as a precursor in the synthesis of osmocenylmethanol, **19**. Osmocenecarboxaldehyde, **27**, was prepared by two different methods, Vilsmeier formylation and formylation by lithiation (Scheme 3.1). In method A, Vilsmeier formylation, osmocene, **26**, was treated with phosphorous oxychloride and *N*-methylformanilide, in toluene. Osmocenecarboxaldehyde, **27**, was isolated in 51.8% yield as a bright yellow powder. This method did not yield a di-formylated product.

In method B, formylation was achieved by lithiation of osmocene, **26**, with *tert*-butyllithium and potassium *tert*-butoxide in tetrahydrofuran at -78 °C. The lithiated osmocenyl species was then formylated with dimethylformamide. Both mono-formylated and di-formylated products were formed, but higher yields of osmocenecarboxaldehyde, **27**, were obtained (79.5% yield) as a bright yellow powder. The disubstituted product, osmocenedicarboxaldehyde, was obtained in 19.5% yield as a pale orange powder. Method B, lithiation of osmocene, is far more efficient than the Vilsmeier formylation (Method A), due to osmocene being activated by the formation of a lithiated complex. Due to this reactivity, both mono-substituted and di-substituted formylated products are

formed.[1] Separation of **27** from Method A (Vilsmeier Method) was achieved using column chromatography with hexane: diethyl ether (3:4) as eluent. The unreacted osmocene eluted first, followed by the bright yellow osmocenecarboxaldehyde, **27**, which can easily be seen on the column as it elutes. For the separation of **27** from Method B (lithiation), different solvents were used to elute each compound. Unreacted osmocene, **26**, was first eluted using *n*-hexane. The more polar osmocenecarboxaldehyde, **27** was eluted using pure dichloromethane. The most polar compound in the column, osmocenedicarboxaldehyde, **37** (a pale orange powder), was then eluted using a 1:1 mixture of dichloromethane and diethyl ether.

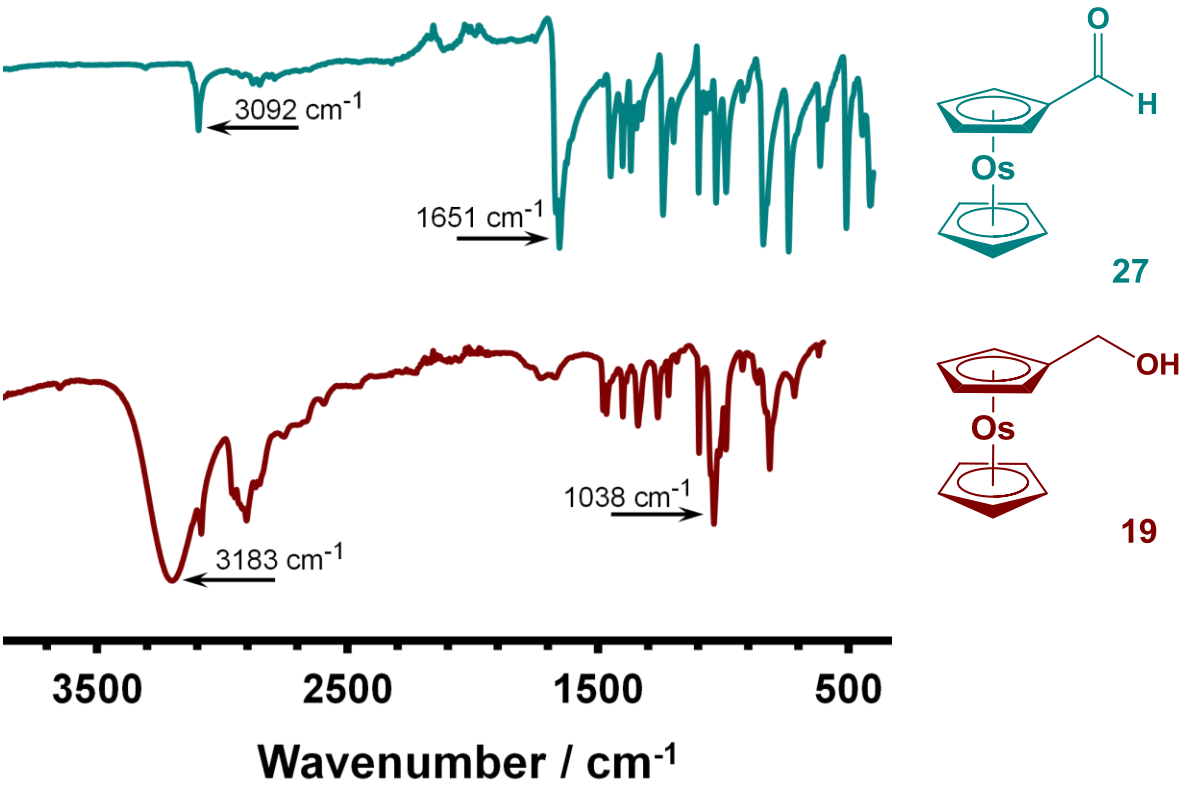

Figure 3.2: Infrared spectra of osmocenecarboxaldehyde, 27, and osmocenylmethanol, 19.

Osmocenylmethanol, **19**, was obtained by the reduction of **27** with lithium aluminium hydride in tetrahydrofuran. The white powder of **19** was isolated in 91.3% yield. Tetrahydrofuran instead of diethyl ether was used as reaction solvent due to its higher boiling point. This allowed the reaction to reflux for an hour at higher temperatures, without leading to issues of dryness of the reaction mixture, allowing the reaction to go to completion. The crude product was pure for analytical purposes.

The infrared spectra of **19** and **27** are shown in Figure 3.2. For osmocenecarboxaldehyde, **27**, the C=O stretching frequency is observed at 1651 cm^{-1} and the C-H aldehyde stretch at 3092 cm^{-1}. These peaks do not appear in the spectrum for osmocenylmethanol, **19**, which instead indicates the C-O stretching frequency at 1038 cm^{-1} and a broad O-H peak at 3183 cm^{-1}. This peak is very distinctive for alcohols, since broad O-H infrared peaks are seen due to hydrogen bonding.[2]

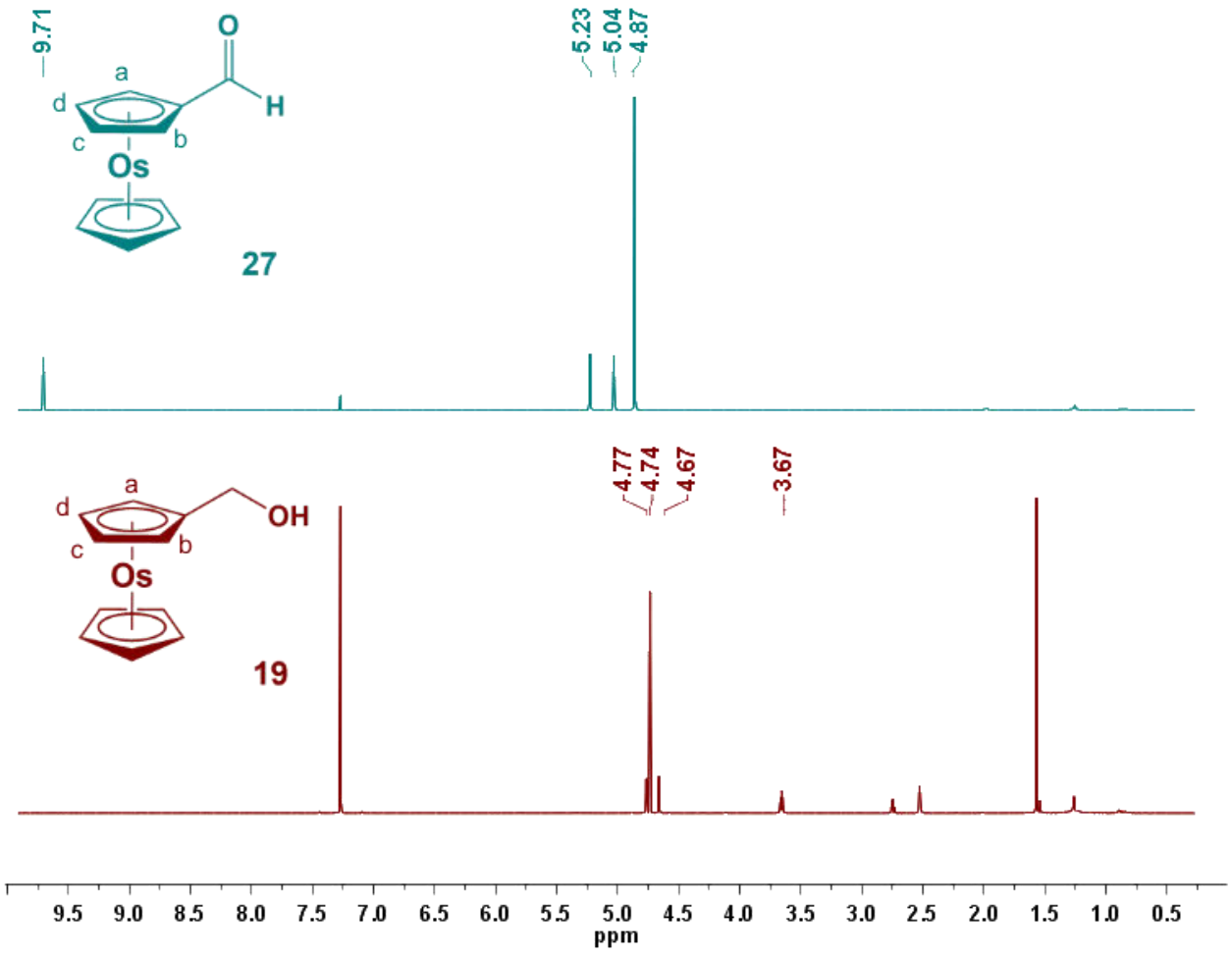

Figure 3.3: ^{1}H NMR spectra of osmocenecarboxaldehyde, 27, and osmocenylmethanol, 19.

The electronegative effects of the different osmocenyl substituents of **19** and **27** can be seen from the NMR spectrum of each compound shown in Figure 3.3. The carbonyl group of **27** is highly electron-withdrawing and this effect can be seen from the NMR spectra of **27**. The carbonyl group pulls electrons away from the aldehyde proton, which causes a large deshielding effect, causing the aldehyde proton to resonate at 9.71 ppm. The electron withdrawing effect of the carbonyl in **27** and the electron-donating effect of the methylene group in **19** are observed more prominently from the

NMR spectra of the substituted cyclopentadienyl rings on the osmocenyl group. The two sets of equivalent protons, labelled **a/b** and **c/d** in Figure 3.3 have different shielding/deshielding effects due to the substituents on **27** and **19**. The carbonyl group of **27** deshields **a/b** and **c/d**, whereby both of these appear downfield (5.23 ppm and 5.04 ppm respectively) as compared to the unsubstituted cyclopentadienyl ring at 4.87 ppm. The methylene group of **19** shields **a/b** and **c/d**, whereby **a** and **b** will be slightly more shielded than **c** and **d**. This is observed in the NMR of **19**, where **a** and **b** are at 4.67 ppm and **c** and **d** are at 4.77 ppm. The unsubstituted cyclopentadienyl ring, is observed at 4.74 ppm. This shows the electron-donating effect of the methylene group.

3.2.2 2-Osmocenylethanol

2-Osmocenylethanol, **20**, the second alcohol in the series with $1 \leq n \leq 4$ (Figure 3.1) was synthesised in five steps, according to Scheme 3.2.

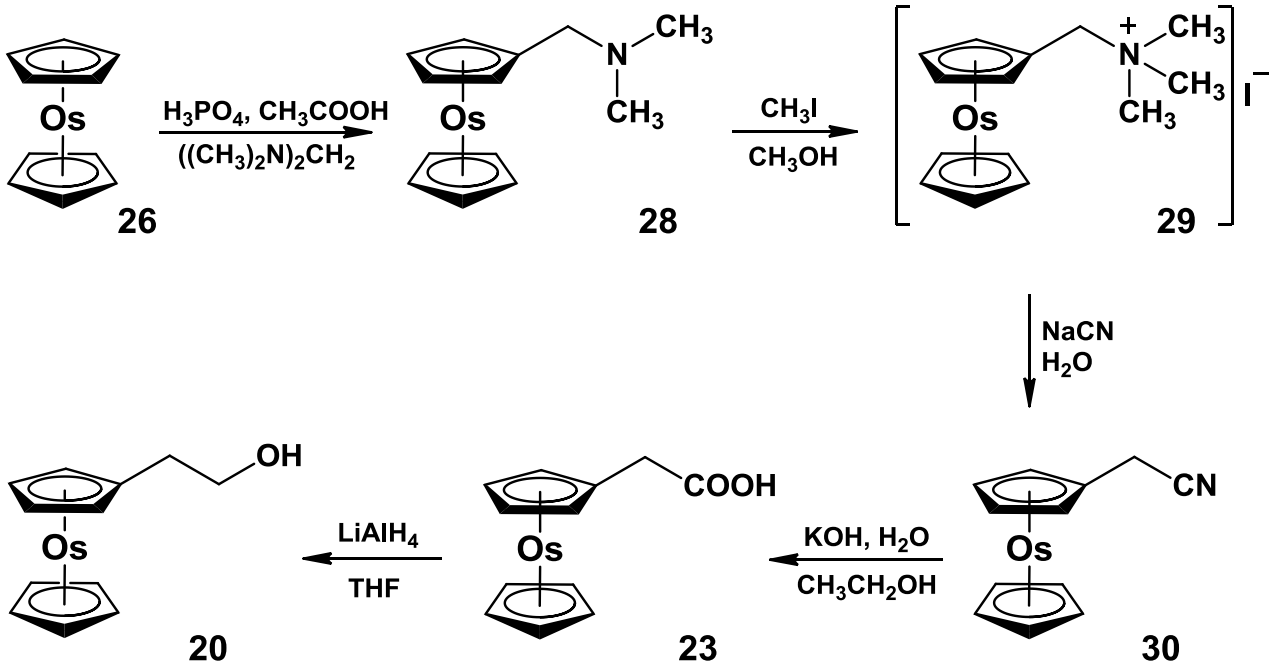

Scheme 3.2: Synthesis of 2-osmocenylethanol, 20.

N,N-dimethylaminomethyl osmocene, **28**, was synthesised by the Mannich reaction which utilises phosphoric acid, acetic acid and bis(dimethylamino)methane. The product, **28**, a white powder, was formed in 44.5% yield. This method was adapted for the less reactive osmocene, whereby the quantities of phosphoric acid, acetic acid and bis(dimethylamino)methane were used in a ten-fold excess, unlike that of the reaction with ferrocene.[3] The method of lithiation followed by reaction with Eschenmoser's salt, for the preparation of **28**, did not work for osmocene as described for ruthenocene in literature.[4] This could be due to the less soluble osmocene precipitating out of solution before the lithiated osmocene had enough time to react with the Eschenmoser's salt. It was observed that lithiated osmocene did not immediately precipitate out of solution when brought to room temperature, however, after 12 hours a white precipitate was seen which was the unreacted osmocene. Compound **28** is very unstable and could not be stored for 12 hours. It had to be reacted immediately with iodomethane to prepare **29**.

N,N,N-trimethylaminomethyl osmocene iodide, **29**, was then prepared from iodomethane in methanol solution, which yielded **29** quantitatively as a white powder. Compound **29** was also found to be unstable and decomposed overnight. It was therefore not purified, but used immediately in the following reaction. 2-Osmocenylacetonitrile, **30**, was synthesised using sodium cyanide in aqueous solution as the cyanation source. The product was obtained in 36.2% yield as a stable white crystalline powder. It was found from multiple reactions of preparing **28** and **29** that both of these compounds tend to decompose very quickly. For the preparation of these compounds to be done successfully, the reactions were done in quick succession of each other until obtaining 2-osmocenylacetonitrile, **30**, within one day. The crystal structure of **30** was solved, see Section 3.4.1. Hydrolysis of **30**, utilising potassium hydroxide and water in ethanol solution, yielded 44.2% of 2-osmocenylethanoic acid, **23** as white crystals. No further purification after normal aqueous workup (see Experimental 4.4.6.) was necessary. Separation of unreacted **30** was achieved by extraction of the reaction mixture, before acidification. The acidified mixture then allowed for separation of **23**. 2-Osmocenylethanol, **20**, was then formed by reduction of **23**, utilising lithium aluminium hydride in tetrahydrofuran solution. The white powder of **20** was isolated in 91.2% yield.

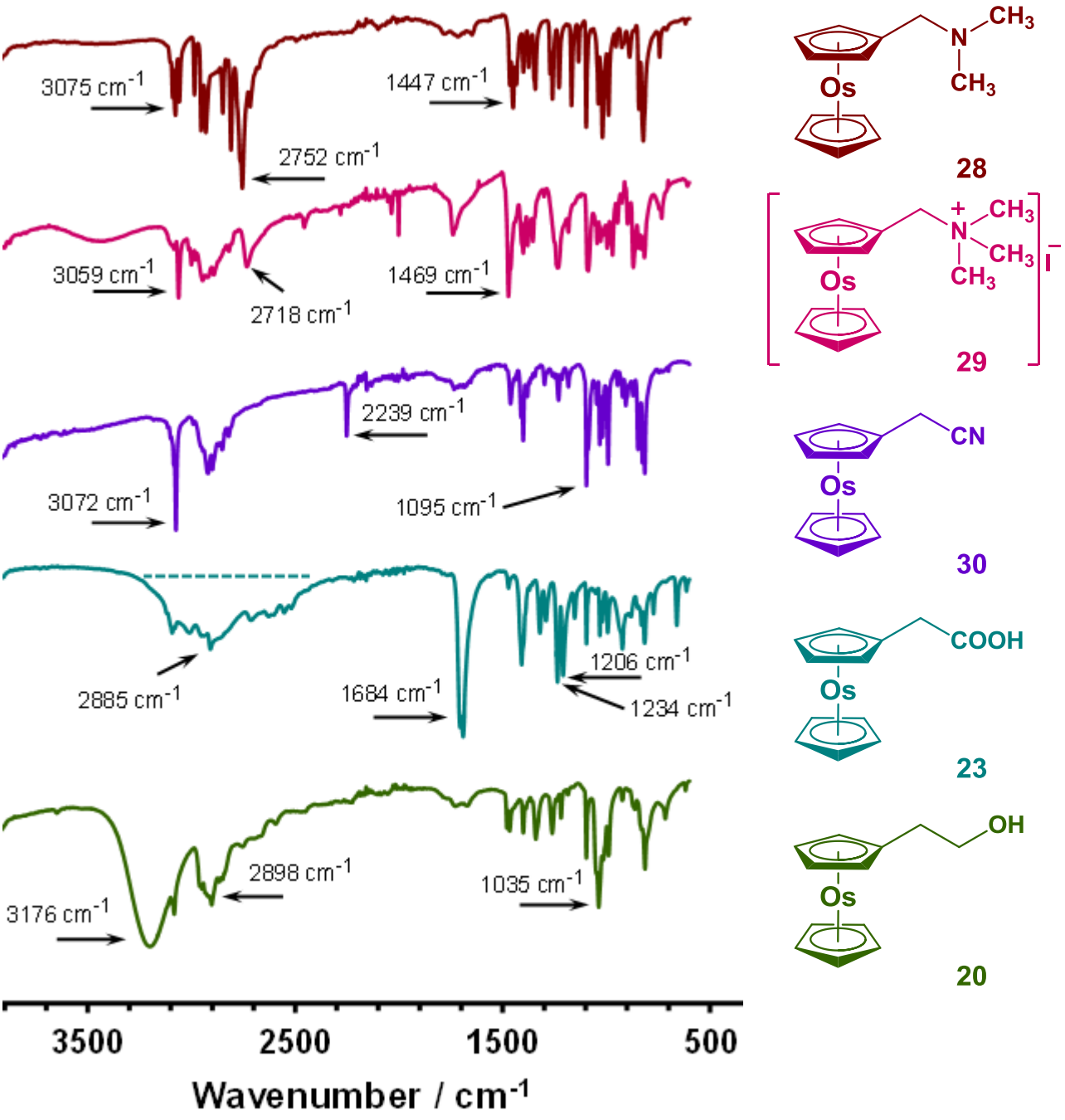

Figure 3.4: Infrared spectra of the series of osmocenyl intermediates required to synthesise the target molecule, 2-osmocenylethanol, 20.

The infrared peak assignments for *N,N*-dimethylaminomethyl osmocene, **28**, consist of CH_3 bending frequency signal at 1447 cm^{-1}, the aliphatic C-H stretches at 2752 cm^{-1} and the aromatic C-H stretches in the region of 3075 cm^{-1} (Figure 3.4). The peaks are seen to shift in *N,N,N*-trimethylaminomethyl osmocene iodide, **29**, due to the positive charge on the nitrogen atom.

The CH_3 peak for **29** is at 1469 cm^{-1}, which represents a shift of 22 wavenumbers from that observed for **28**. The CH_3 peaks in these two infrared spectra can be seen due to the CH_3 functionality being more prominent in the molecule than the other functional groups. The intensity of this peak is also seen to increase for the extra methyl group in **29**, compared to that of **28**. The aliphatic C-H stretch is at 2718 cm^{-1} and the aromatic C-H stretch is shown at 3059 cm^{-1}. The aromatic C-H stretch of **29** was shifted with 25 wavenumbers and the aliphatic C-H stretch with about 40 wavenumbers. The strong C≡N (nitrile) stretching vibration for the IR spectrum of **30** is observed at 2239 cm^{-1}. This peak then disappears in the IR spectrum of **23**, where a prominent C=O stretching vibration is observed at 1684 cm^{-1}. The broad OH vibration of the COOH functionality is found between 2500 and 3300 cm^{-1}. Bond vibrations for the C-O single bond of **23** can also be seen at 1206 cm^{-1} and 1234 cm^{-1}. The spectrum for **20** presents a distinctive broad peak for the O-H bond between 3000 and 3400 cm^{-1}, with the peak maximum at 3176 cm^{-1}. The C-O bond vibration for **20** is observed at 1035 cm^{-1}.

Figure 3.5 shows the osmocenyl fragments of the ^1H NMR spectra for **28** and **30**. The ^1H NMR for **28a** and **28b** were recorded in deuterated tetrahydrofuran as the NMR solvent and **30** was recorded in deuterated chloroform. A few drops of deuterated H_2SO_4 was added to **28a** and then the NMR spectrum was recorded, which then resulted in **28b**. The equivalent protons **a** and **b** for **28a** appear upfield at 4.63 ppm due to the electron-donating methylene group on the substituted cyclopentadienyl ring. The other equivalent protons, **c** and **d** are observed at 4.74 ppm and the singlet for the unsubstituted cyclopentadienyl ring is observed at 4.64 ppm. The positive nitrogen cation that results with the addition of H^+ causes the two triplets for **a/b** and **c/d** to shift further downfield.

This is due to the deshielding effect of the positive charge of the nitrogen atom (because the quaternary ammonium cation is a stronger electron-withdrawing group than the tertiary amine), which causes the electron-donation from the methylene group to stabilise this charge, rather than donating electrons back into the cyclopentadienyl ring. The protons **a/b** for **30** are pulled slightly upfield compared to that of **28b**, and are observed at 4.85 ppm. The unsubstituted cyclopentadienyl protons are at 4.78 ppm and **c/d** are at 4.70 ppm. The nitrile functionality deshields the substituted cyclopentadienyl ring, however, not to the same extent as the quaternary ammonium cation.

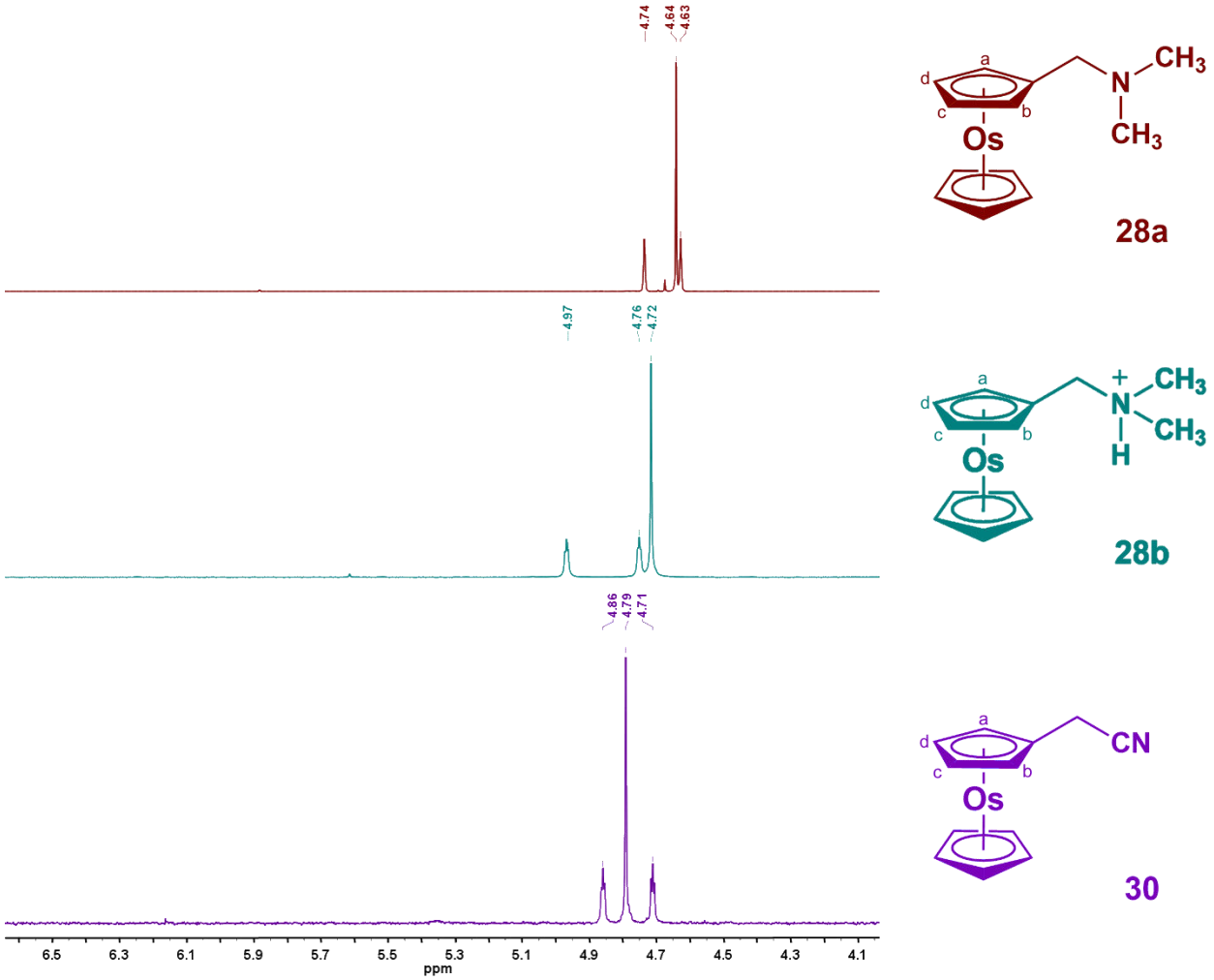

Figure 3.5: ^{1}H Spectra of osmocenyl fragments of *N,N*-dimethylaminomethylosmocene, 28a, *N*-hydrogen-*N,N*,-dimethylaminomethylosmocene cation, 28b and 2-osmocenylacetonitrile, 30.

3.2.3 3-Osmocenylpropanol

3-Osmocenylpropanol, **21**, the third alcohol in the series having n = 3 (Figure 3.1) was synthesised according to Scheme 3.3.

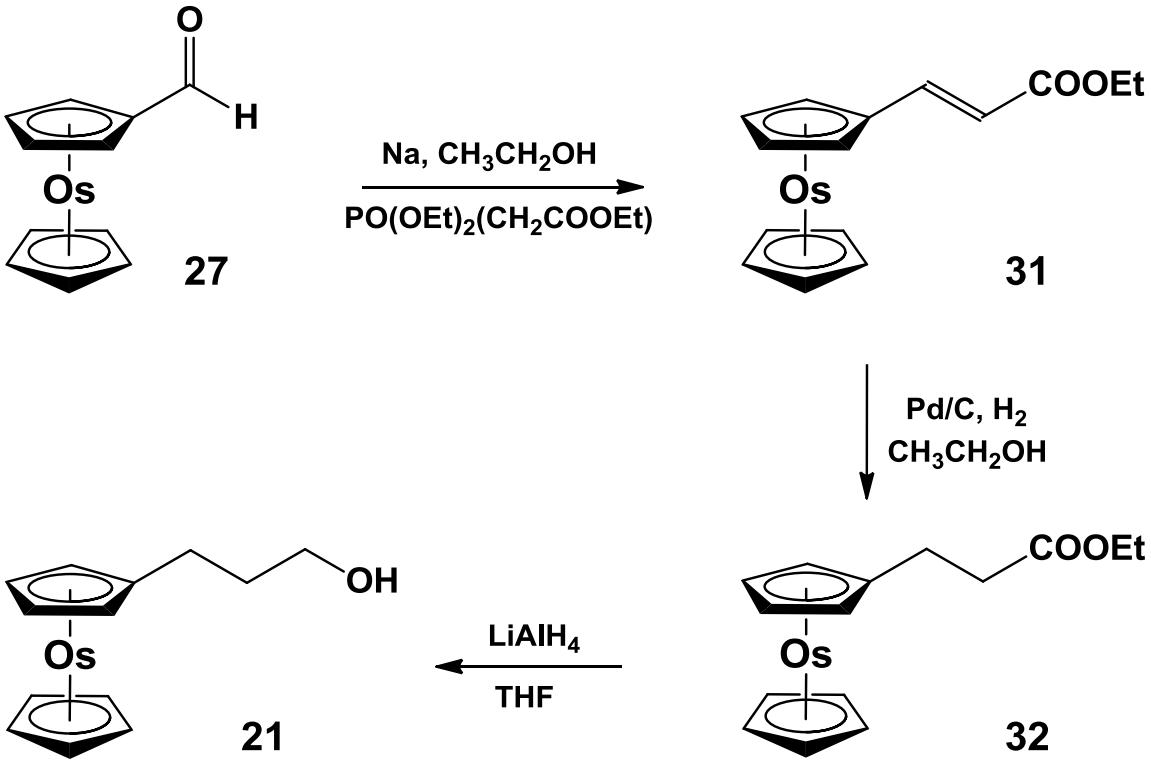

Scheme 3.3: Synthesis of 3-osmocenylpropanol, 21.

Ethyl-3-osmocenylethenoate, **31**, was prepared from osmocenecarboxaldehyde, **27**, using the Wittig reaction. Sodium ethoxide was formed *in situ* from sodium metal and ethanol, followed by formation of the phosphonium ylide utilising triethylphosphonoacetate. The product, **31**, was then formed by the addition of **27**, to yield 90.1% of a yellow powder. Compound **31** was purified using column chromatography with ethyl acetate and *n*-hexane (5:95) as eluent. Only one bright yellow band was observed in the column, which was **31**. No unreacted **27** was recovered. Hydrogenation of **31** was then achieved utilising a 5% palladium on carbon catalyst and hydrogen gas, in ethanol solution. The reaction was stirred in a hydrogen gas atmosphere for 15 hours. This reaction gave 70.2% yield of ethyl-3-osmocenylethanoate, **32**, as an off-white powder. Purification of **32** was achieved using column chromatography using *n*-hexane and diethyl ether (3:4) as eluent. Only **32** was eluted from the column, with impurities being left behind on the surface of the column. No

unreacted **31** was recovered. 3-Osmocenylpropanol, **21**, was then prepared by reduction of **32** utilising lithium aluminium hydride in tetrahydrofuran. The white powder of **21** was isolated in 93% yield.

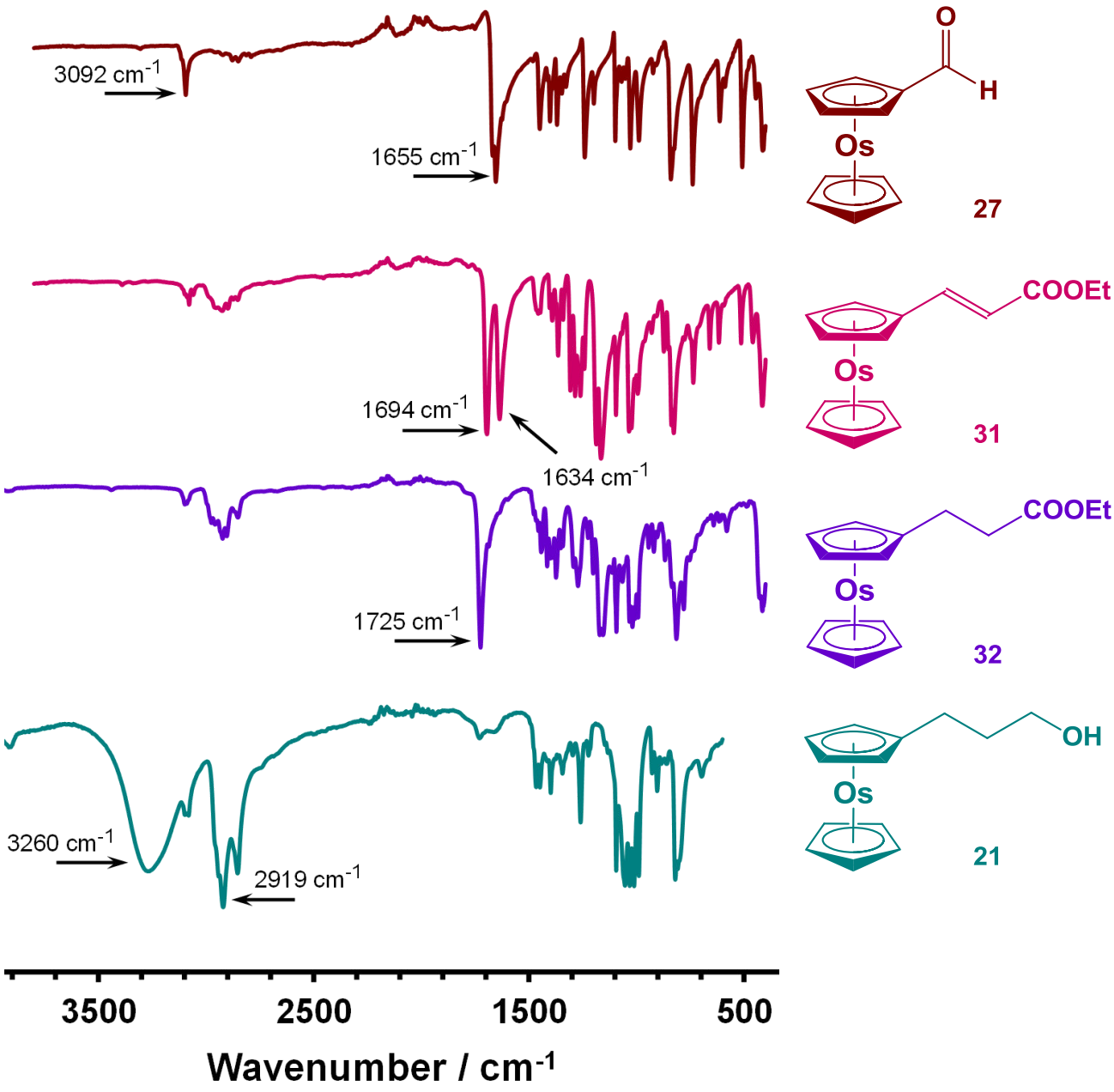

Figure 3.6: Infrared spectra of all osmocenyl derivatives used to reach the target molecule, 3-osmocenylpropanol, 21.

Figure 3.6 presents the infrared spectra for all the compounds synthesised in Scheme 3.3. The C=O stretching frequency shifts from 1655 cm^{-1} for **27** to 1694 cm^{-1} for **31**. The C=C double bond

vibration is observed at 1634 cm^{-1}. The assignment for C=O is made from the larger dipole moment of the carbonyl oxygen to that of the carbon-carbon double bond. This is because larger dipole moments have stronger infrared absorption peaks.[2] The delocalisation of electrons through the alkyl chain to the carbonyl group in **31** is removed in **32**, this results in a higher stretching frequency of 1725 cm^{-1} for the C=O vibration in **32**. The C=C bond is also no longer visible for **32**. The increase in methylene groups for **21** resulted in a stronger C-H stretching vibration at 2919 cm^{-1}. A broad hydrogen bonded O-H vibration is also observed at 3260 cm^{-1} for **21**. The C-O single bond vibration of the esters for **31** and **32** are observed at 1161 cm^{-1} and 1160 cm^{-1} respectively. However, for **21**, the C-O vibrations are observed between 1093 cm^{-1} and 987cm^{-1}.

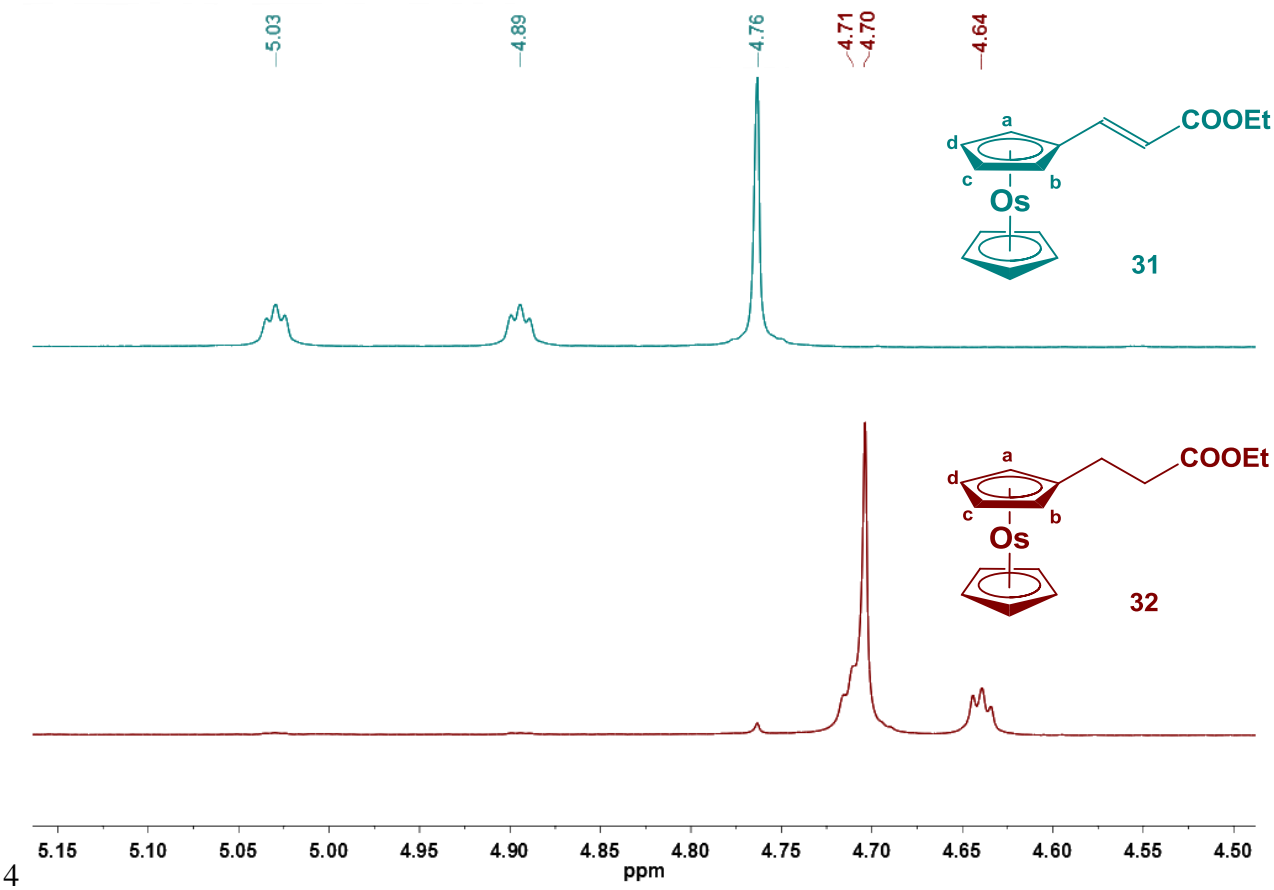

4

Figure 3.7: ^{1}H NMR spectra of osmocenyl fragments for ethyl-3-osmocenylethenoate, 31, and ethyl-3-osmocenylethanoate, 32.

Figure 3.7 presents the osmocenyl fragments of **31** and **32**, indicating the effect of electron donating and withdrawing substituents on the cyclopentadienyl ligands of osmocene, in the

presence and absence of conjugation. The electron withdrawing effects of the alkene and carbonyl substituents of **31** allow delocalisation of the electrons from the osmocenyl fragment, through to the carbonyl carbon. This effect will not be present in **32**, since the alkene moiety no longer exists for this compound. Evidence of this effect can be seen in Figure 3.7. The effect of the π-electron cloud of the alkene group of **31** as well as the C=O electron-withdrawing substituent of **31** deshields the protons on the cyclopentadienyl rings of osmocene. This causes protons **a** and **b** of **31** to resonate more downfield at 5.03 ppm, since they are closest to the substituted carbon on the ring. The triplet for **c** and **d** of **31** appears at 4.89 ppm. All protons on the unsubstituted cyclopentadienyl ring are equivalent and appear as a singlet at 4.76 ppm for **31**.

The electron-donating properties of the methylene groups on **32** can be observed in the ^{1}H NMR spectrum (Figure 3.7) when compared to the ^{1}H NMR signals of the protons on **31**. Both sets of proton signals on the substituted cyclopentadienyl ring of **31** are further upfield than those compared to the same protons of **32**. Protons **a** and **b** on **32** are further upfield (4.71 ppm) compared to that of **31** (5.03 ppm) and overlaps with the unsubstituted cyclopentadienyl protons at 4.70 ppm. The triplet of **c** and **d** of **32** appears at 4.64 ppm, which is much further upfield than that of the same protons in **31** which appear further downfield at 4.89 ppm. The electron-withdrawing effects of the substituents on **31** can also be seen from the osmocene core of the metallocenyl moiety, from the differences in shifts of the singlets of each compound. The singlet of **32** appears upfield (4.70 ppm) compared to that of the singlet of **31** (4.76 ppm).

3.2.4 3-Osmocenylpropanoic acid

3-Osmocenylpropanoic acid, **24**, was not only prepared as a precursor to 3-osmocenylpropanol, **21**. The ester (ethyl-3-osmocenylethanoate, **32**) was also prepared as a precursor to the carboxylic acid, 3-osmocenylpropanoic acid, **24**. Within the framework of this study, **33** was never reduced to **24** as **24** could easily be obtained from **32**.

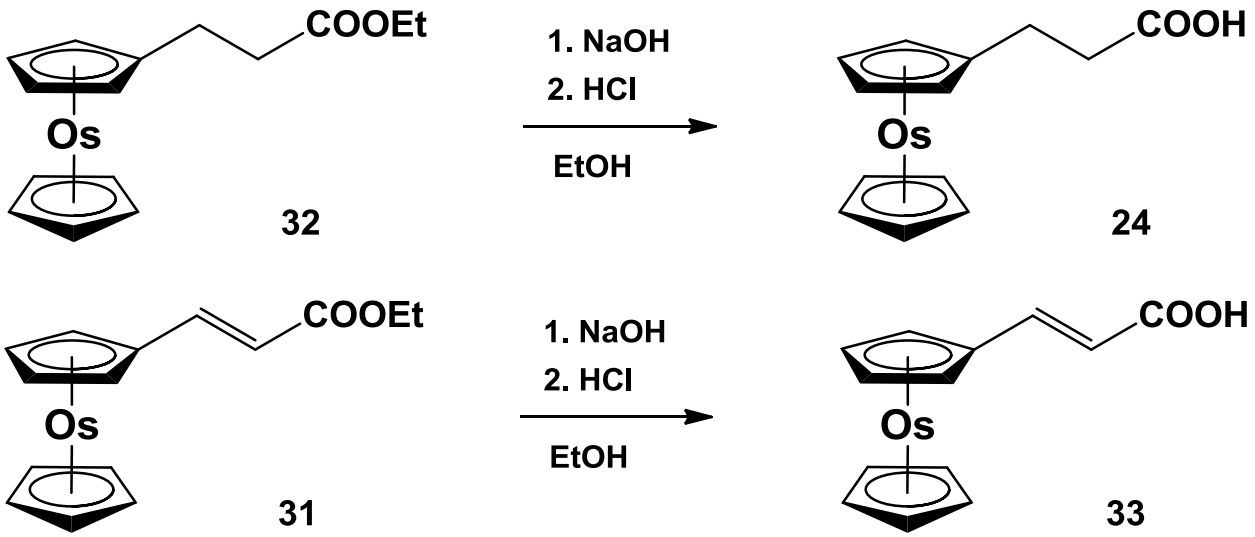

Scheme 3.4: Synthesis of 3-osmocenylpropanoic acid, 24, and 3-osmocenylpropenoic acid, 33.

Ethyl-3-osmocenylethanoate, **32**, was hydrolysed in the presence of sodium hydroxide to prepare 3-osmocenylpropanoic acid, **24**, in 56.8% yield as a yellow powder. The infrared spectrum of **24** (Appendix, Spectrum 32) has a C=O bond vibration at 1691 cm^{-1} and a broad peak at 2903 cm^{-1} which is distinctive for hydrogen bonded O-H vibrations of carboxylic acids. The same reaction conditions were used to hydrolyse ethyl-3-osmocenylethenoate, **31**, to 3-osmocenylpropenoic acid, **33**, in 60.3% yield as a yellow precipitate. The infrared spectrum of **33**, (Appendix, Spectrum 33) contains the C=C stretching vibration at 1617 cm^{-1} and the C=O stretching vibration at 1669 cm^{-1}. The carboxylic acid functionality can also be identified from the broad peak between 2400 and 3200 cm^{-1}, and having the vibration maximum at 2747 cm^{-1} as a result of the carboxylic acid O-H group. These broad peaks do not appear in the infrared spectrum of the ester derivatives of both these compounds, **31** and **32**, as shown in Figure 3.6.

3.2.5 4-Osmocenylbutanol

4-osmocenylbutanol, **21**, the last alcohol in the series having n = 4 (Figure 3.1) was synthesised in two steps, according to Scheme 3.6. The acylating agent required for the Friedel-Crafts acylation of osmocene was prepared according to known methods, as shown in Scheme 3.5.[5]

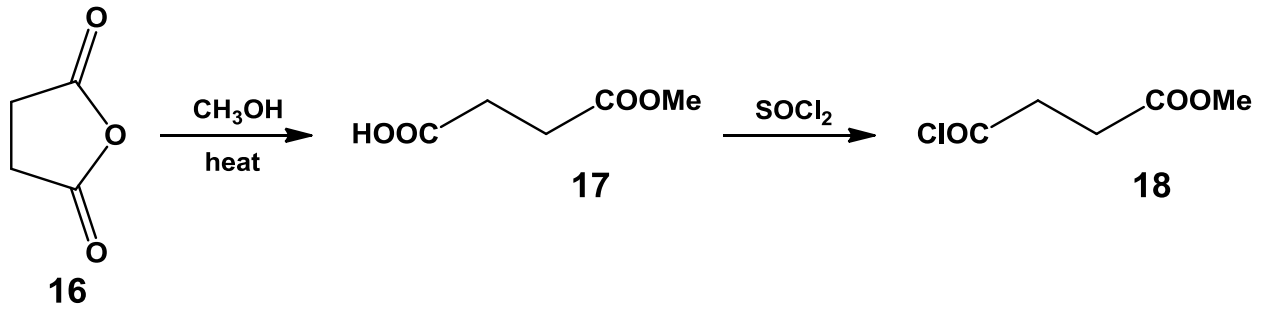

Scheme 3.5: Synthesis of 3-carbomethoxypropionyl chloride, 18, used as acylating agent of osmocene, 26.

To obtain 3-carbomethoxypropionyl chloride, **18**, succinic anhydride, **16**, was heated in excess methanol to form 3-carbomethoxypropionic acid, **17**, in 93.2% yield as a white solid. This product, **17**, was kept under vacuum to remove excess methanol, then immediately reacted with thionyl chloride. 3-carbomethoxypropionyl chloride, **18**, was then distilled at 65 °C and 3-5 mmHg to yield 84.5% of **18** as a colourless liquid. To prevent large scale decomposition of **18** during distillation, the oil bath was heated prior to the setup, and added to the distillation setup once the required vacuum was achieved. The acid chloride, **18**, was stored in a properly sealed flask under argon, away from light, to minimise fast decomposition. Compound **18** was observed to decompose slowly over time (2 months), while stored in this method. Over time the colour became darker, from colourless to beige to brown.

Friedel-Crafts acylation of osmocene, **26**, which utilised 3-carbomethoxypropionyl chloride, **18**, and aluminium trichloride in dichloromethane, produced methyl-3-osmocenoylpropanoate, **34**, in 8.83% yield as a pale yellow liquid. The conditions used for the preparation of **34** were extremely harsh compared to the conditions required for the Friedel-Crafts acylation of ruthenocene.[6] The catalyst, aluminium chloride, was used in 6-fold excess compared to that of the ruthenocene reaction in literature.[6] It was also observed that the longer the reaction time, the less product was

obtained. This could be due to decomposition of the product under these harsh conditions, at long reaction times. During one attempted synthesis of **34**, under the same conditions mentioned, half of the reaction mixture was worked up after refluxing for 6 hours, and the other half was worked up after refluxing for a further 16 hours. The first half of the reaction mixture yielded 4.92% of **34**, whereas the remaining reaction mixture yielded no product. The optimum reaction time was 16 hours, which resulted in the highest yield of 8.83%.

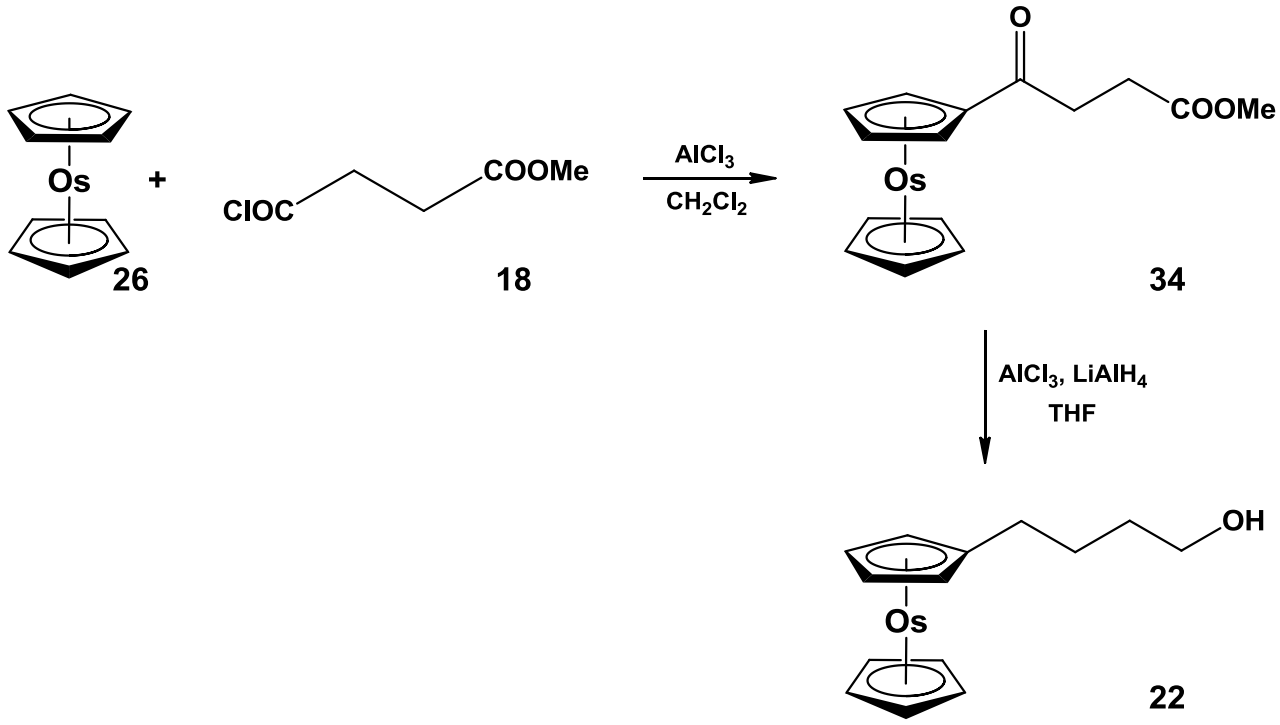

Scheme 3.6: Synthesis of 4-osmocenylbutanol, 22.

To achieve the reduction of **34** to 4-osmocenylbutanol, **22**, aluminium chloride and lithium aluminium hydride in tetrahydrofuran solution was utilised. This yielded 17.2% as an off-white powder. Unlike the reductions used for the preparation of **19**, **20**, and **12**, this reaction required two additional hours of refluxing. This was for the reduction of the keto carbonyl group of **34**, which was reduced using aluminium chloride.

Figure 3.8 presents the infrared spectra of the osmocene derivatives prepared in Scheme 3.6, methyl-3-osmocenoylpropanoate, **34**, and 4-osmocenylbutanol, **22**. The two carbonyl groups for **34** are observed at 1661 cm^{-1} (keto C=O) and 1724 cm^{-1} (ester C=O). The broad O-H bond vibration

for **22** is observed at 3336 cm^{-1}. The C-H bond stretches from the four methylene groups are also observed at 2927 cm^{-1}. The C-O single bond vibrations for **31** and **32** are observed at 1162 cm^{-1} and 1012 cm^{-1} respectively.

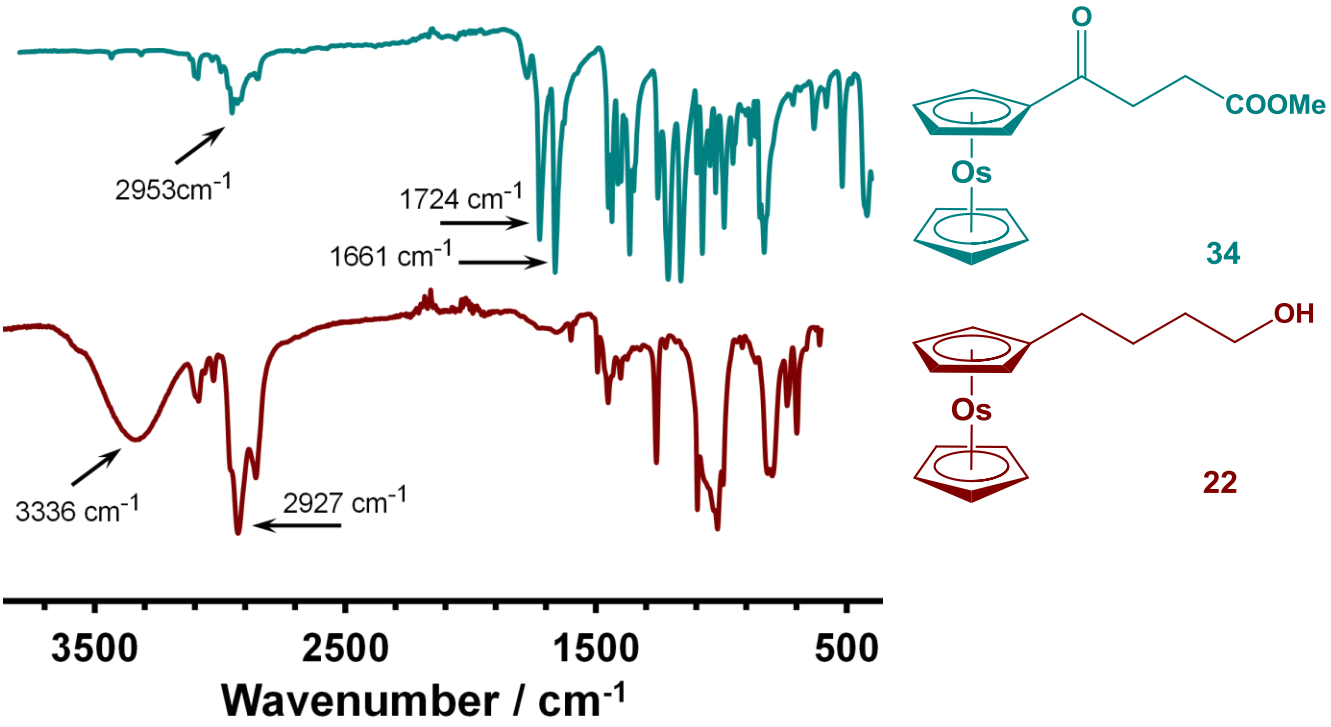

Figure 3.8: Infrared spectra of methyl-3-osmocenoylbutanoate, 34, and 4-osmocenylbutanol, 22.

3.2.6 4-Osmocenylbutanoic acid

The synthesis of 4-osmocenylbutanoic acid, **25**, required an altered synthetic route from the alcohol counterpart, **22**. The synthetic route can be seen in Scheme 3.7.

Clemmensen reduction was used to reduce the keto carbonyl of **34** to form methyl-4-osmocenylbutanoate, **35**, which yielded 45.6% of product. The zinc/mercury amalgam utilised in this reaction was freshly prepared using zinc granules and mercuric chloride, and was immediately used in the Clemmensen reduction reaction. The ester, **35**, was then hydrolysed in the presence of base to prepare 4-osmocenylbutanoic acid, **25**, in 34.5% yield. The product was precipitated in a cold acidic medium.

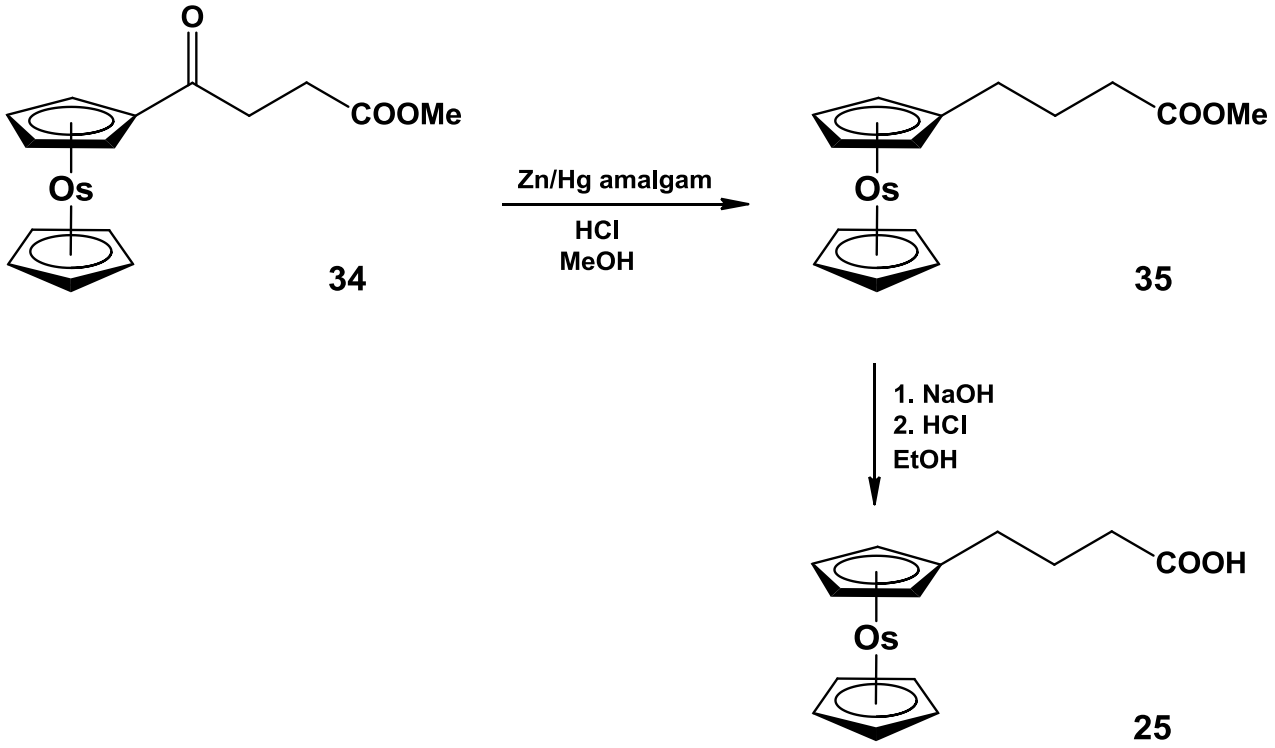

Scheme 3.7: Synthesis of 4-osmocenylbutanoic acid, 25.

Figure 3.9 presents the infrared spectra of the compounds involved in the synthesis of 4-osmocenylbutanoic acid, **25**, (Scheme 3.7). The reduction of the keto carbonyl of methyl-4-osmocenylbutanoate, **35**, can be confirmed by the disappearance of the peak at 1661 cm^{-1} leaving only the ester carbonyl bond vibration at 1734 cm^{-1}. Osmium(II), like iron(II) in ferrocene and ruthenium(II) in ruthenocene, is too stable to be reduced to osmium metal by the Zn/Hg amalgam. The infrared spectrum of 4-osmocenylbutanoic acid, **25**, contains a C=O bond vibration at 1702 cm^{-1}. The carboxylic acid functional group is seen by the broadening of the base of the C-H aliphatic stretch at 2920 cm^{-1}.

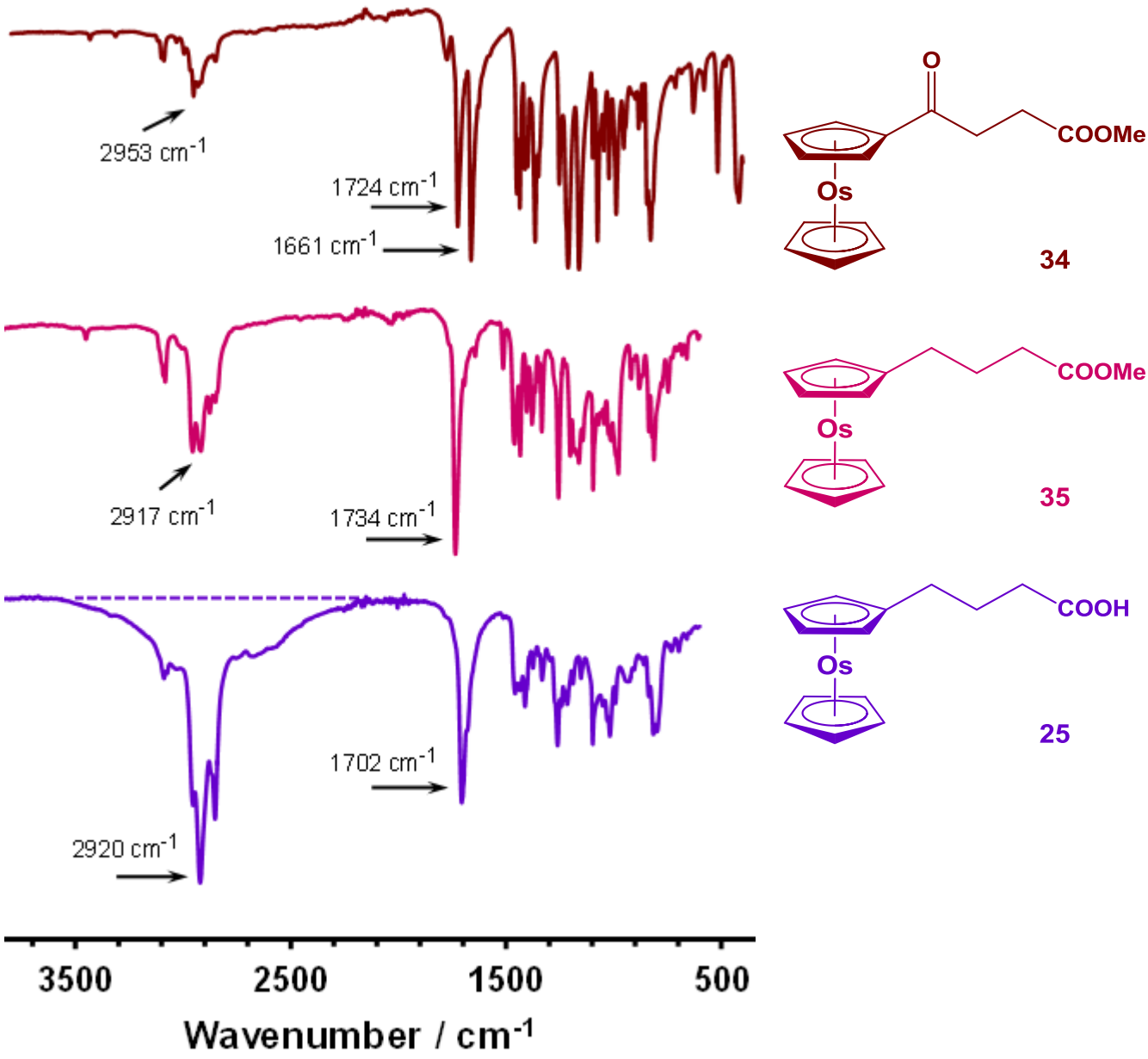

Figure 3.9: Infrared spectra of methyl-3-osmocenoylpropanoate, 34, methyl-4-osmocenylbutanoate, 35, and 4-osmocenylbutanoic acid, 25.

3.3 Cyclic voltammetry

Cyclic voltammetry was conducted on $Oc(CH_2)_mCOOH$, where m = 1, 2 and 3, and $Oc(CH_2)_nOH$, where n = 1, 2, 3 and 4, as per goals (iii) and (iv) in Chapter 1 respectively. The effect of the alkyl chain lengths (m and n) on the electrochemistry of osmocenyl carboxylic acid and alcohol derivatives were determined.

All compounds studied were dissolved in dichloromethane, in concentrations of 0.5 mmol dm^{-3}. All solutions contained $[NBu_4][B(C_6F_5)_4]$ as supporting electrolyte, in concentrations of 0.1 mol dm^{-3}. The electrochemical cell was composed of three electrodes, a platinum wire as the auxiliary electrode, a silver wire for the reference electrode and a glassy carbon working electrode. All compounds were referenced against Fc^*/Fc^{*+} (decamethylferrocene/decamethylferrocenium ion) as the internal standard, which has a formal reduction potential (E°′) of -615 mV. The voltammograms were then used to calculate the peak anodic potentials (E_{pa}), peak cathodic potentials (E_{pc}), peak anodic currents (i_{pa}), peak cathodic currents (i_{pc}), formal reduction potentials (E°′) and the ratio i_{pc}/i_{pa}. The electrochemical data for all osmocene derivatives synthesised in this study, including the osmocene-containing carboxylic acids and alcohols, obtained using cyclic voltammetry, is summarised in Table 3.1. The cyclic voltammetric measurements of **19**, **28** and **29** were done immediately after synthesis of these compounds, due to their instability.

3.3.1 Cyclic voltammetry of osmocene-containing carboxylic acids

Figure 3.10 shows the cyclic voltammograms of the osmocene-containing carboxylic acids synthesised in this study, 2-osmocenylethanoic acid, **23**, 3-osmocenylpropanoic acid, **24**, and 4-osmocenylbutanoic acid, **25**, with and without the internal standard (decamethylferrocene). Two reduction waves are observed from **23** and **24**, however the internal standard seems to overlap the second reduction wave of these compounds, and therefore the voltammograms without the internal standard are also presented.

The effect of an increasing number of CH_2 spacers can be seen electrochemically by observing oxidation waves of each compound. Formal reduction potentials, E°′, could not be used because of the weak or absent E_{pc} peaks for **23** and **24**. Compound **23** which contains one CH_2 spacer, has an E_{pa} of 445.5 mV at 100 mV/s scan rate. The E_{pa} values for **24** and **25** with two and three more CH_2 spacers, are 395.8 mV and 348.8 mV respectively, at 100 mV/s scan rate. Therefore, as the number

of CH_2 spacers increase between the osmocenyl moiety and the COOH moiety, the osmium becomes easier to oxidise. The CH_2 spacers decrease the electron withdrawing effect of the COOH moiety, from the osmocenyl moiety, making the compound easier to oxidise when the number of electron-donating CH_2 spacers is increased. This effect of the CH_2 spacers can also been seen on the reduction waves for **23**, **24** and **25**.

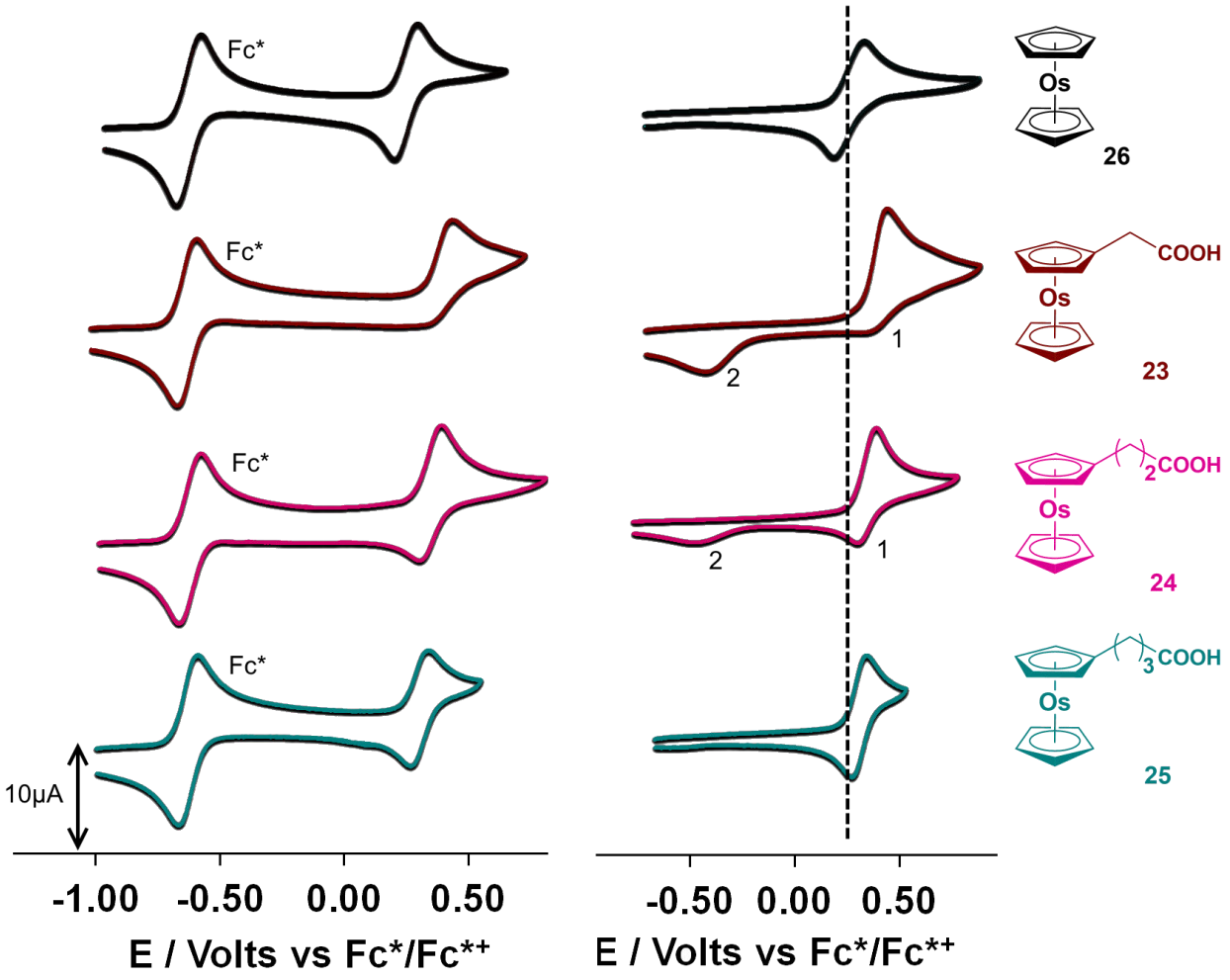

Figure 3.10: Cyclic voltammograms of 0.5 mmol dm^{-3} DCM solutions of 23 – 26 in the presence of $[NBu_4][B(C_6F_5)_4]$ at a scan rate of 100 mV/s. Cyclic voltammograms on the left contain the internal reference decamethylferrocene.

Two reduction waves are seen for **23**, the first at 380.7 mV and the second at -404.6 mV, for the 100 mV scan in Figure 3.10. Two reduction waves are also observed for **24**, the first at 314.3 mV and the second at -472.5 mV, for the 100 mV scan in Figure 3.10.

Both the solvent (DCM) and electrolyte ($[NBu_4][B(C_6F_5)_4]$) employed in these measurements are non-coordinating compounds, therefore the possibility for dimerisation of the reduced osmocenium species is favoured. This dimerisation effect can especially be enhanced when electron-withdrawing groups pull electrons away from the osmium core of the osmocenyl moiety. The dimer could be obtained either as a metal-metal dimer or a metal-cyclopentadienyl dimer. As the number of CH_2 spacers are increased in the osmocenyl carboxylic acid derivatives synthesised in this study, the second reduction wave disappears. This may be due to the diminished electron-withdrawing effect of the COOH moiety. Compound **25** only has one reduction wave and the system resembles one with electrochemical reversibility, where ΔE_p = 66.2 mV and i_{pc}/i_{pa} = 0.90. The possible dimerisation, similar to that of ruthenocene in literature, is observed electrochemically and depicted in Figure 3.11.[6] For osmocene, crystal structures of the equivalent osmocene dimers have been reported in literature by Taube *et al*.[7]

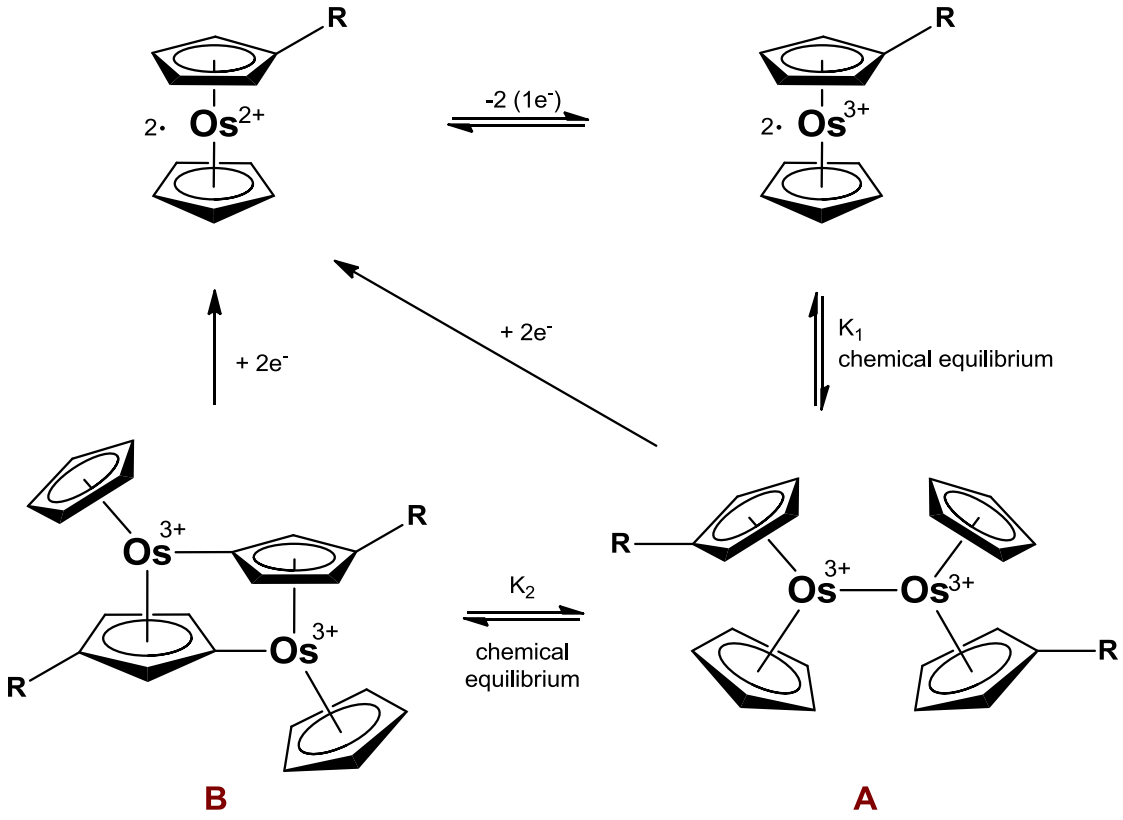

Figure 3.11: Expected dimerisation of osmocene derivatives due to the electrochemical oxidation of the osmocenyl core, where R = $(CH_2)_mCOOH$ with m = 1, 2 and 3, or R = $(CH_2)_nOH$ with n = 1, 2, 3 and 4.

The dimerisation effects depicted in Figure 3.11 can be seen electrochemically for **23** and **24** in Figure 3.10, from the two reduction waves of these compounds. The dimerisation of **23** is also observed at various scan rates (100, 200, 300, 400, 500 and 2000 mV/s) as depicted in Figure 3.12.

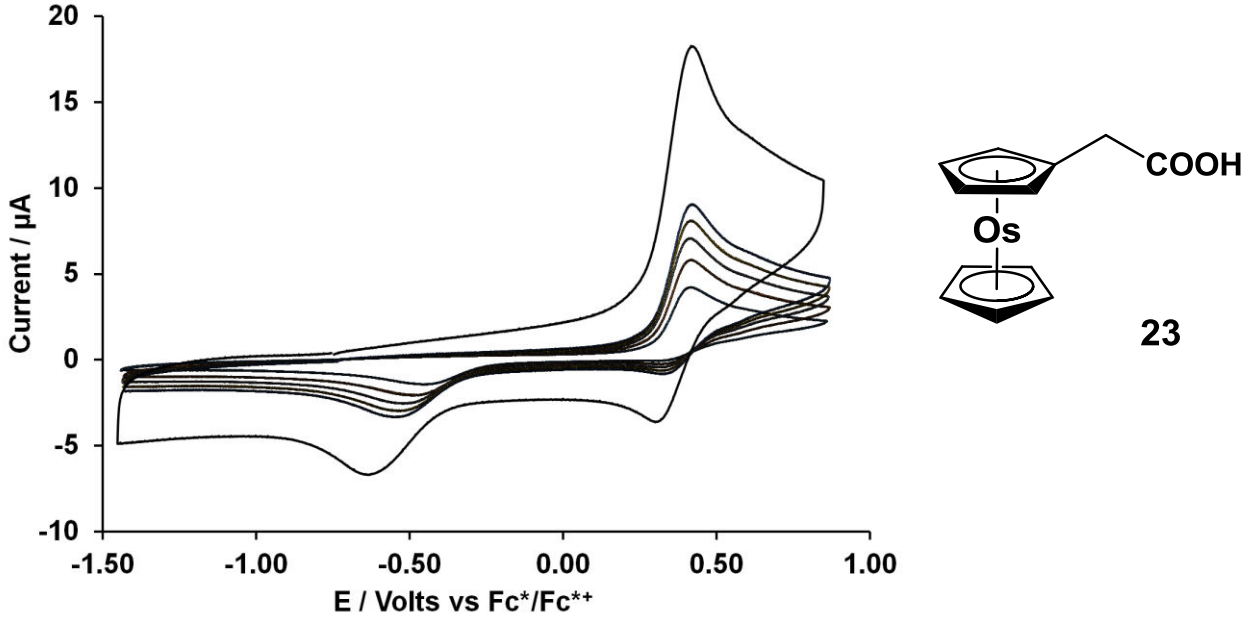

Figure 3.12: Cyclic voltammograms of 0.5 mmol dm^{-3} DCM solutions of 23 in the presence of [NBu$_4$][B(C$_6$F$_5$)$_4$] at scan rates 100, 200, 300, 400, 500 and 2000 mV/s, showing the effect of dimerisation by increasing scan rates.

The cyclic voltammograms of **23** are observed to have two reduction waves (380.7 mV and -404.6 mV for the 100 mV/s scan rate) for all the scan rates measured between 100 to 2000 mV/s). However, the i_{pc}/i_{pa} values for **23** increases slightly as the scan rate is increased (from 0.24 to 0.38). The increasing scan rate reduces the Os^{3+} in a quicker time frame, therefore decreasing the availability of Os^{3+} species for dimerisation. The same effect is seen for **24** but to a lesser extent, where the i_{pc}/i_{pa} increases from 0.73 to 0.78. The second reduction wave of **24** is much smaller than that of **23**, therefore the dimerisation is slower for **24** due to the extra CH_2 spacer in the alkyl chain, which stabilises the Os^{3+} species via electron-donation.

Figure 3.13 shows the relationship between the formal reduction potentials (E°´) and the number of CH_2 spacers, **m**, in the osmocenyl carboxylic acids synthesised in this study. The graph indicates that the formal reduction potentials decrease as the number of CH_2 spacers increase. This indicates that the osmocenyl moiety becomes easier to oxidise when more CH_2 (electron-donating groups) are present on the cyclopentadienyl ring. Since only three compounds were synthesised in this series, only a slight trend (due to the lack of enough data points) can be observed, which is shown by the solid trend line. Due to the time constraints of this study, the simplest osmocenecarboxylic

acid, Oc(COOH) with m = 0 was not synthesised. Once it has been obtained, it is expected that Figure 3.13 would assume a more hyperbolic shape with the inclusion of an m = 0 datapoint.

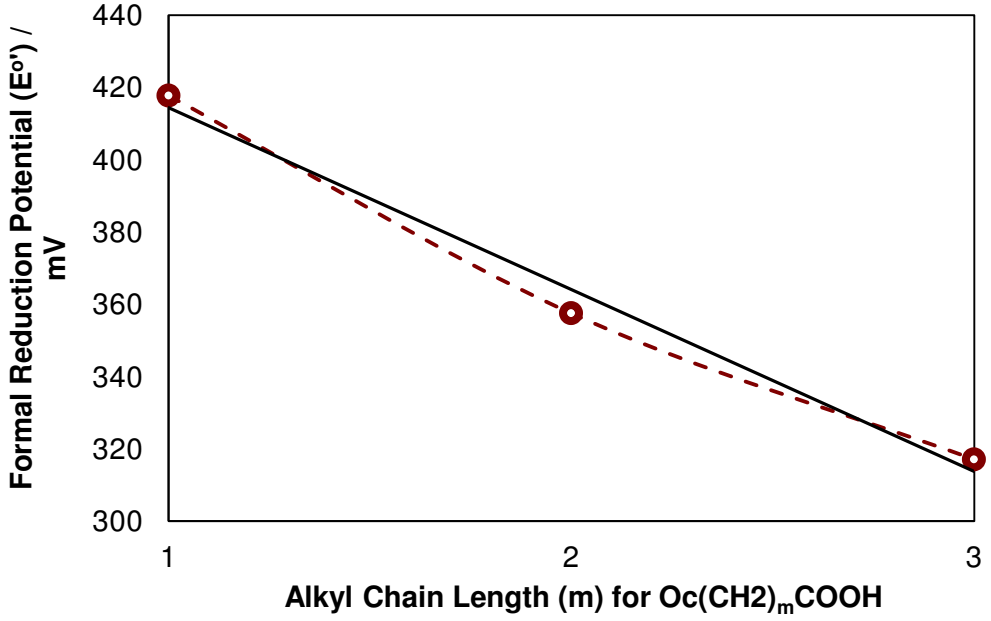

Figure 3.13: Relationship between formal reduction potentials and alkyl chain lengths, m, in osmocenyl carboxylic acids $Oc(CH_2)_mCOOH$.

3.3.2 Cyclic voltammetry of osmocene-containing alcohols

Figure 3.14 shows the cyclic voltammograms of the osmocene-containing alcohols that were synthesised in this study, osmocenylmethanol, **19**, 2-osmocenylethanol, **20**, 3-osmocenylpropanol, **21**, and 4-osmocenylbutanol, **22**, with and without the internal standard (decamethylferrocene).

As mentioned at the beginning of this section, the cyclic voltammetry of **19** was measured immediately after synthesis of the compound, due to its instability. However, from the voltammogram in Figure 3.14, decomposition of **19** is shown by the small peaks to the right of that of **19**. A second reduction wave is also not observed for **19**, which may be a result of its decomposition. Compounds **20** and **21**, however, do have two reduction waves, which may also be caused from dimerisation products, as those mentioned for the carboxylic acids in section 3.3.1.

An influence of increasing CH_2 spacers can also be observed for compounds **20**, **21** and **22**, from the disappearance of the second reduction wave. Compound **20** has an i_{pc}/i_{pa} of 0.47, which

increases to 0.96 for **21** and 0.94 for **22**. Compound **22** indicates that four CH_2 spacers between the osmocenyl moiety and the OH moiety, allows for both chemical and electrochemical reversibility.

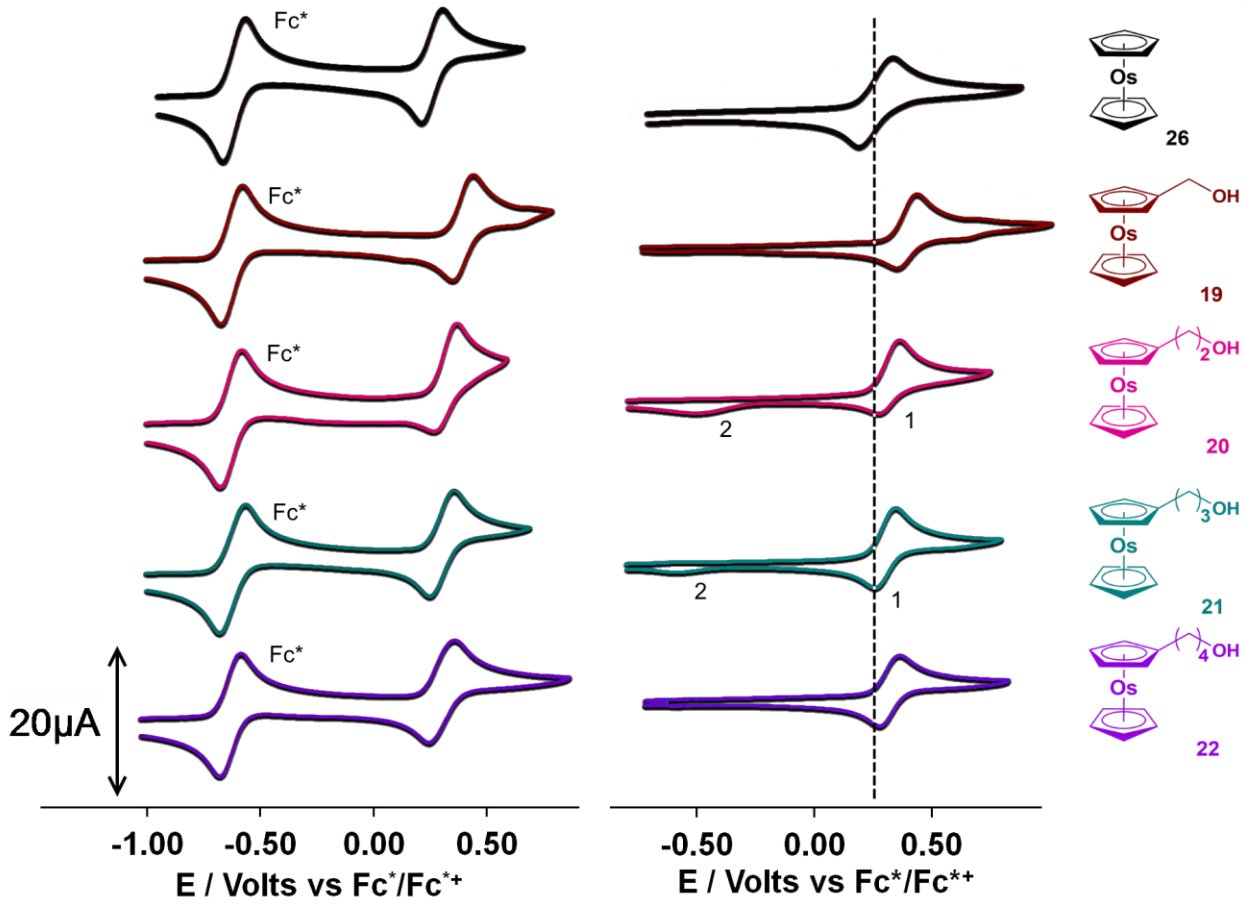

Figure 3.14: Cyclic voltammograms of 0.5 mmol dm^{-3} DCM solutions of 19 – 22 and 26 in the presence of $[NBu_4][B(C_6F_5)_4]$ at a scan rate of 100 mV/s. Cyclic voltammograms on the left are referenced against decamethylferrocene.

The cyclic voltammograms referenced against decamethylferrocene in Figure 3.14, show that the reduction waves are influenced by the addition of the internal standard. The first reduction waves of **19**, **20** and **21** are shown to have increasing Nernstian character when in the presence of decamethylferrocene (i.e. i_{pc}/i_{pa} are closer to 1 for wave 1 in the presence of decamethylferrocene). This may be due to decamethylferrocene promoting electron transfer properties between the osmocenium species and the electrode.

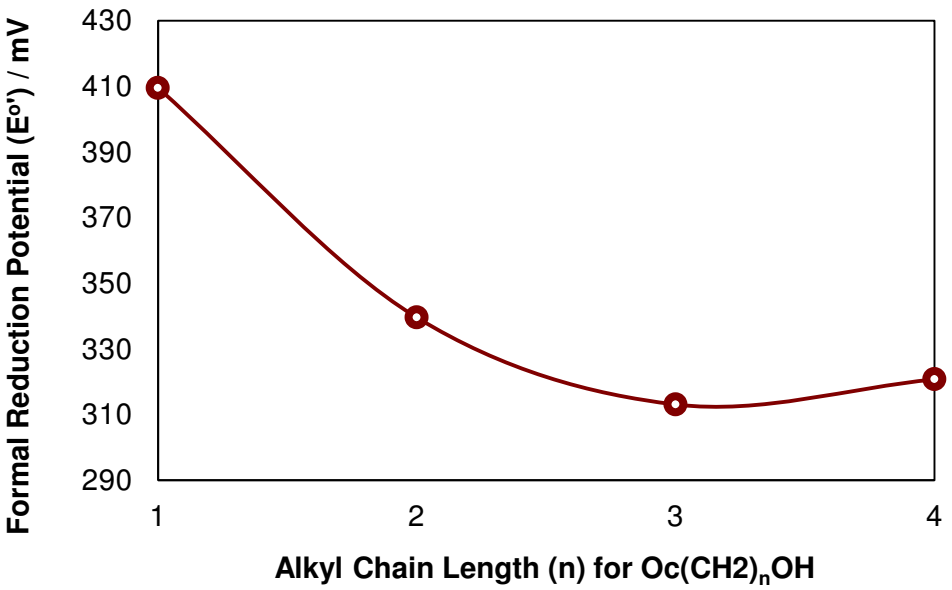

Figure 3.15: Relationship between formal reduction potentials and alkyl chain lengths, n, in osmocenyl alcohols $Oc(CH_2)_nOH$.

Figure 3.15 shows the relationship between the formal reduction potentials (E°´) and the CH_2 spacers, n, for the osmocenylalcohols synthesised in this study. The formal reduction potentials decrease dramatically for **19**, **20** and **21** with one, two and three CH_2 spacers respectively. For **22**, which has four CH_2 spacers, the potential increases again with a small amount (8 mV). One would expect that for a long chain derivative, E°´ should strive asymptotically to a constant potential (313 mV) or just less. The slight rise in potential of **22** (n = 4) is thus not regarded as significant. It is probably more associated with instrumental drift/accuracy.

The cyclic voltammograms of **31** and **32** are shown in Figure 3.16, in scan rates of 100, 200, 300, 400 and 500 mV/s. Compound **31** is comprised of an alkene and ester functionality, both of which are electron-withdrawing groups. Due to this effect, the electrons from the substituted cyclopentadienyl group are delocalised across the alkene to the carbonyl group of the ester. This conjugation effectively pulls electrons away from the osmium core, which destabilizes the Os^{3+} species and also makes it harder to oxidise. The effect of oxidation can be compared to that of the alkane counterpart, **32**, using the formal reduction potentials (E°´) of each compound. The formal reduction potential decreases from 490 mV for **31** to 341 mV for **32**, a difference of 149 mV. This large shift in the formal reduction potential is due to the absence of the double bond, which isolates

the osmocenyl moiety from the ester moiety in **32**. Therefore, the conjugation of electrons from the osmocenyl moiety to the ester moiety in **31** is not present in **32**. Instead, the opposite effect, electron-donation of the CH_2 group next to the osmocenyl moiety, dominates for **32**.

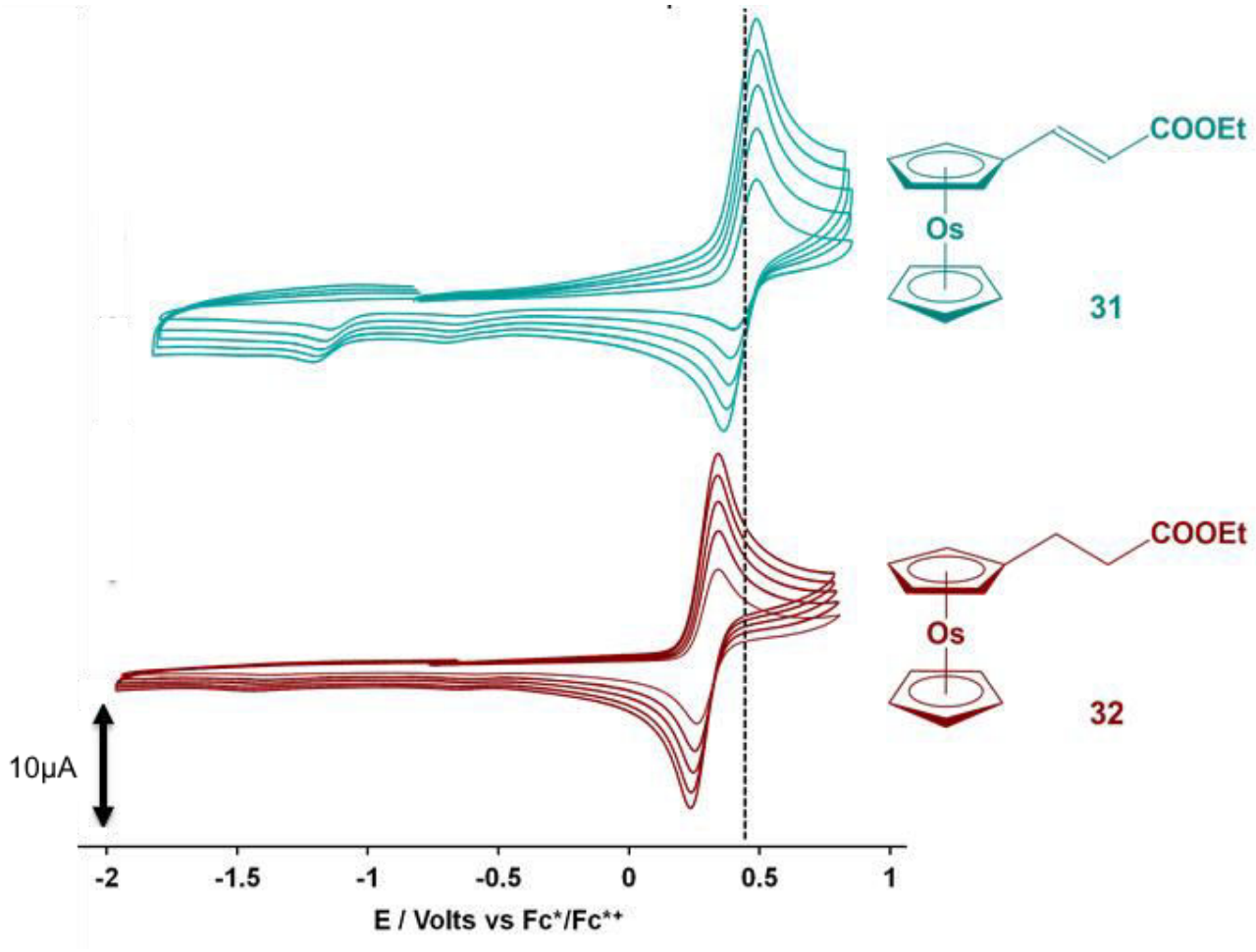

Figure 3.16: Cyclic voltammograms of 0.5 mmol dm^{-3} DCM solutions of ethyl-3-osmocenylethenoate, 31, and ethyl-3-osmocenylethanoate, 32, in the presence of $[NBu_4][B(C_6F_5)_4]$ at scan rates of 100, 200, 300, 400 and 500 mV/s.

The effect of dimerisation on the Os^{3+} species can also be seen for **31** and **32**. Additional reduction waves are observed for **31**. They are likely assignable to decomposition products resulting from the interaction of the oxidised Os^{3+} species with the alkene functionality. No additional reduction waves are present for **32**, since the alkane derivative of **31** has electron-donating CH_2 substituents, rather than CH=CH substituents. Instead, the i_{pc}/i_{pa} for **32** is 0.94, as compared to 0.63 for **31** for

the 100 mV/s scan rate. Therefore, the CH_2 groups on **32** allow for its electrochemistry to have more Nernstian character, compared to that of the alkene substituent.

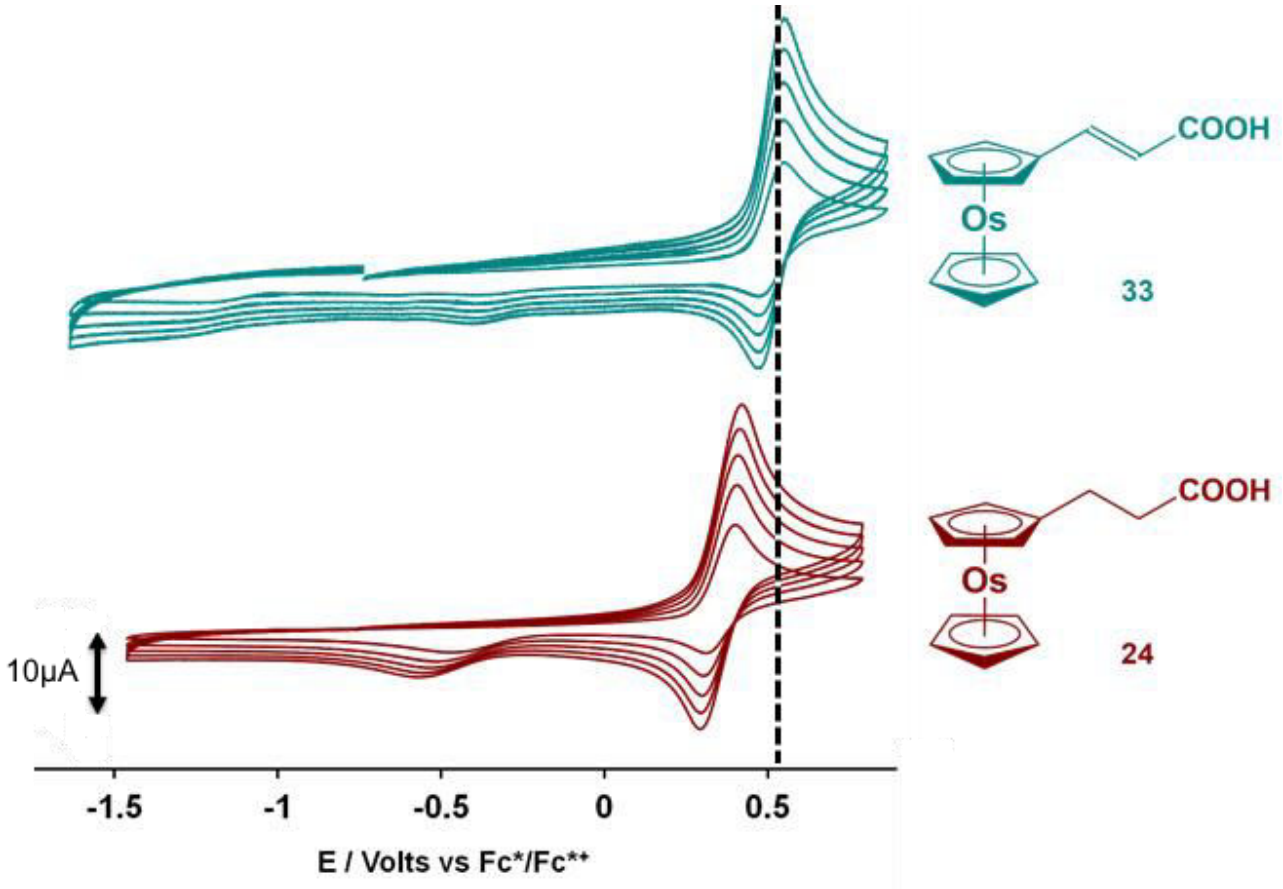

Figure 3.17: Cyclic voltammograms of 0.5 mmol dm^{-3} DCM solutions of 3-osmocenylpropenoic acid, 33, and 3-osmocenylpropanoic acid, 24, in the presence of $[NBu_4][B(C_6F_5)_4]$ at scan rates of 100, 200, 300, 400 and 500 mV/s.

Figure 3.17 shows the cyclic voltammograms of **33** and **24** which were prepared from their ester counterparts, **31** and **32**, in Figure 3.16. The effect of the delocalisation of electrons on the alkene can be seen by the formal reduction potential of **33** when compared to **24**. The value shifts from 510 mV for **33** to 357 mV for **24**, which is a large difference of 153 mV. Compound **33** is harder to oxidise due to the reduced electron density at the osmium core, which is caused by the delocalisation of electrons through the carbon double bond chain to the carboxylic acid moiety. This is not the case for **24**, therefore the osmium is easier to oxidise, which is seen by a smaller formal reduction potential. The esters (**31** and **32**) and acids (**33** and **24**) show a similar difference in the shifts of the formal reduction potentials, which are 149 mV and 153 mV respectively. The

ethyl group on the esters (**31** and **32**) may assist in the very slight difference between this shift, since it donates electrons to the adjacent carbonyl, whereas the hydrogen in the acid counterparts (**33** and **24**) do not have this ability.

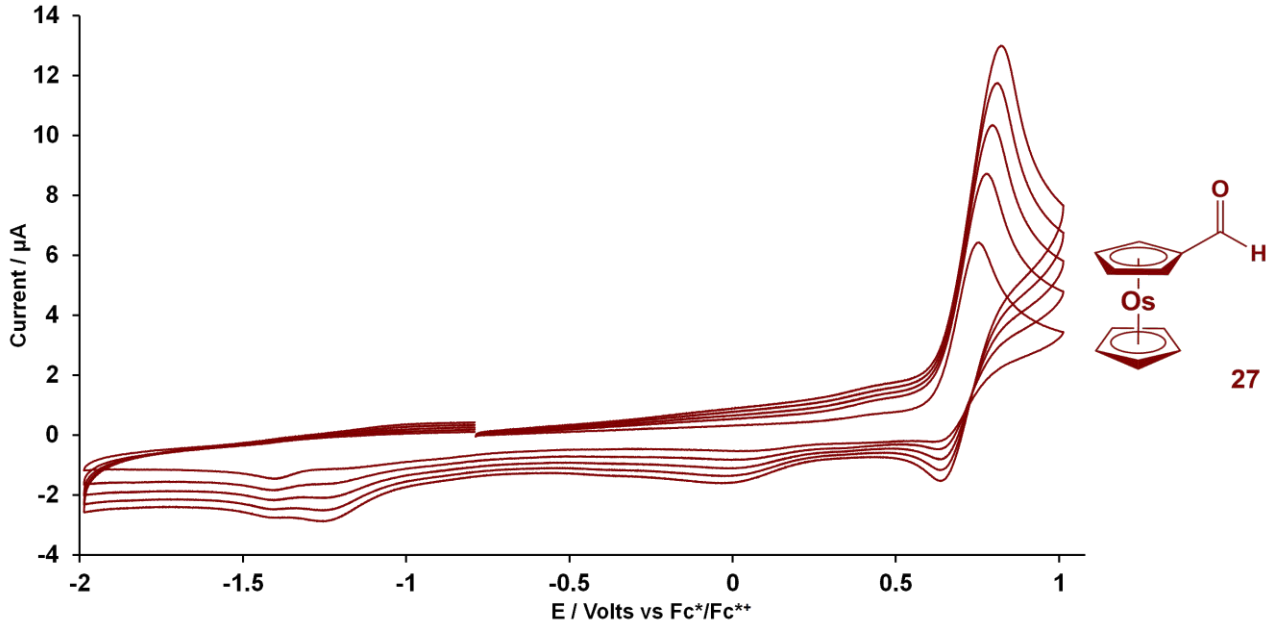

Figure 3.18: Cyclic voltammograms of 0.5 mmol dm^{-3} DCM solutions of osmocenecarboxaldehyde, 27, in the presence of [NBu$_4$][B(C$_6$F$_5$)$_4$] at scan rates of 100, 200, 300, 400 and 500 mV/s.

The cyclic voltammogram of osmocenecarboxaldehyde, **27**, are shown in Figure 3.18. Compound **27** does not exhibit chemical reversibility due to the i_{pc}/i_{pa} having a value of 0.29 for the 100 mV/s scan rate. As the scan rates are increased, the redox behaviour of **27** becomes slightly more chemically reversible, since the i_{pc}/i_{pa} value increases to 0.39 for the 500 mV/s scan rate. The ΔE_p for the 100 mV/s scan rate is 95.6 mV, which also indicates that it is only electrochemically quasi-reversible. Dimerisation products are also visible for **27** due to the formation of multiple reduction waves. Dimerisation of **27** is possible because of the aldehyde moiety on the compound, which is a very strong electron-withdrawing group. The electron poor environment around the osmium core may then allow for dimerisation of the Os^{3+} cation with other Os^{3+} species or cyclopentadienyl ligands, like that described in Figure 3.11. This electron-withdrawing effect of the carbonyl aldehyde also makes the osmium harder to oxidise, whereby **27** has a formal reduction potential of 683 mV.

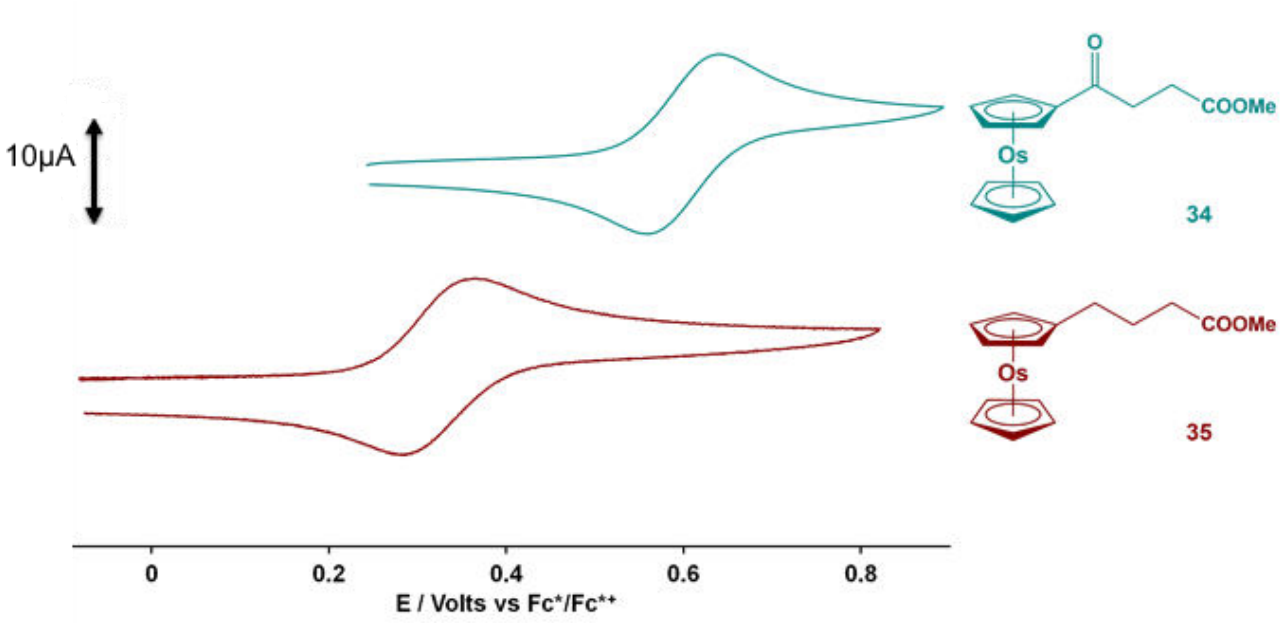

Figure 3.19: Cyclic voltammograms of 0.5 mmol dm^{-3} DCM solutions of methyl-3-osmocenoylpropanoate, 34, and methyl-4-osmocenylbutanoate, 35, in the presence of $[NBu_4][B(C_6F_5)_4]$ at scan rate 100 mV/s.

The cyclic voltammograms of **34** and **35** are presented in Figure 3.19, at 100 mV/s scan rate. Both compounds exhibit chemical reversibility, as their i_{pc}/i_{pa} values are 0.92 and 0.99 respectively, for the 100 mV/s scan rate. Both compounds also exhibit electrochemical reversibility, since their ΔE_p values are 83.4 mV and 76.4 mV respectively, also for the 100 mV/s scan rate. The change in the functionalisation of **34** and **35**, however, is highlighted electrochemically by their formal reduction potentials. The influence of the keto carbonyl in **34** in withdrawing electrons from the osmocenyl moiety, is observed by a formal reduction potential of 597 mV. Compound **35**, however, has a much lower formal reduction potential of 324 mV (a difference of 273 mV), due to the presence of three methylene groups, which donate electrons into the osmocenyl moiety. The keto carbonyl of **34** does not cause as large a shift as that of the aldehyde carbonyl of **27** (Figure 3.18). The two methylene groups next to the keto carbonyl of **34** may contribute to this observation as they donate electrons to the carbonyl, which makes the withdrawal of electron-density from the osmocenyl moiety by the carbonyl of **34** far less than that in **27**. Also, the large difference in the formal reduction potentials of **34** and **35** (a value of 273 mV) may be due to the electron-donating influence of the three methylene groups.

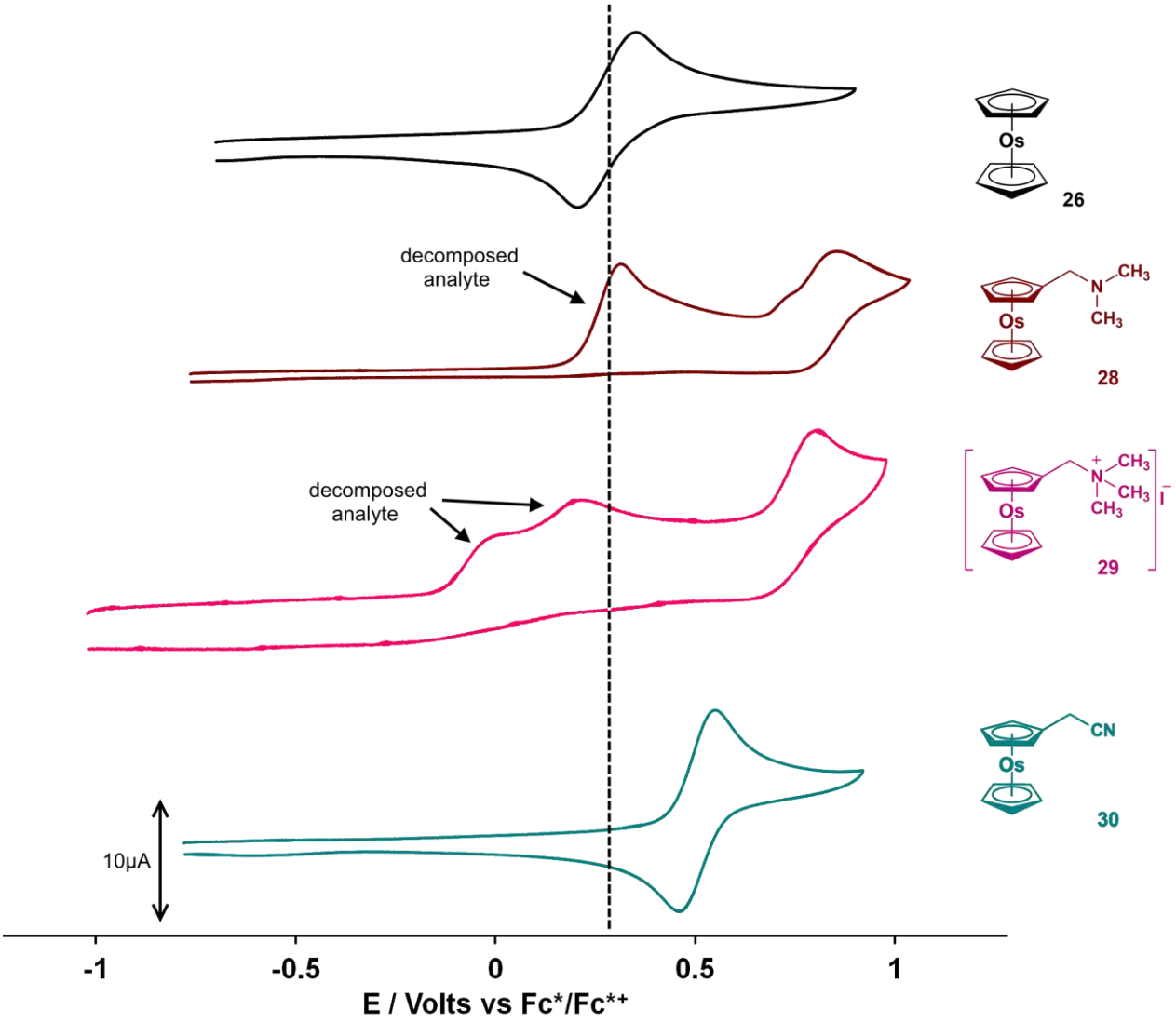

Figure 3.20: Cyclic voltammograms of 0.5 mmol dm^{-3} DCM solutions osmocene, 26, *N,N*-dimethylaminomethylosmocene, 28, *N,N,N*-trimethylaminomethylosmocene iodide, 29 and 2-osmocenylacetonitrile, 30, in the presence of $[NBu_4][B(C_6F_5)_4]$ at scan rate 100 mV/s. The peaks labelled "decomposed analyte" may be due to the instability of the analyte (100% decomposition within hours). They are not associated to decomposition as a result of the electrochemical experiment itself.

The cyclic voltammograms of **28**, **29** and **30** are presented in Figure 3.20, along with a comparison of the CV of osmocene, **26**. Cyclic voltammetry measurements for **28** and **29** were performed immediately after synthesis of these compounds, however, decomposition (due to the very short shelf-life of both compounds) can be seen electrochemically by the additional oxidation peaks present. The onset of reduction for **28** and **29** is observed for the reverse scan at 893 mV and 822 mV respectively. This is used to identify the peaks for **28** and **29**. However, both **28** and **29** are not electrochemically reversible, due to their ΔE_p values (122 mV and 131 mV respectively for 100 mV/s scan rate) being greater than 90 mV. The cyclic voltammetry of **30** exhibits both chemical and electrochemical reversibility, having a ΔE_p of 91 mV and i_{pc}/i_{pa} of 0.83. The formal reduction potentials for **28** and **29** (772 mV and 723 mV) are considerably higher than that of osmocene, **26**, however, **30** has a lower formal reduction potential of 506 mV. The stability of **30** and the delocalisation of electrons from the nitrile moiety to the osmocenyl moiety allows for a chemically and electrochemically reversible voltammogram.

Table 3.1: Cyclic voltammetry data (potentials versus Fc^*/Fc^{*+}) at a glassy carbon electrode of 0.5 mmol dm^{-3} solutions of osmocene derivatives in dichloromethane containing 0.1 mol dm^{-3} $[NBu_4][B(C_6F_5)_4]$ as the supporting electrolyte.

	Scan rate	E_{pa} / mV	E_{pc} / mV	ΔEp / mV	$E^{o'}$ / mV	i_{pc} / µA	i_{pa} / µA	i_{pc}/i_{pa}	Oxidation 2		Oxidation 3	
									E_{pa} 2 / mV	i_{pa} 2 / µA	E_{pa} 3 / mV	i_{pa} 3 / µA
Osmocene	100	315	225	90	270	1.3	1.3	1.01				
	200	329	220	109	275	1.8	1.8	1.01				
	300	335	216	119	276	2.2	2.3	0.96				
	400	341	206	135	274	2.6	2.4	1.05				
	500	343	195	148	269	2.9	2.7	1.06				
Average					273			1.02				
$Oc(CH_2)NMe_2$, **28**	100	822	700	122	761	6.4	5.2	1.22	289	10.55		
	200	835	703	132	769	8.9	7.2	1.24	303	13.49		
	300	842	704	138	773	10.6	8.6	1.23	315	16.62		
	400	850	705	145	778	11.2	9.7	1.16	328	20.75		
	500	852	705	147	779	11.9	10.5	1.14	337	23.77		
Average					772			1.20				
[Oc(CH2)NMe3]I, **29**	100	784	653	131	719	1.4	2.8	0.50	-69.7	1.70	195.6	0.83
	200	799	633	166	716	1.5	3.9	0.38	-55.0	2.46	196.8	0.99
	300	809	632	177	721	1.6	4.6	0.35	-36.7	2.92	210.3	1.03
	400	818	635	183	727	1.4	5.1	0.27	-25.7	3.46	217.6	1.15
	500	824	638	186	731	1.2	5.6	0.21	-12.2	3.88	228.6	1.20
Average					723			0.34				
$Oc(CH_2)CN$, **30**	100	549	458	91	504	9.8	11.8	0.83				
	200	559	452	107	506	14.7	16.4	0.90				
	300	566	446	120	506	18.0	19.9	0.90				
	400	571	440	131	506	20.5	22.7	0.90	Reduction 2			
	500	576	438	138	507	22.8	25.3	0.90	E_{pc} 2 / mV	i_{pc} 2 / µA		
Average					506			0.89				
$Oc(CH_2)COOH$, **23**	100	445.5	380.7	64.8	413	1.1	4.6	0.24	-404.6	0.99		
	200	451.8	378.9	72.9	415	1.5	4.9	0.30	-433.0	1.44		
	300	460.8	378	82.8	419	1.9	6.1	0.32	-459.3	1.79		
	400	462.6	377.1	85.5	420	2.4	7.0	0.34	-478.7	2.08		
	500	467.1	374.4	92.7	421	2.9	7.7	0.38	-491.2	2.18		
Average					418			0.32				
$Oc(CH_2)_2OH$, **20**	100	370.8	286.3	84.5	329	5.5	11.6	0.47	-483.6	2.64		
	200	387.1	284.7	102.4	336	7.9	16.4	0.48	-539.7	4.35		
	300	402.6	283.9	118.7	343	10.3	19.4	0.53	-557.9	5.53		
	400	405	282.4	122.6	344	12.5	22.3	0.56	-575.2	6.27		
	500	411.9	280.8	131.1	346	15.0	25.2	0.60	-601.1	6.83		
Average					340			0.53				

	Scan rate	E_{pa} / mV	E_{pc} / mV	ΔEp / mV	E°' / mV	i_{pc} / μA	i_{pa} / μA	i_{pc}/i_{pa}
Oc(CHO), **27**	100	721.9	626.3	95.6	674	1.8	6.3	0.29
	200	739.9	624.2	115.7	682	2.6	8.1	0.33
	300	749.5	621	128.5	685	3.3	9.4	0.35
	400	760.1	611.5	148.6	686	4.0	10.7	0.37
	500	769.6	607.2	162.4	688	4.6	11.9	0.39
Average					683			0.35
$Oc(CH_2)OH$, **19**	100	451	365	86	408	10.0	8.5	1.17
	200	457	360	97	409	14.1	13.1	1.07
	300	463	356	107	410	17.3	16.0	1.08
	400	468	354	114	411	19.4	19.0	1.03
	500	472	350	122	411	22.1	21.0	1.05
Average					410			1.08
$Oc(CH_2)OH$, **19** Decomposition peak	100	694.9	669.8	25.1	682	0.25	0.69	0.36
	200	699.2	672	27.2	686	0.27	0.69	0.39
	300	704.6	673.5	31.1	689	0.30	0.66	0.45
	400	708.1	674.6	33.5	691	0.31	0.57	0.54
	500	714.6	676.7	37.9	696	0.34	0.25	1.36
Average					689			0.62
Oc(CH=CHCOOEt), **31**	100	526.2	450.2	76	488	4.2	6.6	0.63
	200	543.3	441.2	102.1	492	6.3	10.0	0.63
	300	544.1	437.1	107	491	7.5	11.8	0.63
	400	551.5	431.4	120.1	491	8.7	13.6	0.64
	500	552.3	427.3	125	490	9.6	15.4	0.62
Average					490			0.63
$Oc(CH_2)_2COOEt$, **32**	100	383.1	296.8	86.3	340	10.2	10.8	0.95
	200	392.1	288.7	103.4	340	14.3	14.8	0.96
	300	397.5	285.1	112.4	341	17.3	18.5	0.93
	400	402.9	280.6	122.3	342	19.9	21.3	0.94
	500	405.6	279.7	125.9	343	22.2	23.7	0.93
Average					341			0.94
Oc(CH=CH)COOH, **33**	100	546.9	477.6	69.3	512	5.2	5.2	1.00
	200	547.8	475.9	71.9	512	5.7	6.8	0.85
	300	542.9	475.1	67.8	509	7.3	8.6	0.84
	400	546.1	471.8	74.3	509	8.6	10.3	0.84
	500	546.1	472.7	73.4	509	10.3	11.8	0.87
Average					510			0.88

Reduction 2		Reduction 3	
E_{pc} 2 / mV	i_{pc} 2 / μA	E_{pc} 3 / mV	i_{pc} 3 / μA
-576.8	0.47	-1102	1.29
-588.8	0.57	-1263	1.62
-611.9	0.57	-1134	1.70
-605.9	0.57	-1116	1.72
-629.0	0.60	-1144	1.77

	Scan rate	E_{pa} / mV	E_{pc} / mV	ΔEp / mV	E°' / mV	i_{pc} / µA	i_{pa} / µA	i_{pc}/i_{pa}	Reduction 2	
$OC(CH_2)_2COOH$, **24**	100	395.8	314.3	81.5	355	7.2	9.9	0.73		
	200	406.4	309.4	97	358	10.6	14.4	0.74		
	300	408.8	306.2	102.6	358	13.8	18.2	0.76		
	400	412.9	302.9	110	358	16.9	21.7	0.78		
	500	416.9	301.3	115.6	359	19.3	24.9	0.78	E_{pc} 2 / mV	i_{pc} 2 / µA
Average					357			0.76		
$Oc(CH_2)_3OH$, **21**	100	359.5	260.4	99.1	310	10.4	10.9	0.96	-498.3	0.98
	200	371.8	249.8	122	311	14.3	15.1	0.94	-537.0	1.48
	300	383.3	241.6	141.7	312	17.5	18.6	0.94	-548.3	1.96
	400	391.5	240	151.5	316	19.9	21.4	0.93	-559.6	2.46
	500	398	235.1	162.9	317	22.7	24.1	0.94	-568.1	2.60
Average					313			0.94		
$Oc(COCH_2CH_2COOMe)$, **34**	100	637.3	553.9	83.4	596	9.2	9.8	0.93	-473.5	1.55
	200	642.2	549	93.2	596	13.0	14.0	0.93	-497.3	1.82
	300	648	548	100	598	16.0	17.4	0.92	-506.2	2.43
	400	652	544.1	107.9	598	18.3	20.0	0.92	-520.6	2.73
	500	655.9	540.2	115.7	598	20.1	22.1	0.91	-541.9	3.19
Average					597			0.92		
$Oc(CH_2)_4OH$, **22**	100	376.5	261.5	115	319	8.3	8.8	0.94	-597.6	1.05
	200	379.2	257.9	121.3	319	11.6	13.2	0.88	-611.6	1.36
	300	387.2	253.4	133.8	320	14.3	15.3	0.94	-628.6	1.51
	400	393.5	251.6	141.9	323	16.3	17.6	0.93	-635.4	1.89
	500	395.3	251.6	143.7	323	18.8	20.0	0.94	-646.9	2.05
Average					321			0.92		
$Oc(CH_2)_3COOMe$, **35**	100	363.3	286.9	76.4	325	2.5	2.5	0.99		
	200	365.1	283.3	81.8	324	3.5	3.5	0.98		
	300	367.8	279.7	88.1	324	4.3	4.3	1.00		
	400	369.8	278.8	91	324	4.9	4.9	1.00		
	500	371.4	277	94.4	324	5.6	5.5	1.02		
Average					324			1.00		
$Oc(CH_2)_3COOH$, **25**	100	348.8	282.6	66.2	316	2.1	2.3	0.90		
	200	349.5	286.2	63.3	318	3.0	3.4	0.89		
	300	353.2	280.4	72.8	317	3.7	4.3	0.88		
	400	353.9	281.1	72.8	318	4.2	4.9	0.86		
	500	355.4	280	75.4	318	4.7	5.6	0.84		
Average					317			0.88		

3.4 Crystallography

The author acknowledges Dr. M. Landman from the University of Pretoria for data collection and solving the crystal structures discussed in this thesis. Two structures are presented, that of 2-osmocenylacetonitrile, **30**, and 2-osmocenylethanol, **20**. Both structure determinations are perfectly valid, but due to crystal quality even after repeated crystallisations, the best efforts to refine all data did not allow us to identify the source of the stray electron densities of 15.37 and 21.96 e $Å^3$ reported in Tables 3.2 and 3.5, respectively.

3.4.1 2-Osmocenylacetonitrile

The crystal structure of 2-osmocenylacetonitrile, **30**, was determined using X-Ray diffraction (XRD) techniques, as an additional characterization technique. The high resolution data (0.499 Å, R = 5.65%) resulted in the highest residual electron density peak of 15.37 e $Å^3$, less than 1 Å from Os1, and most of the remaining peaks with significant electron density are approximately 1 Å from the metal atom. Reducing the resolution of the data to 0.80 Å (R = 4.39 %) reduces the highest residual electron density peak to a value of 4.01 e $Å^3$, less than 1 Å from Os1, and again most of the remaining peaks with significant electron densities are also approximately 1 Å from the metal atom. Although these values are high, this effect is often seen in the presence of heavier metal-containing structures. No chemically significant assignments could be associated with any of these peaks. The high resolution data was used as the highest residual electron density peaks in both solutions are in very similar positions, only the intensities vary. Figure 3.21 shows the perspective views of **30** determined by crystallography. The crystallographic data for **30** is presented in Tables 3.2, 3.3 and 3.4.

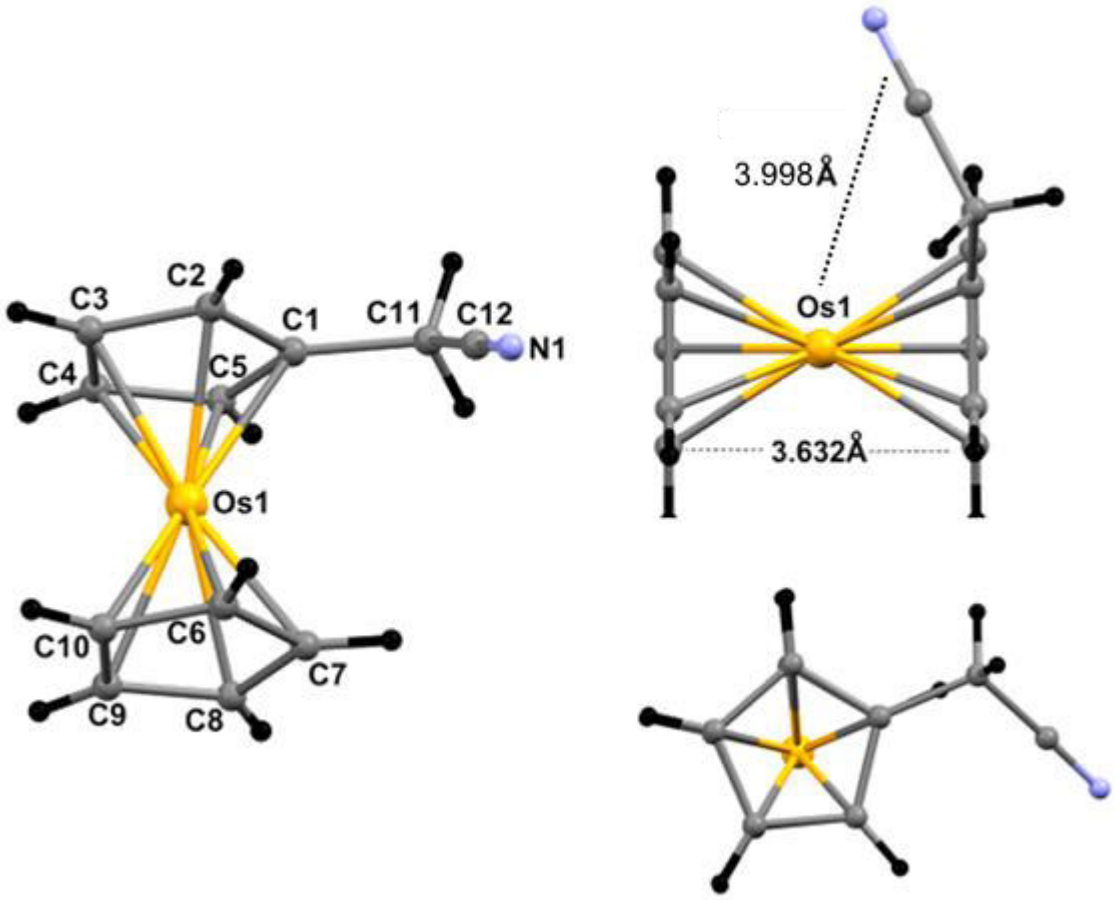

Figure 3.21: Molecular structure of 2-osmocenylacetonitrile, 30, with atom labelling (Left), side view of 30 (top right) and top view of 30 (bottom right).

Table 3.2: Crystallographic data for Oc(CH_2)CN, 30.

Chemical formula	$C_{12}H_{11}NOs$	Radiation type	Mo Kα
Mr	359.42	μ (mm^{-1})	12.91
Crystal system	Monoclinic	Crystal size (mm)	0.368 × 0.092 × 0.061
Space group	*P* $2_1/c$	No. of measured, independent and observed [I > 2σ(I)] reflections	122802, 8317, 5354
Temperature (K)	283 - 303		
Unit Cell Dimensions	a = 13.4941 (8) Å b = 5.6014 (3) Å c = 13.5604 (8) Å α = 90 ° β = 106.190 (2) ° γ = 90 °	R_{int}	0.3338
		(sin θ/λ)max (Å−1)	1.003
		R[F2 > 2σ(F2)], wR(F2), S	0.057, 0.160, 1.08
		No. of reflections	8317
V ($Å^3$)	984.33 (10)	No. of parameters	127
Z	4	Δρmax, Δρmin (e $Å^3$)	15.37, −6.27

Refinement done with *SHELXL*-2014 (Sheldrick, 2014).

2-Osmocenylacetonitrile, **30**, crystallised in dichloromethane to give a monoclinic crystal system with prismatic point group and $P2_1/c$ space group, according to Hermann–Mauguin notation. The crystal structure is of high crystal quality due to a low R value of 0.057 and low estimated standard deviations, 0.003 – 0.008 Å for bond lengths and 0.1 – 0.4° for bond angles.

The C=C bond lengths in the substituted cyclopentadienyl ring range from 1.426(7) Å to 1.436(6) Å, whereby the average is 1.433 Å. The C=C bond lengths on the unsubstituted cyclopentadienyl ring ranges from 1.423(6) Å to 1.440(6) Å, with an average of 1.429 Å. These variations are due to the delocalisation of electrons, therefore the distances of these bonds lie between that of conventional sp^3 and sp^2 C-C bonds. The bond length between C1-C11 (sp^2-sp^3) is 1.499(5) Å, whereas that for C11-C12 (sp^3-sp) is 1.472(7) Å. The C≡N bond length (C12-N1) is 1.145(8) Å. The distance between the two cyclopentadienyl rings were determined by first calculating centroids for both rings followed by determining the distance between those centroids. The distance between these centroids is 3.632 Å.

The dihedral angles are used to show the deviation of the eclipsed conformation of the cyclopentadienyl rings. The dihedral angle for C11-C1-C7-H7 is 0.22° and the dihedral angle for H3-C3-C10-H10 is 0.93°. The dihedral angle for the nitrile and the osmocenyl moiety,

C12-C11-C1-Os01, is 60.56°. The two cyclopentadienyl rings are not parallel to each other, as the planes for each ring were determined, and the angle between the two planes is 1.30°. The almost linear bond angle between C11-C12-N1 for the nitrile moiety is 178.75(7)°. The bond angle between the osmocenyl moiety and the nitrile, C1-C11-C12, is 110.80(4)°.

The added acetonitrile functionality to osmocene, to make **30**, changed the crystal system to monoclinic, whereas osmocene itself has an orthorhombic crystal system[8]. The sandwiching cyclopentadienyl rings in unsubstituted osmocene are 3.64 Å apart, which is slightly further away than that of **30**, which are 3.623 Å apart. Unlike **30**, where the eclipsed conformation of the cyclopentadienyl rings deviate with an angle of 0.93°, these rings in osmocene are eclipsed and lie on a crystallographic mirror plane, with D_{5h} symmetry.[8]

Table 3.3: Bond lengths for Oc(CH_2)CN, 30.

Atom1-Atom2	Length / Å	Atom1-Atom2	Length / Å
Os01-C9	2.188(6)	C4-C3	1.436(6)
Os01-C1	2.170(4)	C4-C5	1.432(5)
Os01-C4	2.192(4)	C6-C10	1.416(6)
Os01-C6	2.190(4)	C6-C7	1.433(6)
Os01-C10	2.186(4)	C11-C12	1.472(7)
Os01-C7	2.189(4)	C7-C8	1.432(7)
Os01-C3	2.186(4)	C3-C2	1.426(7)
Os01-C2	2.188(5)	C12-N1	1.145(8)
Os01-C5	2.184(3)	C1-C11	1.499(5)
Os01-C8	2.186(4)	C1-C2	1.434(5)
C9-C10	1.440(6)	C1-C5	1.435(5)
C9-C8	1.423(6)		

Table 3.4: Bond angles for $Oc(CH_2)CN$, 30.

Atom1-Atom2-Atom3	Bond Angle / °	Atom1-Atom2-Atom3	Bond Angle / °
C9-Os01-C1	160.2(2)	C2-C1-C5	107.8(3)
C9-Os01-C4	112.9(2)	Os01-C4-C3	70.6(2)
C9-Os01-C6	63.7(2)	Os01-C4-C5	70.6(2)
C9-Os01-C10	38.4(2)	C3-C4-C5	107.7(3)
C9-Os01-C7	64.1(2)	Os01-C6-C10	71.0(2)
C9-Os01-C3	127.1(2)	Os01-C6-C7	70.9(2)
C9-Os01-C2	160.4(2)	C10-C6-C7	108.8(3)
C9-Os01-C5	126.8(2)	Os01-C10-C9	70.9(3)
C9-Os01-C8	38.0(2)	Os01-C10-C6	71.2(2)
C1-Os01-C4	64.3(1)	C9-C10-C6	108.0(4)
C1-Os01-C6	125.6(1)	C1-C11-C12	110.8(4)
C1-Os01-C10	159.3(1)	Os01-C7-C6	70.9(2)
C1-Os01-C7	111.0(2)	Os01-C7-C8	70.8(3)
C1-Os01-C3	64.2(2)	C6-C7-C8	107.0(4)
C1-Os01-C2	38.4(2)	C6-Os01-C8	63.5(2)
C1-Os01-C5	38.5(1)	C6-Os01-C10	37.8(1)
C1-Os01-C8	126.0(1)	C6-Os01-C7	38.2(2)
C4-Os01-C6	161.2(1)	C6-Os01-C3	127.1(2)
C4-Os01-C10	127.7(1)	C6-Os01-C2	112.4(2)
C4-Os01-C7	159.4(2)	C6-Os01-C5	159.3(1)
C4-Os01-C3	38.3(2)	C4-Os01-C5	38.2(1)
C4-Os01-C2	63.9(2)	C4-Os01-C8	126.5(2)
C10-Os01-C7	63.9(2)	Os01-C3-C4	71.1(2)
C10-Os01-C3	113.1(2)	Os01-C3-C2	71.0(3)
C10-Os01-C2	126.3(2)	C4-C3-C2	108.3(4)
C10-Os01-C5	161.3(1)	Os01-C2-C1	70.1(2)
C10-Os01-C8	63.7(2)	Os01-C2-C3	70.9(3)
C7-Os01-C2	126.1(2)	C1-C2-C3	108.1(4)
C7-Os01-C5	125.4(2)	Os01-C5-C1	70.2(2)

Atom1-Atom2-Atom3	Bond Angle / °	Atom1-Atom2-Atom3	Bond Angle / °
C7-Os01-C8	38.2(2)	Os01-C5-C4	71.2(2)
C3-Os01-C2	38.0(2)	C1-C5-C4	108.2(3)
C3-Os01-C5	64.0(2)	Os01-C8-C9	71.1(3)
C3-Os01-C8	160.4(2)	Os01-C8-C7	71.0(3)
C2-Os01-C5	64.0(2)	C9-C8-C7	108.8(4)
C2-Os01-C8	160.1(2)	C11-C12-N1	178.7(7)
C5-Os01-C8	112.2(1)	Os01-C1-C11	126.6(3)
Os01-C9-C10	70.7(3)	Os01-C1-C2	71.5(2)
Os01-C9-C8	70.9(3)	Os01-C1-C5	71.3(2)
C10-C9-C8	107.4(4)	C11-C1-C2	126.5(4)
C11-C1-C5	125.5(3)		

3.4.2 2-Osmocenylethanol

The crystal structure of 2-osmocenylethanol, **20**, was also determined by X-ray diffraction techniques. This dataset was collected to high resolution (0.649 Å, R = 10.39%) and resulted in the highest residual electron density peak of 29.57 e $Å^3$, at a distance of 0.24 Å from C10, and some of the remaining peaks with significant electron density are close to (ca 1 Å) one of the Os atom. Reducing the resolution of the data to 0.80 Å (R = 9.91%) reduces the highest residual electron density peak to a value of 21.96 e $Å^3$, at a distance of 0.24 Å from C10, and some of the remaining peaks with significant electron densities are approximately 1 Å from one of the Os atom. This highest electron density peak could not even be used in modelling of disorder of the ring system. The anisotropic displacement factors for the ring atoms had to be linked to avoid that most of these atoms turn non-positive definite, and placing an atom at this position made no chemical sense. The second most significant peak appears on a special position (0, 0, ½) in both solutions, and is located approximately in the centre of the void in the packing diagram. However, refinement with a variety of elements (e.g. O in H_2O) in this position suggests that this atom is included in this position in a random ratio. No chemically significant assignments could be associated with this peak. The lower resolution data was used as the highest residual electron density peaks in both solutions are in very similar positions, only the intensities vary. The quality of the data collected does not permit any better solution in this case. Perspective views of **20** are shown in Figure 3.22.

The packing of the crystal lattice is shown in Figure 3.23 and the crystallographic data is given in Table 3.5.

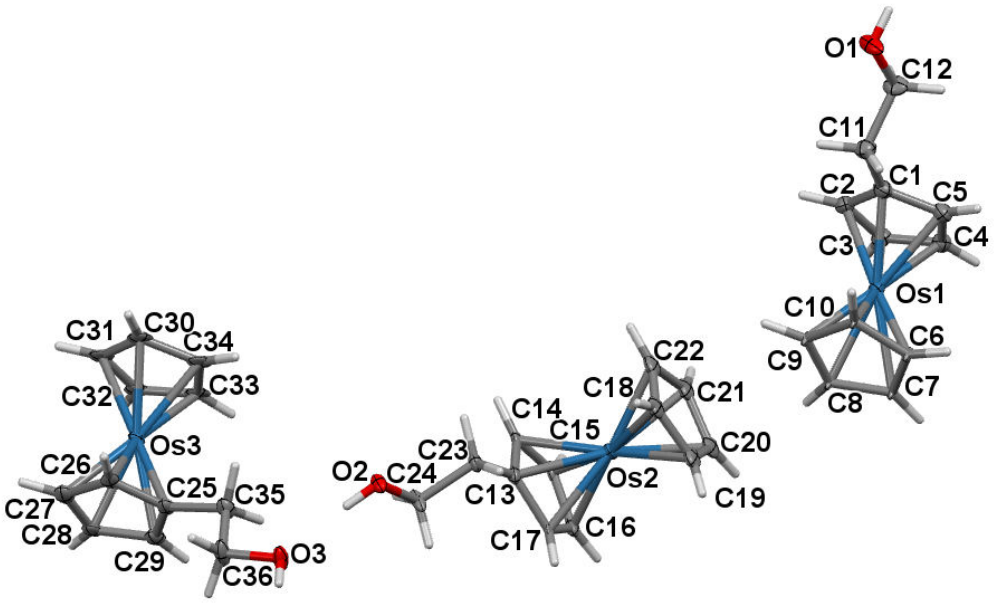

Figure 3.22: Perspective views of 2-osmocenylethanol, 20, including atom labelling.

2-Osmocenylethanol, **20**, as depicted in Figure 3.22 has a trigonal crystal system with space group *P*-3. The crystal quality is less than ideal and resulted in an R value of 0.0921; due to the time limitations of this study, better crystals could not be found. The structure was solved using three molecules of **20**, however the empirical formula is $C_{12}H_{14}OOs$ and the molecular weight was determined to be 364.43 g/mol as shown in Figure 3.22.

The C=C bond lengths on the substituted cyclopentadienyl ring range from 1.418(2) Å to 1.422(3) Å with an average of 1.420 Å. These are almost the same as the C=C bond lengths on the unsubstituted ring, with a range of 1.419(2) – 1.422(3) Å and an average of 1.420 Å. These bond lengths are smaller than that discussed for 2-osmocenylacetonitrile, **30** (Section 3.4.1), however for **20**, electrons are donated into the ring by the two methylene groups. Therefore the C=C bond lengths for **20** are smaller, due to stronger bonds, and the slightly larger bonds in **30** are due to weaker bonds that are caused from the delocalisation of electrons to the nitrile group.

Table 3.5: Crystallographic data for 2-osmocenylethanol, 20.

Chemical formula	$C_{12}H_{14}OOs$	Radiation type	Mo Kα
Mr	364.43	μ (mm^{-1})	12.059
Crystal system	Trigonal	Crystal size (mm)	0.246 × 0.101 × 0.100
Space group	*P*-3	No. of measured, independent and observed [I > 2σ(I)] reflections	122032, 6484, 5989
Temperature (K)	150		
Unit Cell Dimensions	a = 30.2956 (19) Å b = 30.2956 (19) Å c = 5.9679 (4) Å α = 90 ° β = 90 ° γ = 120 °	R_{int}	0.081
		(sin θ/λ)max (Å−1)	0.625
		R[F2 > 2σ(F2)], wR(F2), S	0.092, 0.229, 1.33
		No. of reflections	6484
V ($Å^3$)	4743.6 (7)	No. of parameters	253
Z	18	Δρmax, Δρmin (e $Å^3$)	21.96, -5.96

Refinement done with *SHELXL*-2014 (Sheldrick, 2014).

The bond length of the alkyl chain between C13-C23 (sp^2-sp^3) is 1.500(2) Å and C23-C24 (sp^3-sp^3) is 1.505(3) Å. The C-O bond length (C24-O2) is 1.405(2) Å. The O-H alcohol bond (O2-HO2) has a bond length of 0.839(3) Å. The distance between the two sandwiching cyclopentadienyl rings is 3.640 Å. The Cp-Cp distance for the equivalent ferrocene derivative, 2-ferrocenylethanol, is 3.393 Å in literature.[9] A larger distance is expected for **30** due to osmium being a much larger atom than iron. The dihedral angle between H17-C17-Os2-C19 is 5.33° which indicates a deviation from the eclipsed conformation of the sandwiching cyclopentadienyl rings. The two sandwiching cyclopentadienyl rings are approximately parallel to each other; the angle between the two planes for these rings are 0.64°.

Figure 3.23 shows the hydrogen bonding interaction of **20** from the top view of the interaction, whereby six molecules interact together to form a hexagonal pattern. The hydrogen bond interactions each have a distance of 2.691 Å. This hydrogen bond interaction, depicted in Figure 3.23, is also observed for 2-ferrocenylethanol, however the distance between the interactions are significantly smaller (2.687 Å).

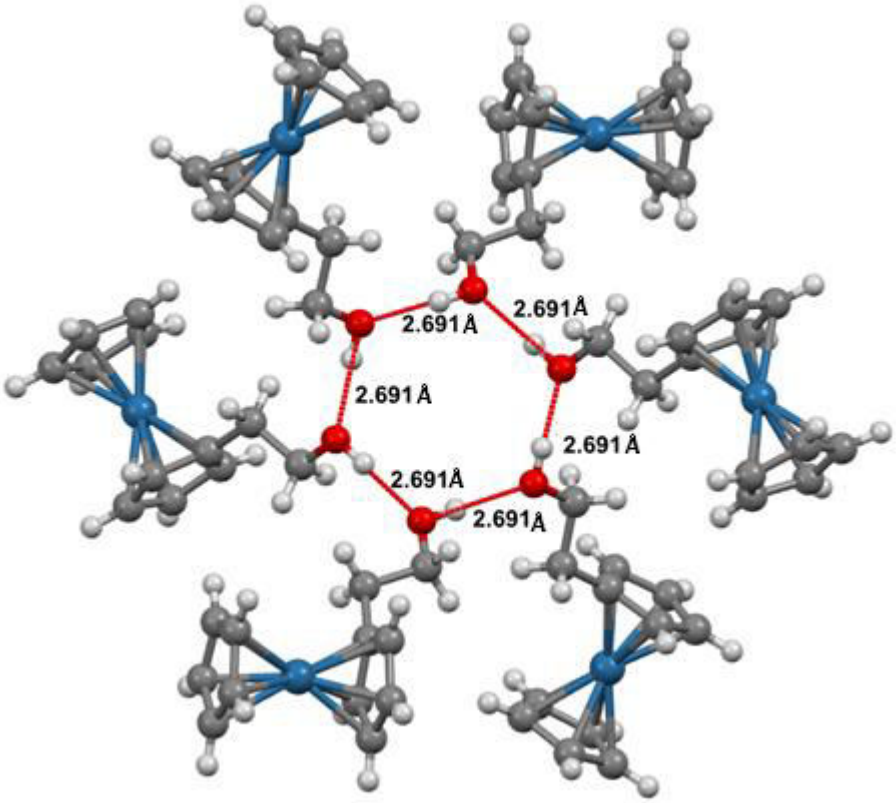

Figure 3.23: Crystal structure of 2-osmocenylethanol, 20, showing the hydrogen bond interaction and the bond length of these hydrogen bonds.

Table 3.6: Bond lengths for 2-osmocenylethanol, 20.

Atom1-Atom2	Bond Length / Å	Atom1-Atom2	Bond Length / Å
Os(1)-C(10)	1.785(15)	Os(3)-C(25)	2.182(14)
Os(1)-C(6)	1.976(14)	Os(3)-C(27)	2.194(15)
Os(1)-C(9)	2.002(14)	Os(3)-C(34)	2.183(15)
Os(1)-C(2)	2.166(15)	Os(3)-C(33)	2.186(15)
Os(1)-C(3)	2.170(15)	Os(3)-C(30)	2.197(14)
Os(1)-C(1)	2.189(15)	Os(3)-C(29)	2.194(14)
Os(1)-C(4)	2.195(15)	Os(3)-C(32)	2.202(15)
Os(1)-C(5)	2.207(15)	C(1)-C(2)	1.42(2)
Os(1)-C(7)	2.273(12)	C(1)-C(5)	1.42(2)
Os(1)-C(8)	2.287(12)	C(1)-C(11)	1.50(2)
Os(2)-C(21)	2.181(15)	C(2)-C(3)	1.42(2)
Os(2)-C(22)	2.171(15)	C(3)-C(4)	1.42(2)
Os(2)-C(16)	2.178(13)	C(4)-C(5)	1.42(3)
Os(2)-C(20)	2.187(15)	C(6)-C(7)	1.42(3)
Os(2)-C(18)	2.172(15)	C(6)-C(10)	1.42(2)
Os(2)-C(17)	2.188(13)	C(7)-C(8)	1.42(2)
Os(2)-C(15)	2.185(13)	C(8)-C(9)	1.42(2)
Os(2)-C(19)	2.182(15)	C(9)-C(10)	1.42(3)
Os(2)-C(13)	2.200(13)	C(11)-C(12)	1.53(3)
Os(2)-C(14)	2.199(13)	C(13)-C(14)	1.42(2)
Os(3)-C(26)	2.182(14)	C(13)-C(17)	1.42(2)
Os(3)-C(28)	2.201(14)	C(13)-C(23)	1.50(2)
Os(3)-C(31)	2.209(14)	C(14)-C(15)	1.42(2)
O(1)-C(12)	1.42(3)	C(15)-C(16)	1.42(2)
O(2)-C(24)	1.40(2)	C(16)-C(17)	1.42(2)
O(3)-C(36)	1.42(3)	C(27)-C(28)	1.42(3)
C(18)-C(19)	1.42(2)	C(28)-C(29)	1.42(2)
C(18)-C(22)	1.42(2)	C(30)-C(31)	1.42(3)

Atom1-Atom2	Bond Length / Å	Atom1-Atom2	Bond Length / Å
C(19)-C(20)	1.42(2)	C(30)-C(34)	1.42(2)
C(20)-C(21)	1.42(2)	C(31)-C(32)	1.42(2)
C(21)-C(22)	1.42(2)	C(32)-C(33)	1.42(3)
C(23)-C(24)	1.51(3)	C(33)-C(34)	1.42(3)
C(25)-C(29)	1.42(2)	C(35)-C(36)	1.51(3)
C(25)-C(26)	1.42(2)	C(26)-C(27)	1.42(3)
C(25)-C(35)	1.51(2)		

Table 3.7: Bond angles for 2-osmocenylethanol, 20.

Atom1-Atom2-Atom3	Bond Angle / °	Atom1-Atom2-Atom3	Bond Angle / °
C(10)-Os(1)-C(6)	44.0(3)	C(5)-Os(1)-C(7)	130.5(5)
C(10)-Os(1)-C(9)	43.6(3)	C(10)-Os(1)-C(8)	67.4(3)
C(6)-Os(1)-C(9)	70.6(3)	C(6)-Os(1)-C(8)	64.7(3)
C(10)-Os(1)-C(2)	128.3(5)	C(9)-Os(1)-C(8)	37.9(2)
C(6)-Os(1)-C(2)	167.2(5)	C(2)-Os(1)-C(8)	124.9(5)
C(9)-Os(1)-C(2)	111.2(5)	C(3)-Os(1)-C(8)	113.6(5)
C(10)-Os(1)-C(3)	165.4(5)	C(1)-Os(1)-C(8)	156.9(5)
C(6)-Os(1)-C(3)	150.5(5)	C(4)-Os(1)-C(8)	130.2(5)
C(9)-Os(1)-C(3)	127.9(5)	C(5)-Os(1)-C(8)	164.3(5)
C(2)-Os(1)-C(3)	38.2(2)	C(7)-Os(1)-C(8)	36.28(18)
C(10)-Os(1)-C(1)	109.3(5)	C(21)-Os(2)-C(22)	38.1(2)
C(6)-Os(1)-C(1)	129.9(5)	C(21)-Os(2)-C(16)	129.9(5)
C(9)-Os(1)-C(1)	123.6(5)	C(22)-Os(2)-C(16)	164.6(6)
C(2)-Os(1)-C(1)	38.1(2)	C(21)-Os(2)-C(20)	37.9(2)
C(3)-Os(1)-C(1)	63.6(3)	C(22)-Os(2)-C(20)	63.6(3)
C(10)-Os(1)-C(4)	152.6(5)	C(16)-Os(2)-C(20)	113.2(4)
C(6)-Os(1)-C(4)	118.4(5)	C(21)-Os(2)-C(18)	63.7(3)
C(9)-Os(1)-C(4)	163.3(5)	C(22)-Os(2)-C(18)	38.2(2)
C(2)-Os(1)-C(4)	63.6(3)	C(16)-Os(2)-C(18)	156.0(6)
C(3)-Os(1)-C(4)	38.0(2)	C(20)-Os(2)-C(18)	63.6(3)
C(1)-Os(1)-C(4)	63.2(3)	C(21)-Os(2)-C(17)	165.3(5)
C(10)-Os(1)-C(5)	119.8(5)	C(22)-Os(2)-C(17)	155.7(5)
C(6)-Os(1)-C(5)	109.7(5)	C(16)-Os(2)-C(17)	38.0(2)
C(9)-Os(1)-C(5)	156.6(5)	C(20)-Os(2)-C(17)	130.8(5)
C(2)-Os(1)-C(5)	63.4(3)	C(18)-Os(2)-C(17)	124.1(5)
C(3)-Os(1)-C(5)	63.3(3)	C(21)-Os(2)-C(15)	112.5(5)
C(1)-Os(1)-C(5)	37.7(2)	C(22)-Os(2)-C(15)	129.5(5)
C(4)-Os(1)-C(5)	37.6(2)	C(16)-Os(2)-C(15)	38.0(2)

Atom1-Atom2-Atom3	Bond Angle / °	Atom1-Atom2-Atom3	Bond Angle / °
C(10)-Os(1)-C(7)	67.7(3)	C(20)-Os(2)-C(15)	123.6(5)
C(6)-Os(1)-C(7)	38.2(2)	C(18)-Os(2)-C(15)	164.7(6)
C(9)-Os(1)-C(7)	64.7(3)	C(17)-Os(2)-C(15)	63.4(3)
C(2)-Os(1)-C(7)	154.5(5)	C(21)-Os(2)-C(19)	63.6(3)
C(3)-Os(1)-C(7)	122.5(5)	C(22)-Os(2)-C(19)	63.7(3)
C(1)-Os(1)-C(7)	165.7(5)	C(16)-Os(2)-C(19)	124.1(5)
C(4)-Os(1)-C(7)	112.6(5)	C(20)-Os(2)-C(19)	37.9(2)
C(18)-Os(2)-C(19)	38.1(2)	C(34)-Os(3)-C(29)	130.1(5)
C(17)-Os(2)-C(19)	113.7(5)	C(33)-Os(3)-C(29)	113.5(5)
C(15)-Os(2)-C(19)	155.7(5)	C(30)-Os(3)-C(29)	164.7(6)
C(21)-Os(2)-C(13)	155.2(5)	C(26)-Os(3)-C(32)	164.4(6)
C(22)-Os(2)-C(13)	123.6(5)	C(25)-Os(3)-C(32)	156.5(6)
C(16)-Os(2)-C(13)	63.3(3)	C(27)-Os(3)-C(32)	130.0(5)
C(20)-Os(2)-C(13)	165.8(6)	C(34)-Os(3)-C(32)	63.2(3)
C(18)-Os(2)-C(13)	113.4(5)	C(33)-Os(3)-C(32)	37.8(2)
C(17)-Os(2)-C(13)	37.8(2)	C(30)-Os(3)-C(32)	63.0(3)
C(15)-Os(2)-C(13)	63.2(3)	C(29)-Os(3)-C(32)	124.6(5)
C(19)-Os(2)-C(13)	130.9(5)	C(26)-Os(3)-C(28)	63.2(3)
C(21)-Os(2)-C(14)	123.3(5)	C(25)-Os(3)-C(28)	63.2(3)
C(22)-Os(2)-C(14)	112.6(5)	C(27)-Os(3)-C(28)	37.7(2)
C(16)-Os(2)-C(14)	63.3(3)	C(34)-Os(3)-C(28)	164.8(6)
C(20)-Os(2)-C(14)	155.2(5)	C(33)-Os(3)-C(28)	130.2(5)
C(18)-Os(2)-C(14)	130.1(5)	C(30)-Os(3)-C(28)	156.1(6)
C(17)-Os(2)-C(14)	63.2(3)	C(29)-Os(3)-C(28)	37.7(2)
C(15)-Os(2)-C(14)	37.8(2)	C(32)-Os(3)-C(28)	113.6(5)
C(19)-Os(2)-C(14)	165.4(6)	C(26)-Os(3)-C(31)	129.9(5)
C(13)-Os(2)-C(14)	37.7(2)	C(25)-Os(3)-C(31)	164.5(6)
C(26)-Os(3)-C(25)	38.0(2)	C(27)-Os(3)-C(31)	113.4(5)
C(26)-Os(3)-C(27)	37.9(2)	C(34)-Os(3)-C(31)	63.1(3)
C(25)-Os(3)-C(27)	63.3(3)	C(33)-Os(3)-C(31)	63.0(3)

Atom1-Atom2-Atom3	Bond Angle / °	Atom1-Atom2-Atom3	Bond Angle / °
C(26)-Os(3)-C(34)	124.0(5)	C(30)-Os(3)-C(31)	37.6(2)
C(25)-Os(3)-C(34)	113.1(5)	C(29)-Os(3)-C(31)	156.4(5)
C(27)-Os(3)-C(34)	156.1(6)	C(32)-Os(3)-C(31)	37.6(2)
C(26)-Os(3)-C(33)	156.3(6)	C(28)-Os(3)-C(31)	124.6(5)
C(25)-Os(3)-C(33)	124.3(5)	C(2)-C(1)-C(5)	108(1)
C(27)-Os(3)-C(33)	164.6(6)	C(2)-C(1)-C(11)	126.7(14)
C(34)-Os(3)-C(33)	37.9(2)	C(5)-C(1)-C(11)	124.9(13)
C(26)-Os(3)-C(30)	113.0(5)	C(2)-C(1)-Os(1)	70.1(6)
C(25)-Os(3)-C(30)	129.9(5)	C(5)-C(1)-Os(1)	71.8(6)
C(27)-Os(3)-C(30)	124.2(5)	C(11)-C(1)-Os(1)	129.3(13)
C(34)-Os(3)-C(30)	37.8(2)	C(1)-C(2)-C(3)	108(1)
C(33)-Os(3)-C(30)	63.2(3)	C(1)-C(2)-Os(1)	71.8(6)
C(26)-Os(3)-C(29)	63.3(3)	C(10)-C(9)-C(8)	108(1)
C(25)-Os(3)-C(29)	37.9(2)	C(10)-C(9)-Os(1)	60.1(5)
C(27)-Os(3)-C(29)	63.2(3)	C(8)-C(9)-Os(1)	82.0(5)
C(3)-C(2)-Os(1)	71.0(6)	C(9)-C(10)-C(6)	108(1)
C(2)-C(3)-C(4)	108(1)	C(9)-C(10)-Os(1)	76.3(6)
C(2)-C(3)-Os(1)	70.7(6)	C(6)-C(10)-Os(1)	75.2(6)
C(4)-C(3)-Os(1)	72.0(6)	C(1)-C(11)-C(12)	110.9(18)
C(5)-C(4)-C(3)	108(1)	C(21)-C(22)-C(18)	108(1)
C(5)-C(4)-Os(1)	71.6(6)	C(21)-C(22)-Os(2)	71.3(6)
C(3)-C(4)-Os(1)	70.1(6)	C(18)-C(22)-Os(2)	70.9(6)
C(4)-C(5)-C(1)	108(1)	O(1)-C(12)-C(11)	110.4(19)
C(4)-C(5)-Os(1)	70.7(6)	C(14)-C(13)-C(17)	108(1)
C(1)-C(5)-Os(1)	70.5(6)	C(14)-C(13)-C(23)	125.9(12)
C(7)-C(6)-C(10)	108(1)	C(17)-C(13)-C(23)	125.6(12)
C(7)-C(6)-Os(1)	82.3(5)	C(14)-C(13)-Os(2)	71.1(5)
C(10)-C(6)-Os(1)	60.8(6)	C(17)-C(13)-Os(2)	70.6(5)
C(6)-C(7)-C(8)	108(1)	C(23)-C(13)-Os(2)	129.9(11)
C(6)-C(7)-Os(1)	59.5(5)	C(13)-C(14)-C(15)	108(1)

Atom1-Atom2-Atom3	Bond Angle / °	Atom1-Atom2-Atom3	Bond Angle / °
C(8)-C(7)-Os(1)	72.4(5)	C(13)-C(14)-Os(2)	71.2(5)
C(7)-C(8)-C(9)	108(1)	C(15)-C(14)-Os(2)	70.6(5)
C(7)-C(8)-Os(1)	71.3(5)	C(20)-C(21)-Os(2)	71.3(6)
C(9)-C(8)-Os(1)	60.1(5)	C(16)-C(15)-Os(2)	70.7(5)
C(14)-C(15)-C(16)	108(1)	C(17)-C(16)-C(15)	108(1)
C(14)-C(15)-Os(2)	71.6(5)	C(22)-C(21)-C(20)	108(1)
C(17)-C(16)-Os(2)	71.4(5)	C(13)-C(23)-C(24)	111.5(16)
C(15)-C(16)-Os(2)	71.3(5)	O(2)-C(24)-C(23)	111.1(16)
C(16)-C(17)-C(13)	108(1)	C(29)-C(25)-C(26)	108(1)
C(16)-C(17)-Os(2)	70.7(5)	C(29)-C(25)-C(35)	125.2(13)
C(13)-C(17)-Os(2)	71.6(5)	C(26)-C(25)-C(35)	126.5(13)
C(19)-C(18)-C(22)	108(1)	C(29)-C(25)-Os(3)	71.5(5)
C(19)-C(18)-Os(2)	71.3(6)	C(26)-C(25)-Os(3)	71.0(6)
C(22)-C(18)-Os(2)	70.9(6)	C(35)-C(25)-Os(3)	127.6(12)
C(20)-C(19)-C(18)	108(1)	C(27)-C(26)-C(25)	108(1)
C(20)-C(19)-Os(2)	71.2(6)	C(27)-C(26)-Os(3)	71.5(6)
C(18)-C(19)-Os(2)	70.6(6)	C(25)-C(26)-Os(3)	71.0(6)
C(19)-C(20)-C(21)	108(1)	C(26)-C(27)-C(28)	108(1)
C(19)-C(20)-Os(2)	70.8(6)	C(26)-C(27)-Os(3)	70.6(5)
C(21)-C(20)-Os(2)	70.8(6)	C(28)-C(27)-Os(3)	71.4(6)
C(22)-C(21)-C(20)	108(1)	C(28)-C(27)-Os(3)	71.4(6)
C(22)-C(21)-Os(2)	70.6(6)	C(31)-C(32)-Os(3)	71.5(6)
C(29)-C(28)-C(27)	126(1)	C(32)-C(33)-C(34)	108(1)
C(29)-C(28)-Os(3)	123.6(9)	C(32)-C(33)-Os(3)	71.7(6)
C(27)-C(28)-Os(3)	108(1)	C(34)-C(33)-Os(3)	70.9(6)
C(25)-C(29)-C(28)	126(2)	C(30)-C(34)-C(33)	108(1)
C(25)-C(29)-Os(3)	123.9(9)	C(30)-C(34)-Os(3)	71.6(6)
C(28)-C(29)-Os(3)	108(1)	C(33)-C(34)-Os(3)	71.2(6)
C(31)-C(30)-C(34)	126(6)	C(25)-C(35)-C(36)	110.7(17)
C(31)-C(30)-Os(3)	123.6(6)	O(3)-C(36)-C(35)	109.5(18)

Atom1-Atom2-Atom3	Bond Angle / °	Atom1-Atom2-Atom3	Bond Angle / °
C(34)-C(30)-Os(3)	108(1)	C(32)-C(31)-Os(3)	108(1)
C(30)-C(31)-C(32)	126(6)	C(33)-C(32)-C(31)	126(6)
C(30)-C(31)-Os(3)	123.4(9)	C(33)-C(32)-Os(3)	123.9(9)

References

1. R. Sanders and U. T. Mueller-Westerhoff, *J. Organomet. Chem.*, 1996, **512**, 219–224.
2. J. Clayden, N. Greeves, S. Warren and P. Wothers, *Organic Chemistry*, Oxford University Press, New York, 2001.
3. O. A. Tarasova, I. V. Tatarinova, T. I. Vakul'skaya, S. S. Khutsishvili, V. I. Smirnov, L. V. Klyba, G. F. Prozorova, A. I. Mikhaleva and B. A. Trofimov, *J. Organomet. Chem.*, 2013, **745–746**, 1–7.
4. P. Beagley, M. A. L. Blackie, K. Chibale, C. Clarkson, J. R. Moss and P. J. Smith, *J. Chem. Soc. Dalton Trans.*, 2002, **23**, 4426–4433.
5. J. Cason, *Org. Synth. Coll*, 1945, **3**, 169–171.
6. (a) C. C. Joubert, M. Sc. Synthesis and characterisation of ruthenocene-containing complexes with biomedical applications, University of the Free State, 2011.
   (b) J. C. Swarts, A. Nafady, J. H. Roudebush, S. Trupia and W. E. Geiger, *Inorg. Chem.*, 2009, **48**, 2156-2165.
7. M. W. Droege, W. D. Harman and H. Taube, *Inorg. Chem.*, 1987, **26**, 1309–1315.
8. J. C. A. Bobyens, D. C. Levendis, M. I. Bruce and M. L. Williams, *J. Crystallogr. Spectrosc. Res.*, 1986, **16**, 519–524.
9. C. Nataro, W. M. Cleaver, C. C. Landry and C. W. Allen, *Polyhedron*, 1999, **18**, 1471–1473.

4 Experimental

4.1 Introduction

The materials, equipment, experimental procedures and techniques that were used in this study are presented in this chapter.

4.2 Materials

Solid reagents (Strem, Aldrich and Merck) and liquid reagents (Aldrich and Merck) were used without further purification unless otherwise stated. Organic solvents used in this study were dried and distilled according to published methods.[1] Kieselgel 60 (Merck, grain size 0.040 – 0.063 mm) was used to perform column chromatography. Filtration and vacuum evaporation were conducted using a water aspirator. Melting points (m.p.) were measured using the Olympus BX51 microscope equipped with a Linkham THMS 600 heating/cooling apparatus and the values are uncorrected.

4.3 Spectroscopic Measurements

^{1}H NMR spectra were measured at 298 K on a Bruker Avance DPX 300 NMR spectrometer. A few specified ^{1}H and ^{13}C NMR spectra were measured using a Bruker Avance II 600 NMR spectrometer. Chemical shifts are reported relative to $SiMe_4$ (TMS) at 0.00 ppm. The ^{1}H NMR peak for deuterated chloroform ($CDCl_3$) is at 7.27 ppm and the peak for trace amounts of water is at 1.60 ppm. The ^{1}H NMR peaks for deuterated tetrahydrofuran (THF) are at 1.73 and 3.58 ppm and deuterated water (D_2O) has a peak at 4.65 ppm in this solvent. Infra-red measurements were taken using a Nicolet iS50 ATR Fourier transform spectrometer.

4.4 Synthesis of osmocene derivatives

4.4.1 Osmocene carboxaldehyde, 27.

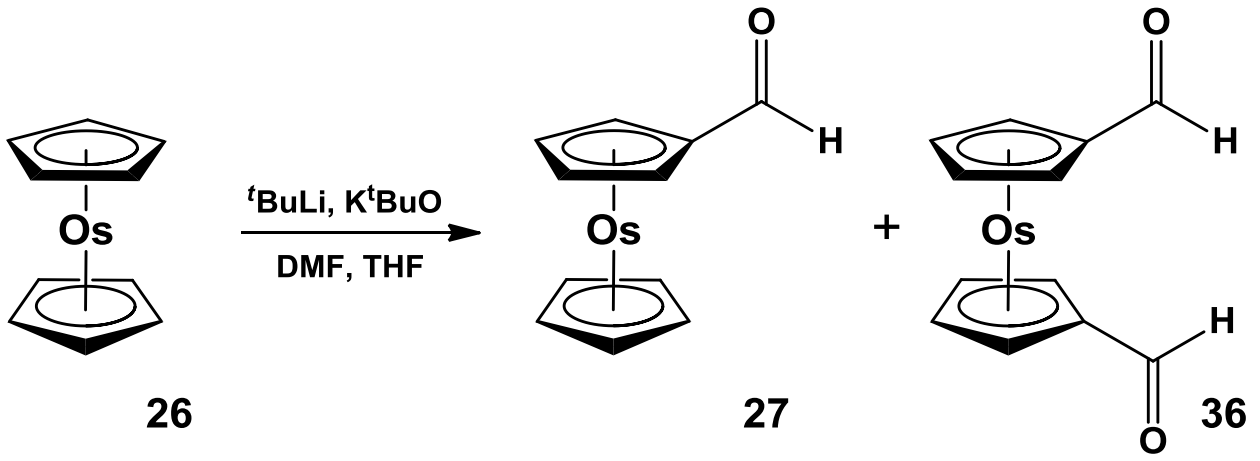

Osmocene (600 mg, 1.872 mmol) and potassium *t*-butoxide (25.84 mg, 0.2304 mmol, 0.12 eq) were dissolved in 58 cm^3 of freshly distilled, dry THF and the solution cooled to -78 °C in a liquid nitrogen/isopropanol bath. Over a period of 5 – 6 minutes, 1.7 M *t*-BuLi in pentane (3.72 mmol, 2.0 cm^3, 2 eq) was added, ensuring the temperature remained below -70 °C. The reaction mixture was then stirred for 26 minutes at -78 °C. DMF (0.4 cm^3, 4.72 mmol, 2.5 eq) was added drop-wise. The temperature was allowed to rise to -40 °C over a period of 15 minutes. Distilled water (10 cm^3) was added, and the reaction mixture extracted using dichloromethane (3 x 25 cm^3), dried over anhydrous $MgSO_4$ and the DCM removed using a rotary evaporator. The crude product was purified by column chromatography by first using *n*-hexane to collect the unreacted osmocene, dichloromethane to collect the mono-substituted aldehyde and finally dichloromethane:diethyl ether 1:1 to collect the di-substituted aldehyde. Yield mono-substituted aldehyde 79.5% (530 mg). Melting point = 114 °C. IR: υ/cm^{-1} = 1655 (C=O). **Spectrum 21**. ^1H NMR (600 MHz, $CDCl_3$)/ppm = 9.71 (s, 1H, CHO), 5.23 (t, J_{HH} = 1.59 Hz, 2H, 0.5 x C_5H_4), 5.04 (t, J_{HH} = 1.58 Hz, 2H, 0.5 x C_5H_4), 4.87 (s, 5H, C_5H_5). **Spectrum 1**. Yield di-substituted aldehyde 19.5% (137 mg). Melting point = 139 – 149 °C. IR: υ/cm^{-1} = 1673 (C=O), 1665 (C=O). **Spectrum 22.** ^1H NMR (300 MHz,

$CDCl_3$)/ppm = 9.70 (s, 2H, CHO), 5.38 (t, J_{HH} = 1.48 Hz, 4H, C_5H_4), 5.14 (t, J_{HH} = 1.27 Hz, 4H, C_5H_4) **Spectrum 2**.* Retention factors: **26** = 0.776; **27** = 0.417; **36** = 0.24.

4.4.2 Osmocene carboxaldehyde using Vilsmeier reaction, 27.

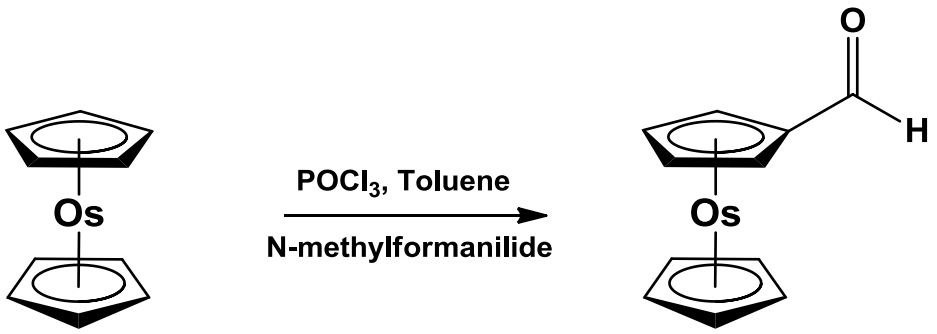

26 **27**

N-methylformanilide (6 cm^3, 48.6 mmol, 52 eq) was degassed under argon while the flask was kept in an ice bath. $POCl_3$ (3.21 cm^3, 34.4 mmol, 37 eq) was then added slowly to the flask, ensuring the solution was kept cool. After addition, the solution was stirred for one hour. Osmocene (308 mg, 0.936 mmol) in dry toluene (5 cm^3) was added to the reaction mixture. The mixture was heated to 80 °C and left to reflux for two hours. The reaction mixture was cooled in an ice bath, CH_3COONa (2.143 g, 26.1 mmol, 28 eq) in water (43 cm^3) was added slowly and the reaction mixture stirred at room temperature for 16 hours. The organic layer was washed with 1 M HCl, distilled water, a saturated solution of Na_2CO_3 and again with distilled water. Anhydrous $MgSO_4$ was used to dry the organic layer, and the solvent distilled off using a rotary evaporator. The crude product was purified by column chromatography using hexane:diethyl ether (3:4) as eluent. Yield 51.8% (169 mg). Melting point = 114 °C. IR: υ/cm^{-1} = 1655 (C=O). **Spectrum 21**. ^1H NMR (300 MHz, $CDCl_3$)/ppm = 9.73 (s, 1H, CHO), 5.24 (t, J_{HH} = 1.59 Hz, 2H, 0.5 x C_5H_4), 5.04 (t, J_{HH} = 1.59 Hz, 2H, 0.5 x C_5H_4), 4.88 (s, 5H, C_5H_5). **Spectrum 1**. Retention factors: **26** = 0.941; **27** = 0.53.

* Although it is an IUPAC rule to always write the cation first, eg: Li^{t}Bu, it has become customary in organic chemistry to write ^{t}BuLi and not Li^{t}Bu. The Organic convention is followed in this thesis when appropriate.

4.4.3 Osmocenylmethanol, 19.

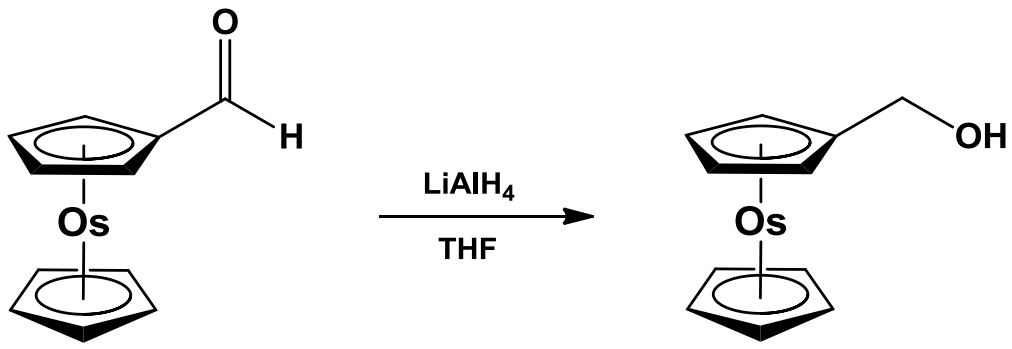

27 **19**

$LiAlH_4$ (33 mg, 0.861 mmol, 3 eq) was added to a round bottom flask under argon. A solution of osmocenecarboxaldehyde (100 mg, 0.287 mmol) in THF (20 cm^3) was added drop-wise to the round bottom flask and refluxed for one hour. After cooling to room temperature, distilled water (15 cm^3) was added slowly. The alcohol was extracted with diethyl ether (2 x 50 cm^3), the ether washed with distilled water, dried over anhydrous $MgSO_4$ and the solvent removed under reduced pressure. Yield 91.3% (97 mg). Melting point = 91.7 – 94.8 °C. IR: υ/cm^{-1} = 1038 (C-O), 3183 (O-H). **Spectrum 23**. ^1H NMR (300 MHz, $CDCl_3$)/ppm = 4.67 (t, J_{HH} = 1.31 Hz, 2H, 0.5 x C_5H_4), 4.74 (s, 5H, C_5H_5), 4.77 (t, J_{HH} = 1.33 Hz, 2H, 0.5 x C_5H_4), 3.95 (s, 2H, $C\underline{H_2}OH$). **Spectrum 3**. $^{13}C\{^1H\}$ NMR (150 MHz, $CDCl_3$)/ppm = 58.39 (CH_2), 63.87 (C_5H_4), 64.05 (C_5H_5), 64.86 (C_5H_4), 89.73 (C_5H_4). Elemental analysis (%): calc for $C_{11}H_{12}OOs$ (350.1): C, 37.7; H, 3.5; found: C, 36.6, H, 3.2.

4.4.4 *N,N,N*-Trimethylaminomethyl osmocene iodide, 29.

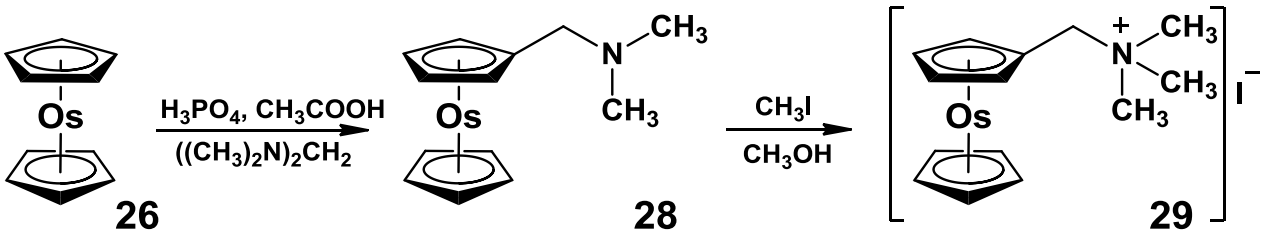

A solution of phosphoric acid (6 cm^3, 115 mmol, 73.7 eq) and glacial acetic acid (30 cm^3, 524 mmol, 335 eq) was flushed with argon, then cooled in an ice bath, and bis(dimethylamino)methane (3.0 cm^3, 23.9 mmol, 15.3 eq) was added drop-wise with stirring. Osmocene (500 mg, 1.560 mmol) was added and the mixture refluxed for 5 hours. The solution was allowed to cool, diluted with 20 cm^3 of cold distilled water, and unreacted osmocene extracted from the acidic medium with diethyl ether (3 x 50 cm^3). The acidic aqueous solution was then treated ice and with 2M NaOH until alkaline, and further extracted with diethyl ether (3 x 50 cm^3). The ether extracts were dried over anhydrous $MgSO_4$ and solvent removed by rotary evaporation, yielding 44.5% (262 mg) as a white powder, of considerable instability. Melting point = 56.7 – 57.2 °C. IR: υ/cm^{-1} = 1447 (CH_3), 2752 (C-H aliphatic), 2811 – 3075 (C-H aromatic). **Spectrum 24**. ^{1}H NMR (600 MHz, THF-d_8)/ppm = 4.74 (t, J_{HH} = 1.33 Hz, 2H, 0.5 x C_5H_4), 4.64 (s, 5H, C_5H_5), 4.63 (t, J_{HH} = 1.33 Hz, 2H, 0.5 x C_5H_4), 3.35 (s, 2H, $C\underline{H}_2N$), 2.48 (s, 6H, $N(C\underline{H}_3)_2$. **Spectrum 4**.*

N,N-dimethylaminomethylosmocene, **28**, (218 mg, 0.577 mmol) was immediately dissolved in methanol (1.5 cm^3) and iodomethane (1.5 cm^3, 24 mmol, 41.5 eq). The reaction mixture was refluxed for one hour. The solvent was removed by rotary evaporation to yield 100% (302 mg) of **29** as a crude white powder, of considerable instability. Melting point = decomposed at 155 °C. IR: υ/cm^{-1} = 1469 (CH_3), 2718 (C-H aliphatic), 2917 – 3059 (C-H aromatic). **Spectrum 25**. ^{1}H NMR (300 MHz, D_2O)/ppm = 6.46 (t, J_{HH} = 11.45 Hz, 2H, 0.5 x C_5H_4), 6.32 (t, J_{HH} = 11.57 Hz, 2H, 0.5 x C_5H_4), 6.22 (s, 5H, C_5H_5), 5.45 (s, 2H, $C\underline{H}_2N$), 4.39 (s, 9H, $N(C\underline{H}_3)_3$. **Spectrum 5**.*

* No elemental analysis was possible due to instability of compound.

4.4.5 2-osmocenylacetonitrile, 30.

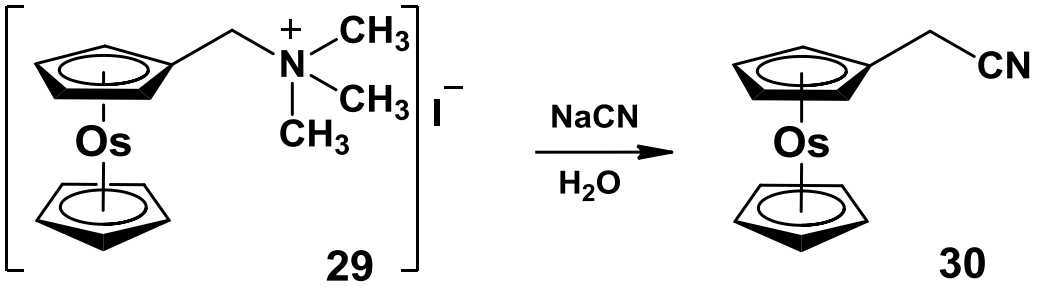

N,N,N-trimethylaminomethyl osmocene iodide, **29**, (300 mg, 0.577 mmol) and NaCN (0.31 g, 6.32 mmol, 11 eq) were dissolved in distilled water (5 cm^3) and refluxed for 4 hours. The solution was cooled, ice added and extracted with diethyl ether (3 x 50 cm^3). The ether extract was dried over anhydrous $MgSO_4$ and the solvent removed by rotary evaporation. The product was purified using column chromatography using diethyl ether:n-hexane (1:1) as eluent, to yield 36.2% (75 mg) as white crystals. Melting point = 114 – 115 °C. IR: υ/cm^{-1} = 2239 (C≡N). **Spectrum 26**. ^{1}H NMR (300 MHz, $CDCl_3$)/ppm = 4.85 (t, J_{HH} = 1.34 Hz, 2H, 0.5 x C_5H_4), 4.78 (s, 5H, C_5H_5), 4.70 (t, J_{HH} = 1.33 Hz 2H, 0.5 x C_5H_4), 3.44 (s, 2H, $C\underline{H_2}CN$). **Spectrum 6**. Retention factor: **30** = 0.56. Elemental analysis (%): calc for $C_{12}H_{11}NOs$ (359.5): C, 40.1; H, 3.0; N, 3.9; found: C, 41.1, H, 3.3; N, 4.0.

4.4.6 2-osmocenylethanoic acid, 23.

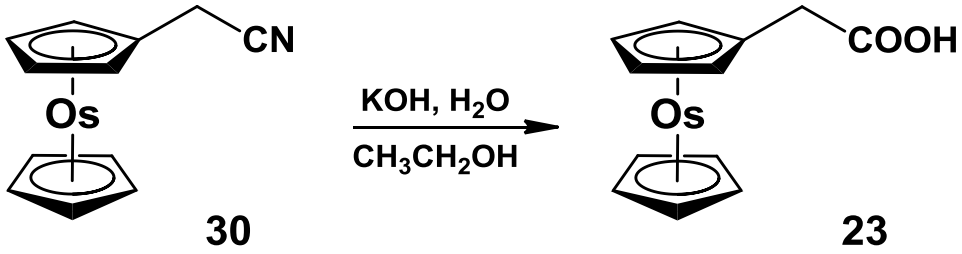

KOH (0.5 g, 8.9 mmol, 45 eq) in distilled water (5 cm^3) was added to a solution of 2-osmocenylacetonitrile (71 mg, 0.197 mmol) in absolute ethanol (2.5 cm^3). The reaction mixture

was refluxed for 5 hours until evolution of ammonia ceased. The ethanol was removed under reduced pressure. The residual suspension was dissolved in distilled water (50 cm^3), extracted with diethyl ether and filtered. The water layer was then acidified with 2 M HCl and left in ice. Once the precipitate was formed, it was filtered and washed with small amounts of cold water, then left to air dry, yielding 44.2% (33 mg) as clear crystals. Melting point = 160 – 163 °C. IR: υ/cm^{-1} = 1206 (C-O), 1234 (C-O), 1684 (C=O), 2407 – 3257 (O-H board peak), 2885 (C-H aromatic). **Spectrum 27**. ^{1}H NMR (300 MHz, $CDCl_3$)/ppm = 4.80 (s, 5H, C_5H_5), 4.76 (m, J_{HH} = 1.45 Hz, 4H, C_5H_4), 3.38 (s, $C\underline{H_2}COOH$). **Spectrum 7**. At time of publishing, the elemental analysis was not available.

4.4.7 2-osmocenylethanol, 20.

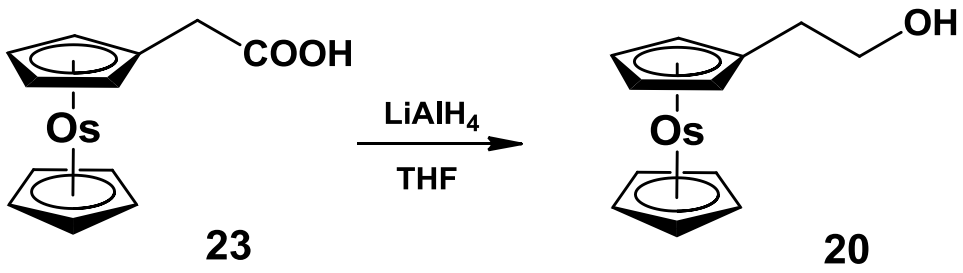

$LiAlH_4$ (34 mg, 0.861 mmol, 10 eq) was added to a round bottom flask under argon. A solution of 2-osmocenylethanoic acid (33 mg, 0.0872 mmol) in THF (15 cm^3) was added drop-wise to the round bottom flask and refluxed for one hour. After cooling to room temperature, distilled water (15 cm^3) was added slowly. The alcohol was extracted with diethyl ether (2 x 50 cm^3), and washed with distilled water, dried over anhydrous $MgSO_4$ and the solvent removed under reduced pressure. Yield 91.2% (29 mg). Melting point = 82.6 – 84.0 °C. IR: υ/cm^{-1} = 1035 (C-O), 2898 (C-H aliphatic), 3176 (O-H broad peak). **Spectrum 28**. ^{1}H NMR (300 MHz, $CDCl_3$)/ppm = 4.75 (t, J_{HH} = 2.02 Hz, 2H, 0.5 x C_5H_4), 4.73 (s, 5H, C_5H_5), 4.65 (t, J_{HH} = 1.27 Hz, 2H, 0.5 x C_5H_4), 3.65 (q, J_{HH} = 6.03 Hz, 2H, $CH_2C\underline{H_2}OH$), 2.52 (t, J_{HH} = 5.80 Hz, 2H, $C\underline{H_2}CH_2OH$). **Spectrum 8**. $^{13}C\{^1H\}$ NMR (150 MHz, $CDCl_3$)/ppm = 23.15 (CH_2), 33.73 (CH_2OH), 63.51 (C_5H_4), 64.48 (C_5H_5), 65.32 (C_5H_4), 81.83 (C_5H_4). Elemental analysis (%): calc for $C_{12}H_{14}OOs$ (364.5): C, 39.5; H, 3.8; found: C, 39.2, H, 3.8.

4.4.8 Ethyl-3-osmocenylethenoate, 31.

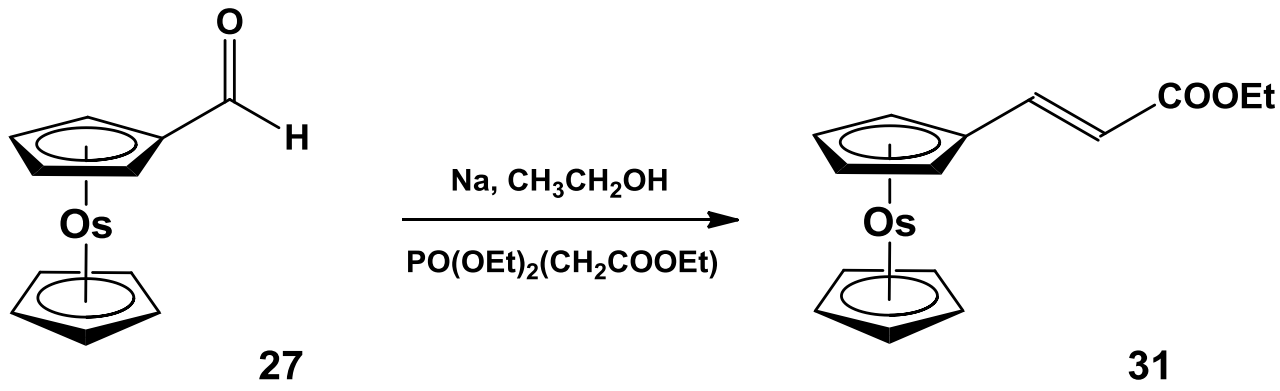

27 **31**

Sodium (72 mg, 2.72 mmol, 1.8 eq) was dissolved in dry ethanol (16 cm^3) at 0 ºC under argon. A mixture of triethylphosphonoacetate (0.3 cm^3, 1.435 mmol, 0.95 eq) and osmocenyl aldehyde (526 mg, 1.51 mmol) in absolute ethanol (40 cm^3) was added drop-wise to the sodium ethoxide solution and stirred for an hour. The ethanol was removed by rotary evaporation and the product purified using column chromatography with ethyl acetate:hexane as eluent (5:95). Yield 90.1% (570 mg). Melting point = 107 °C. IR: υ/cm^{-1} = 1634 (C=C), 1694 (C=O). **Spectrum 29**. ^{1}H NMR (300 MHz, $CDCl_3$)/ppm = 7.42 (d, J_{HH} = 15 Hz, 1H, $C\underline{H_2}$=$CH_2COOCH_2CH_3$), 5.93 (d, J_{HH} = 15 Hz, 1H, CH_2=$C\underline{H_2}COOCH_2CH_3$), 5.01 (t, J_{HH} = 1.44 Hz, 2H, 0.5 x C_5H_4), 4.87 (t, J_{HH} = 1.44 Hz, 2H, 0.5 x C_5H_4), 4.74 (s, 5H, C_5H_5), 4.18 (q, J_{HH} = 7.14 Hz, 2H, $COOC\underline{H_2}CH_3$), 0.88 (t, 3H, $COOCH_2C\underline{H_3}$). **Spectrum 9**. Retention factors: **27** = 0.02; **31** = 0.571.

4.4.9 Ethyl-3-osmocenylethanoate, 32.

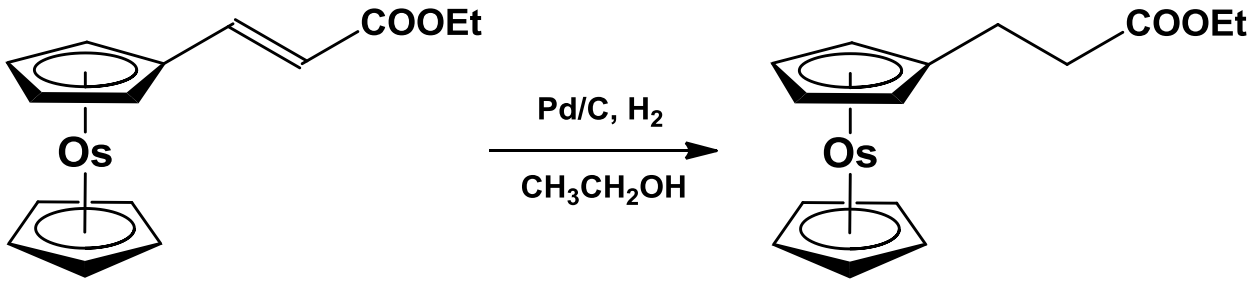

31 **32**

Ethyl-3-osmocenylethenoate (149 mg, 0.356 mmol) and palladium on charcoal (28 mg, 5% Pd/C) was suspended in absolute ethanol (20 cm^3). The suspension was stirred under 10 bar hydrogen atmosphere for 15 hours, followed by filtration through 3 cm of silica gel. Cold water was added to the filtrate and the product extracted with diethyl ether (3 x 50 cm^3). The ether was washed with distilled water, dried over anhydrous $MgSO_4$ and the solvent removed by rotary evaporation. Yield 70.2% (105 mg). Melting point = 44.7 – 45.8 °C. IR: υ/cm^{-1} = 1725 (C=O). **Spectrum 30**. ^{1}H NMR (300 MHz, $CDCl_3$)/ppm = 4.71 (t, J_{HH} = 3.52 Hz, 2H, 0.5 x C_5H_4), 4.70 (s, 5H, C_5H_5), 4.64 (t, J_{HH} = 3.23 Hz, 2H, C_5H_4), 4.16 (q, J_{HH} = 7.14 Hz, 2H, $COOC\underline{H_2}CH_3$), 2.50 (m, 4H, $C\underline{H_2}C\underline{H_2}COOEt$), 1.29 (t, J_{HH} = 5.84 Hz, 3H, $COOCH_2C\underline{H_3}$). **Spectrum 10**.

4.4.10 3-osmocenylpropanol, 21.

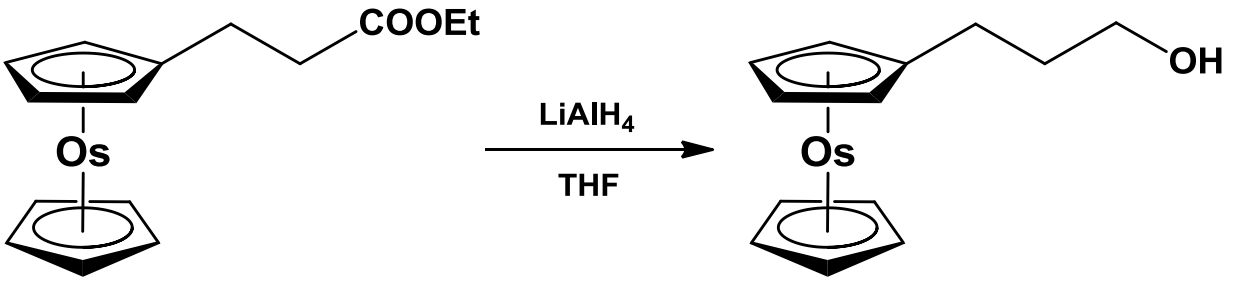

32 **21**

$LiAlH_4$ (16.28 mg, 0.429 mmol, 2.95 eq) was added to a round bottom flask under argon. A solution of ethyl-3-osmocenylethanoate (61 mg, 0.145 mmol) in tetrahydrofuran (20 cm^3) was added drop-wise to the round bottom flask and left to reflux for one hour. After cooling to room temperature, distilled water (15 cm^3) was added slowly. The alcohol was extracted with diethyl ether (2 x 50 cm^3), and washed with distilled water, dried over anhydrous $MgSO_4$ and the solvent removed under reduced pressure. Yield 93% (55 mg) as a white powder. Melting point = 120.6 – 123.4 °C. IR: υ/cm^{-1} = 3260 (O-H broad peak). **Spectrum 31**. ^1H NMR (300 MHz, $CDCl_3$)/ppm = 4.71 (t, J_{HH} = 1.33 Hz, 2H, 0.5 x C_5H_4), 4.68 (s, 5H, C_5H_5), 4.63 (t, J_{HH} = 1.33 Hz, 2H, 0.5 x C_5H_4), 3.68 (q, J_{HH} = 6.03 Hz, 2H, $CH_2CH_2C\underline{H_2}OH$), 2.32 (t, J_{HH} = 5.80 Hz, 2H, $C\underline{H_2}CH_2CH_2OH$), 1.69 (m, 2H, $CH_2C\underline{H_2}CH_2OH$). **Spectrum 11**. $^{13}C\{^1H\}$ NMR (150 MHz, $CDCl_3$)/ppm = 25.88 ($CH_2\underline{C}H_2CH_2$), 34.85 (CH_2), 62.81 ($\underline{C}H_2OH$), 63.13 (C_5H_4), 64.01 (C_5H_5), 65.08 (C_5H_4), 85.64 (C_5H_4). Elemental analysis (%): calc for $C_{13}H_{16}OOs$ (378.5): C, 41.3; H, 4.3; found: C, 44.1, H, 5.4.

4.4.11 3-osmocenylpropanoic acid, 24.

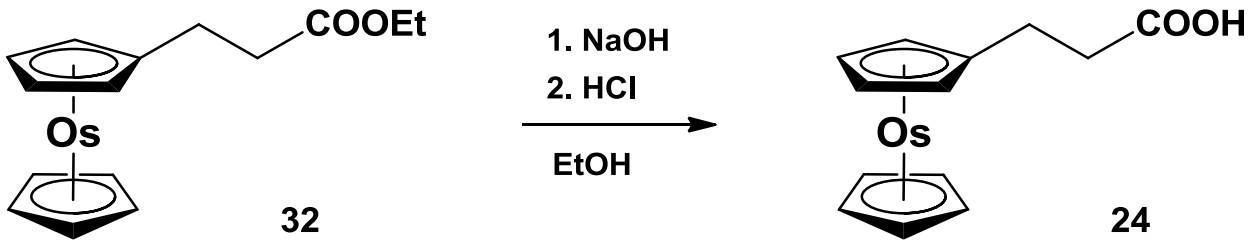

Ethyl-3-osmocenylethanoate, **32**, (15 mg, 0.035 mmol) was dissolved in absolute ethanol (2.5 cm^3), followed by the addition of 2 M NaOH (2.5 cm^3, 5 mmol, 142 eq). The reaction mixture was stirred for 1 hour at room temperature, followed by addition of ice (2.5 cm^3). The mixture was extracted with diethyl ether (3 x 50 cm^3). The aqueous layer was then acidified with 1 M HCl and left in ice. The precipitate was filtered, washed with small amounts of cold diethyl ether and air dried. Yield 56.8% (8 mg). Melting point = 174.1 – 176.5 °C. IR: υ/cm^{-1} = 1691 (C=O, acid), 2567 - 3107 (O-H broad peak), 2903 (C-H aromatic). **Spectrum 32**. ^{1}H NMR (300 MHz, $CDCl_3$)/ppm = 4.71 (t, J_{HH} = 1.24 Hz, 2H, 0.5 x C_5H_4), 4.69 (s, 5H, C_5H_5), 4.63 (t, J_{HH} = 1.24 Hz, 2H, 0.5 x C_5H_4), 2.52 (m, 4H, CH_2CH_2COOH). **Spectrum 12**. Elemental analysis (%): calc for $C_{13}H_{14}O_2Os$ (392.5): C, 39.7; H, 3.6; found: C, 38.7, H, 3.4.

4.4.12 3-osmocenylpropenoic acid, 33.

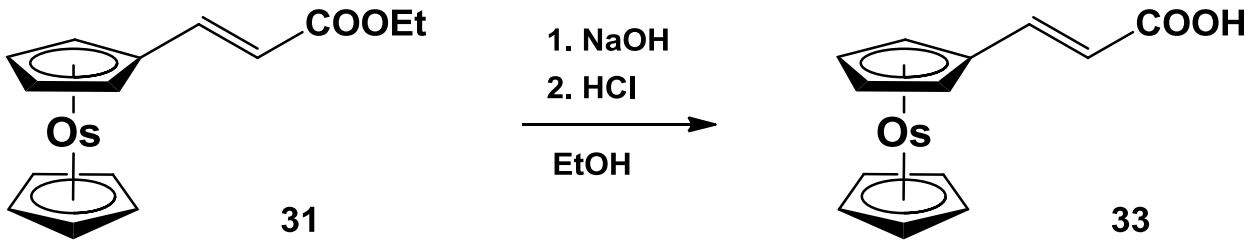

Ethyl-3-osmocenylethenoate, **31**, (14 mg, 0.034 mmol) was dissolved in absolute ethanol (2.5 cm^3), followed by the addition of 2 M NaOH (2.5 cm^3, 5 mmol, 147 eq). The reaction mixture was stirred overnight at room temperature, followed by addition of ice (2.5 cm^3). The mixture was extracted with diethyl ether (3 x 50 cm^3). The aqueous layer was then acidified with 1 M HCl and left in ice. The precipitate was filtered, washed with small amounts of cold diethyl ether and air dried. Yield 60.3% (8 mg). Melting point = 215.9 – 221.1 °C. IR: υ/cm^{-1} = 1617 (C=C), 1669 (C=O), 2477 – 3102 (O-H broad peak), 2747 (C-H). **Spectrum 33**. ^{1}H NMR (300 MHz, $CDCl_3$)/ppm = 7.53

(d, J = 15.7 Hz, 1H, C<u>H</u>=CHCOOH), 5.93 (d, J = 15.6 Hz, 1H, CH=C<u>H</u>COOH), 5.03 (t, J_{HH} = 1.33 Hz, 2H, 0.5 x C_5H_4), 4.91 (t, J_{HH} = 1.33 Hz, 2H, 0.5 x C_5H_4), 4.78 (s, 5H, C_5H_5). **Spectrum 13**. Elemental analysis (%): calc for $C_{13}H_{12}O_2Os$ (390.5): C, 40.0; H, 3.1; found: C, 32.9, H, 3.3.

4.4.13 3-(Carbomethoxy)propionic acid, 17.

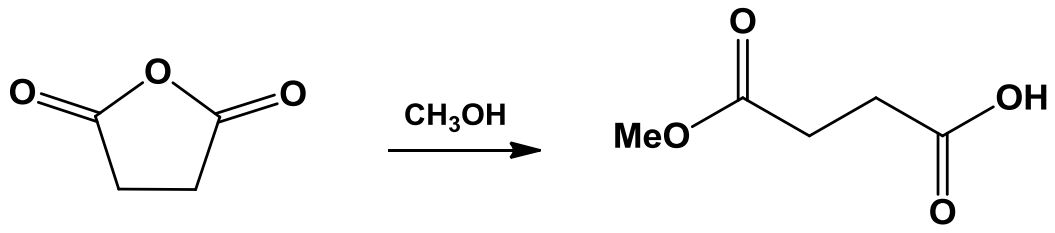

16 **17**

Succinic anhydride (10 g, 100 mmol) and methanol (5 cm^3, 120 mmol) were refluxed for 30 minutes on a steam bath. The mixture was stirred vigorously and refluxed for a further 30 minutes. The solvent was removed under reduced pressure and the contents was dried under vacuum for 16 hours. Yield 93.2% (12.3g). Melting point = 56.1 – 57.2 °C. IR: υ/cm^{-1} = 1171 (C-O), 1683 (C=O acid), 1727 (C=O ester). **Spectrum 34**. ^{1}H NMR (300 MHz, $CDCl_3$)/ppm = 3.72 (s, 3H, CH_3), 2.68 (m, 4H, CH_2CH_2). **Spectrum 14**.

4.4.14 3-(Carbomethoxy)propionyl chloride, 18.

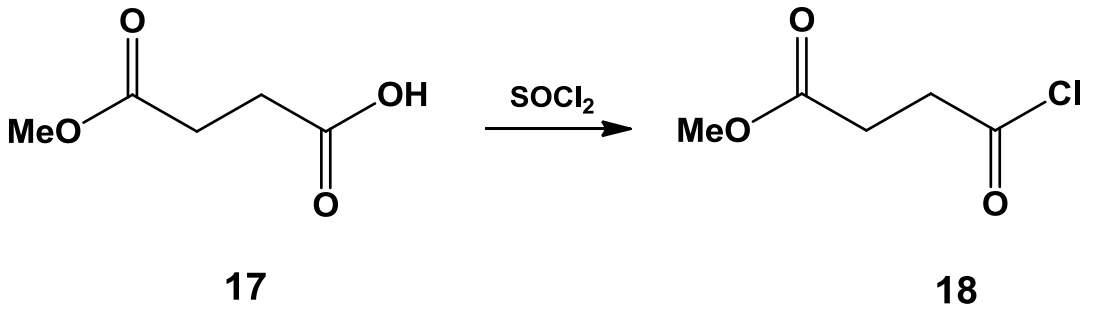

17 18

3-(Carbomethoxy)propionic acid (20.10 g, 151.4 mmol) and thionyl chloride (16.5 cm^3, 227.1 mmol, 1.5 eq) were refluxed at 30 – 40 ºC for 3 hours. The excess thionyl chloride was removed under reduced pressure and the product was collected by distillation under vacuum (below 3 mmHg). Yield 84.56% (19.37 g). Boiling point = 65 °C at 3 – 5 mmHg. IR: υ/cm^{-1} = 1734 (C=O, ester), 1788 (C=O, acid chloride). **Spectrum 35**. ^{1}H NMR (300 MHz, $CDCl_3$)/ppm = 3.67 (s, 3H, OCH_3), 3.19 (t, 2H, $CH_2C\underline{H_2}C(O)Cl$), 2.65 (t, 2H, $C\underline{H_2}CH_2C(O)Cl$). **Spectrum 15**.

4.4.15 Methyl-3-osmocenoyl propanoate, 34.

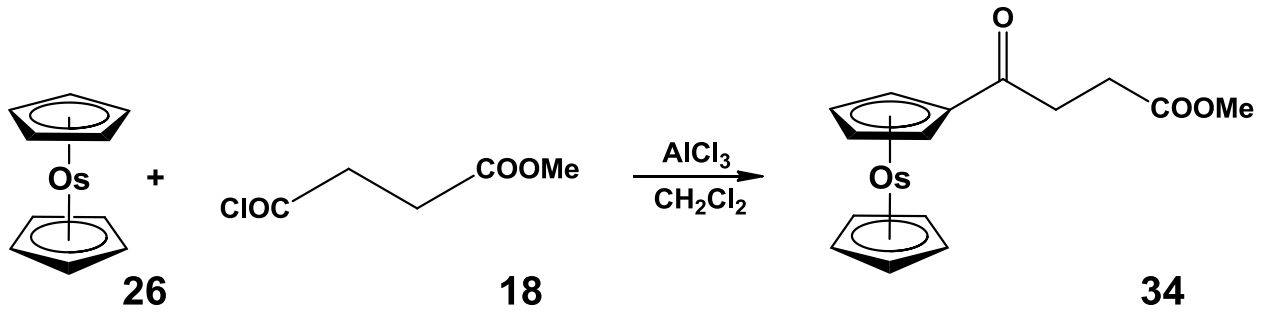

26 18 34

In a Schlenk tube, $AlCl_3$ (5 g, 37.4 mmol, 120 eq) and dry DCM (1 cm^3) were added and degassed. Osmocene (100 mg, 0.312 mmol) in DCM (3 cm^3) was added drop-wise. 3-(carbomethoxy)propionyl chloride (0.132 g, 0.87 mmol, 2.8 eq) in DCM (3 cm^3) added drop-wise over 20 minutes. The reaction was refluxed for 16 hours at room temperature. The reaction was quenched with cold water and extracted with DCM (3 x 50 cm^3). The DCM extracts were washed with water, dried over anhydrous $MgSO_4$ and the solvent removed by rotary evaporation. Purification was done by column chromatography with hexane:diethyl ether 1:1 as eluent. Yield

8.83% (17 mg). Melting point = 67 – 75 °C. IR: υ/cm^{-1} = 1661 (C=O, keto), 1724 (C=O, ester). **Spectrum 36**. ^{1}H NMR (300 MHz, $CDCl_3$)/ppm = 5.29 (t, J_{HH} = 1.33 Hz, 2H, 0.5 x C_5H_4), 4.97 (t, J_{HH} = 1.31 Hz, 2H, 0.5 x C_5H_4), 4.85 (s, 5H, C_5H_5), 3.71 (s, 3H, CO(O)C$\underline{H}_3$), 2.91 (t, J_{HH} = 6.7 Hz, 2H, CH_2), 2.64 (t, J_{HH} = 6.7 Hz, 2H, CH_2). **Spectrum 16**. Retention factors: **26** = 0.942; **34** = 0.63. Elemental analysis (%): calc for $C_{15}H_{16}O_3Os$ (434.5): C, 41.5; H, 3.7; found: C, 44.0, H, 4.4.

4.4.16 4-Osmocenylbutanol, 22.

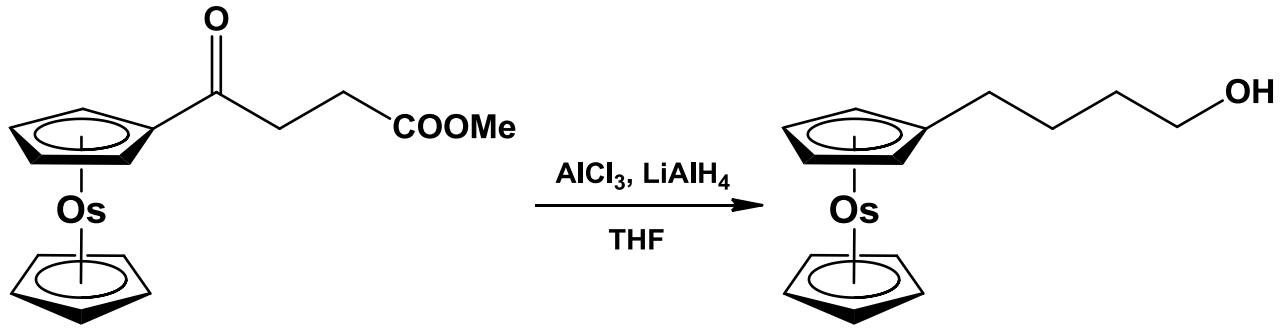

34 **22**

An ice cold suspension of $LiAlH_4$ (17.57 mg, 0.463 mmol, 4.3 eq) in dry THF (5 cm^3) was prepared in a degassed reflux setup. A suspension of $AlCl_3$ (67 mg, 0.504 mmol, 4.7 eq) in dry THF was added. Methyl-3-osmocenoylpropanoate (47 mg, 0.108 mmol) and $AlCl_3$ (57 mg, 0.429 mmol, 4 eq) were dissolved in THF (2.3 cm^3), added to the reaction flask, and left to stir for 30 minutes at room temperature. The mixture was refluxed for 3 hours and then cooled. Ice and water was added to the reaction mixture, followed by a few drops of concentrated sulphuric acid. The mixture was extracted with diethyl ether (3 x 50 cm^3), the solvent dried with anhydrous $MgSO_4$ and removed by rotary evaporation. Yield 75.4% (32 mg). Melting point = 54.6 – 56.7 °C. IR: υ/cm^{-1} = 3336 (O-H broad peak). **Spectrum 37**. ^{1}H NMR (300 MHz, $CDCl_3$)/ppm = 4.69 (t, J_{HH} = 1.38 Hz, 2H, 0.5 x C_5H_4), 4.66 (s, 5H, C_5H_5), 4.62 (t, J_{HH} = 1.27 Hz, 2H, 0.5 x C_5H_4), 3.65 (q, J_{HH} = 6.34 Hz, 2H, $CH_2CH_2CH_2C\underline{H}_2OH$), 2.24 (t, J_{HH} = 5.05 Hz, 2H, $C\underline{H}_2CH_2CH_2CH_2OH$), 1.21 (t, 4H, $CH_2C\underline{H}_2C\underline{H}_2CH_2OH$). **Spectrum 17**. $^{13}C\{^{1}H\}$ NMR = 28.28 ($\underline{C}H_2CH_2OH$), 29.39 ($\underline{C}H_2CH_2CH_2OH$), 32.71 ($\underline{C}H_2$), 62.87 ($CH_2OH$), 63.10 ($C_5H_4$), 63.94 ($C_5H_5$), 65.13 ($C_5H_4$), 86.12 ($C_5H_4$). Elemental analysis (%): calc for $C_{14}H_{18}OOs$ (392.5): C, 42.8; H, 4.6; found: C, 43.6, H, 5.7.

4.4.17 Methyl-4-osmocenylbutanoate, 35.

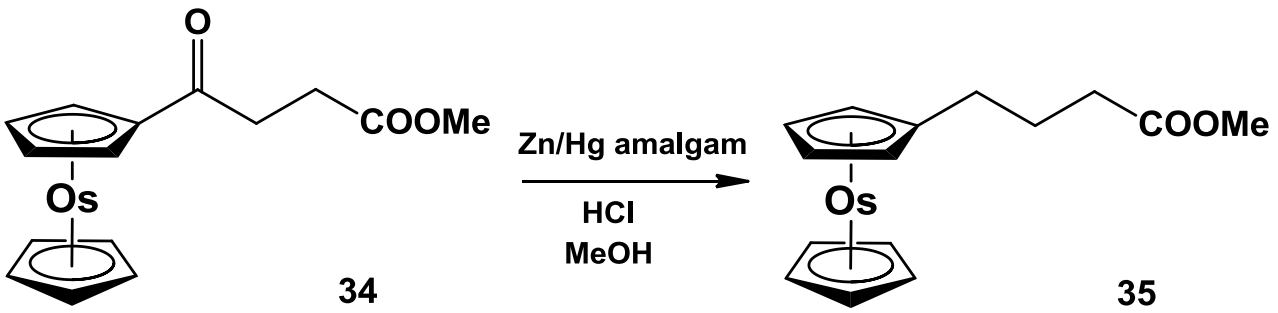

Zn/Hg amalgam:

Zinc granules (10 g) were cut into small pieces, 5 mm^3 or smaller. The granules were poured into a solution of 1 M HCl and left to stand for 5 minutes. The granules were then rinsed with water for 5 minutes. A solution of $HgCl_2$ (0.8 g) in concentrated HCl (0.5 cm^3) and water (11 cm^3). The mixture was stirred vigourously for 10 minutes. The liquid was decanted and the zinc amalgam was washed with water, methanol, 2M HCl and water again.

3-osmocenoylpropionic acid (28 mg, 0.0644 mmol) was added to a mixture of concentrated HCl (6 cm^3), distilled water (12.5 cm^3) and methanol (7.5 cm^3). Zinc/mercury amalgam (10 g) was added, and the reaction mixture was refluxed at 60 °C for 7 days. Every 12 hours, the reaction mixture was topped up with HCl (1cm^3) and methanol (to the original volume of the solution). Once cooled, the mixture was extracted with DCM, dried over $MgSO_4$ and the solvent removed by rotary evaporation. Yield 45.6% (12 mg). Melting point = 42.0 – 43.1 °C. IR: υ/cm^{-1} = 1734 (C=O, ester). **Spectrum 38**. ^{1}H NMR (300 MHz, $CDCl_3$)/ppm = 4.69 (t, J_{HH} = 1.33 Hz, 2H, 0.5 x C_5H_4), 4.68 (s, 5H, C_5H_5), 4.62 (t, J_{HH} = 1.28 Hz, 2H, 0.5 x C_5H_4), 3.67 (s, 3H, OCH_3), 2.35 (t, J_{HH} = 5.20 Hz, 2H, CH_2), 2.24 (t, J_{HH} = 6.69 Hz, 2H, CH_2), 1.74 (m, 2H, $CH_2C\underline{H_2}CH_2$). **Spectrum 18**.

4.4.18 4-osmocenylbutanoic acid, 25.

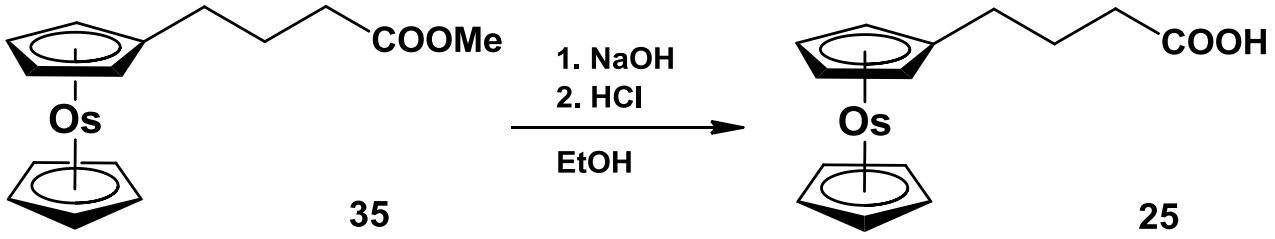

Methyl-4-osmocenylbutanoate (12 mg, 0.035 mmol) was dissolved in absolute ethanol (5 cm^3), followed by the addition of 2 M NaOH (3 cm^3, 6 mmol, 171 eq). The reaction mixture was stirred for 3 hours at room temperature, followed by addition of ice (3 cm^3). The mixture was extracted with diethyl ether (3 x 50 cm^3). The aqueous layer was then acidified with 1 M HCl and left in ice overnight. The precipitate was filtered, washed with small amounts of cold diethyl ether and air dried. Yield 34.5% (4 mg). Melting point = 120.6 – 123.4 °C. IR: υ/cm^{-1} = 1702 (C=O, acid). **Spectrum 39**. ^{1}H NMR (300 MHz, $CDCl_3$)/ppm = 4.69 (t, J_{HH} = 1.24 Hz, 2H, 0.5 x C_5H_4), 4.68 (s, 5H, C_5H_5), 4.62 (t, J_{HH} = 1.24 Hz, 2H, 0.5 x C_5H_4), 2.40 (t, J_{HH} = 5.98 Hz, 2H, CH_2), 2.27 (t, J_{HH} = 6.67 Hz, 2H, CH_2), 1.75 (m, 2H, $CH_2C\underline{H_2}CH_2$). **Spectrum 19**. Elemental analysis (%): calc for $C_{14}H_{16}O_2Os$ (406.5): C, 41.4; H, 4.0; found: C, 46.8, H, 6.5.

4.6 Electrochemistry

Cyclic voltammetry (CV), linear-sweep voltammetry (LSV) and square wave voltammetry (SW) were performed using a Princeton Applied Research PARSTAT 2273. Voltammographs were recorded using Powersuite (version 2.58). A platinum wire was used as an auxiliary electrode and a silver wire as reference electrode. A glassy carbon electrode was used as the working electrode, with surface area 3.14 mm^2. The working electrode was polished on a Buhler polishing mat, utilising 1 micron and then ¼ micron diamond paste. All electrochemical experiments were carried out in a Siemens MBraun Lab Master glovebox, utilising high purity argon (H_2O and O_2 < 10 ppm). Solutions contained 0.5 mM of analyte (osmocene derivative), 0.5 mM of decamethylferrocene as internal standard and 0.1 M tetrabutylammonium tetrakis(pentafluorophenyl)borate as the supporting electrolyte. All complexes were dissolved in 1 cm^3 anhydrous dichloromethane as solvent.

References

1. D. B. G. Williams and M. Lawton, *J. Org. Chem.*, 2010, **75**, 8351–8354.

5 Summary and Future Perspectives

5.1 Summary

This project focused on the synthesis, characterization and electrochemical studies of osmocene-containing carboxylic acids and alcohols.

A series of osmocene-containing carboxylic acids of the type $Oc(CH_2)_mCOOH$, where m = 1, 2 and 3, were synthesised by multiple-step synthetic routes. 2-Osmocenylethanoic acid, **23**, was synthesised under new reaction conditions, to provide an overall yield of 7.1%. The second carboxylic acid in the series, 3-osmocenylpropanoic acid, **24**, was synthesised from stable precursors (osmocenecarboxaldehyde, **27**, and ethyl-3-osmocenylethanoate, **32**). A multi-step reaction path was followed to obtain **24** with good average yields of 56.8%. The overall yield for 3-osmocenylpropanoic acid, **24**, is 28.5%. The last carboxylic acid in the series, 4-osmocenylbutanoic acid, **25**, was synthesised in three steps, however, the first osmocene-derivative, methyl-3-osmocenoylpropanoate, **34**, was difficult to obtain in high yields (8.8%). Therefore, 4-osmocenylbutanoic acid, **25**, was obtained in a very low overall yield of 1.4%. The overall low yields highlight the significantly lower reactivity of osmocene compared to other metallocenes in the same series, e.g. ferrocene and ruthenocene.

A series of osmocene-containing alcohols of the type, $Oc(CH_2)_nOH$ where n = 1, 2, 3 and 4, were also synthesised in this study by multiple-step synthetic routes. The first alcohol in the series, osmocenylmethanol, **19**, was obtained in good yields (91.3%) due to its precursor, osmocenecarboxaldehyde, **27**, being easily synthesised and reactive towards reduction. A good overall yield of 72.6% was obtained for osmocenylmethanol, **19**. The second alcohol in the series, 2-osmocenylethanol, **20**, was synthesised in a low overall yield of 6.5% due to the instability of its precursor compounds (*N,N*-dimethylaminomethylosmocene, **28**, and *N,N,N*-trimethylaminomethyl osmocene iodide, **29**). The third alcohol in the series, 3-osmocenylpropanol, **21**, was synthesised in an overall yield of 46.8%. The last alcohol in this series, 4-osmocenylbutanol, **22**, was difficult to obtain in high yields since the precursor, methyl-3-osmocenylpropanoate, **34**, proved very difficult to synthesise in good yields. Therefore, the overall yield for 4-osmocenylbutanol, **22**, is 6.7%.

All compounds synthesised were characterized using melting points, infrared spectroscopy, ^{1}H nuclear magnetic resonance spectroscopy and electrochemical methods; for two compounds (2-osmocenylacetonitrile and 2-osmocenylethanol) crystal structures were elucidated.

The electrochemical study of osmocene-containing carboxylic acids, $Oc(CH_2)_mCOOH$ where m = 1, 2 and 3 were determined. Cyclic voltammetry experiments were conducted in DCM and 0.1 M $[NBu_4][B(C_6F_5)_4]$ as supporting electrolyte. Dimerisation products were observed electrochemically for 2-osmocenylethanoic acid, **23**, and 3-osmocenylpropanoic acid, **24**. The increasing number of $–CH_2–$ spacers were found to lower the extent of dimerisation of the carboxylic acids; no dimerisation products were observed electrochemically on CV-timescale for 4-osmocenylbutanoic acid, **25**. The formal reduction potentials (E°´) for each compound was also observed to decrease, as the number of $–CH_2–$ spacers were increased. The formal reduction potentials for 2-osmocenylethanoic acid, **23**, 3-osmocenylpropanoic acid, **24** and 4-osmocenylbutanoic acid, **25**, are 418 mV, 357 mV and 317 mV respectively. The increase in $–CH_2–$ spacers isolates the COOH functionality from the osmocenyl moiety. Longer side chains also caused a decrease in dimerisation products.

An electrochemical study of osmocene-containing alcohols, $Oc(CH_2)_nOH$ where n = 1, 2, 3 and 4, was also conducted. The cyclic voltammetry of osmocenylmethanol, **19**, was performed immediately after synthesis, due to the compounds instability. However, decomposition of the compound was observed electrochemically. No dimerisation products were observed electrochemically for osmocenylmethanol, **19**. However, dimerisation was observed electrochemically for 2-osmocenylethanol, **20**, and 3-osmocenylpropanol, **21**. The electrochemistry of 4-osmocenylbutanol, **22**, was observed to be chemically reversible with an i_{pc}/i_{pa} value of 0.92; no dimerisation was observed. A trend between the number of $–CH_2–$ species and the formal reduction potentials for the alcohols was also observed. As the number of $–CH_2–$ spacers increase, the formal reduction potential for the alcohol decreases. The formal reduction potentials for osmocenylmethanol, **19**, 2-osmocenylethanol, **20**, 3-osmocenylpropanol, **21**, and 4-osmocenylbutanol, **22**, are 410 mV, 340 mV, 313 mV and 321 mV, respectively.

The crystal structures of 2-osmocenylacetonitrile, **30**, (monoclinic, $P2_1/c$, Z = 4, R = 0.057) and 2-osmocenylethanol, **20**, (trigonal, $P\bar{3}$, Z = 18, R = 0.092) were determined by single crystal X-ray diffraction (XRD). The alcohol, **20**, showed a hydrogen bond network that involved six interacting

molecules to create a hexagonal pattern between the OH functionalities. The nitrile, **30**, showed the nitrile functionality to be orientated in such a way that it faced the osmium atom side, or in the closest intramolecular proximity.

5.2 Future Perspectives

This study has researched new and optimised methods for the preparation of osmocene-containing carboxylic acids and alcohols. This has opened a new field for osmocene chemistry, which has been fairly limited thus far due to the low reactivity of osmocene, and hence unavailability of osmocene derivatives.

Cytotoxic studies of the synthesised compounds could not be determined during the duration of this study, due to time constraints, but can now be researched. The formal reduction potentials of the carboxylic acids and the alcohols show a trend with the increasing number of $–CH_2–$ in the synthesised compounds. By relating the cytotoxic results with reduction potentials, it may be possible to predict osmocene derivative antineoplastic activity from electrochemical measurements.

The osmocene-containing carboxylic acids and alcohols that were synthesised in this study may also be anchored onto polymeric drug carriers, such as polyaspartamide or polyphosphazene polymers. The electrochemical and cytotoxic studies of these osmocenyl-polymer conjugates may provide more insight into the characteristics and properties of these new compounds. Also, a comparative study of the osmocenyl derivatives and the anchored osmocenyl-polymer conjugates may provide insight on improving the compounds antineoplastic activity.

Ferrocene and ruthenocene-containing chloroquine and aminoquinoline derivatives have showed promising results in antimalarial activity.[1] These compounds were synthesised using the ferrocenyl and ruthenocenyl equivalents of *N,N*-dimethylaminomethylosmocene, **28**, that was synthesised in this study. Therefore, this osmocenyl derivative can be utilised to prepare osmocene-containing chloroquines and aminoquinolines, with potential antimalarial activity.

Ferrocenyl derivatives, such as 4-ferrocenylbutanol, have been shown to possess catalytic activity, in this case a solid propellant catalyst with high-burning rate activity.[2] Ferrocene-containing rhodium complexes have also been found to possess catalytic activity.[3] Catalytic studies on the osmocene-containing carboxylic acids and alcohols synthesised in this study or new osmocenyl derivatives may provide new and useful information on osmocene chemistry.

References

1. P. Beagley, M. A. L. Blackie, K. Chibale, C. Clarkson, J. R. Moss and P. J. Smith, *J. Chem. Soc. Dalton Trans.*, 2002, **23**, 4426–4433.
2. W. L. Davis, R. F. Shago, E. H. G. Langner and J. C. Swarts, *Polyhedron*, 2005, **24**, 1611–1616.
3. J. Conradie and J. C. Swarts, *Dalton Trans.*, 2011, **40**, 5844–5851.

Appendix

^{1}H NMR Spectra

Spectrum 1: Osmocenecarboxaldehyde, 27.

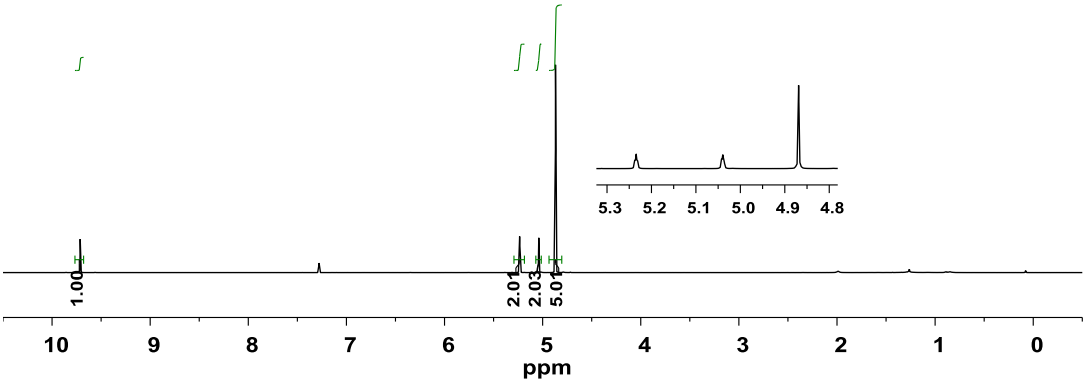

Spectrum 2: Osmocenedicarboxaldehyde, 36.

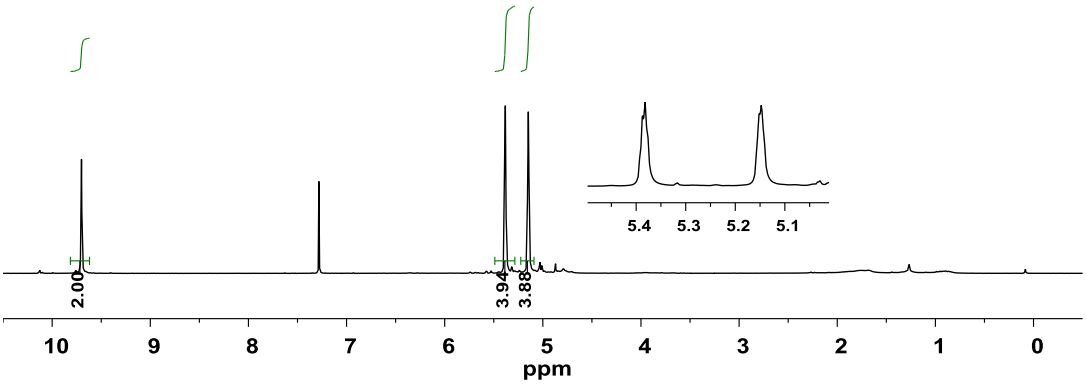

Spectrum 3: Osmocenylmethanol, 19.

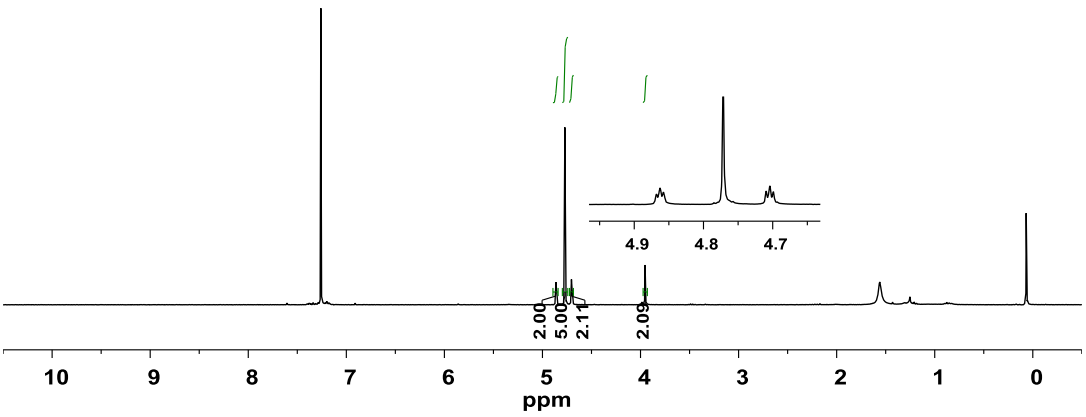

Spectrum 4: N,N-dimethylaminomethyl osmocene, 28, d_4-THF.

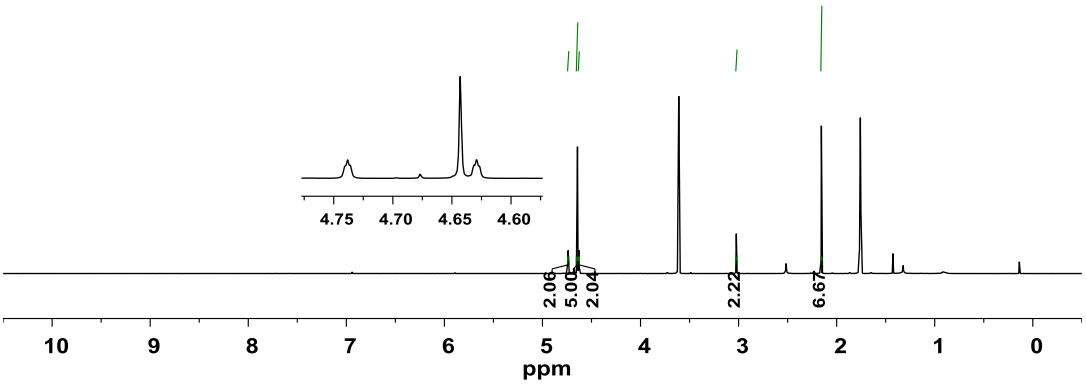

Spectrum 5: N,N,N-trimethylaminomethyl osmocene iodide, 29, in D_2O.

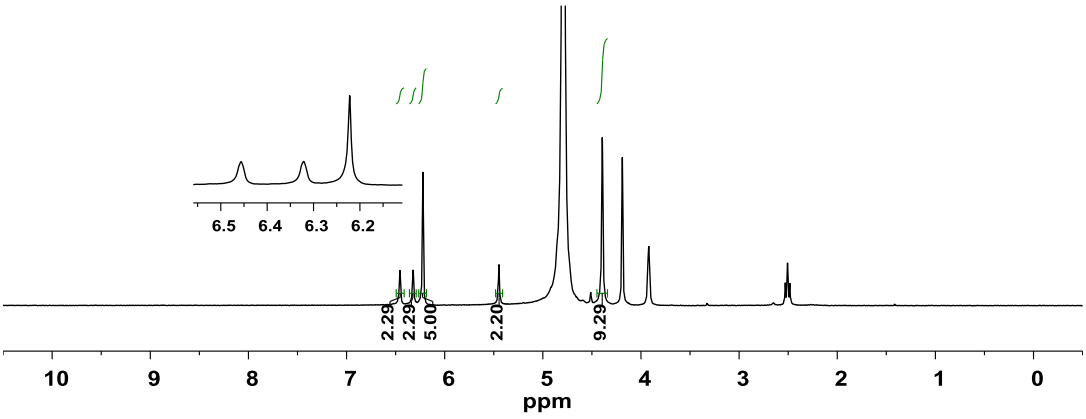

Spectrum 6: 2-osmocenylacetonitrile, 30.

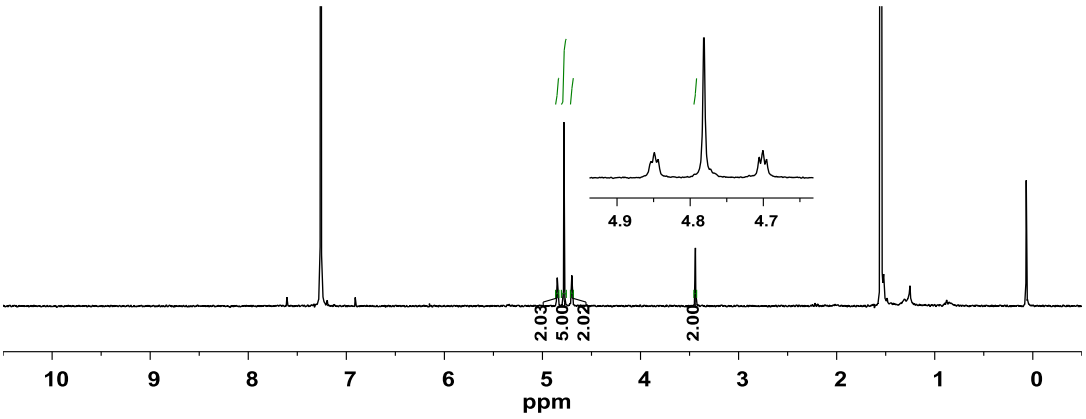

Spectrum 7: 2-osmocenylethanoic acid, 23.

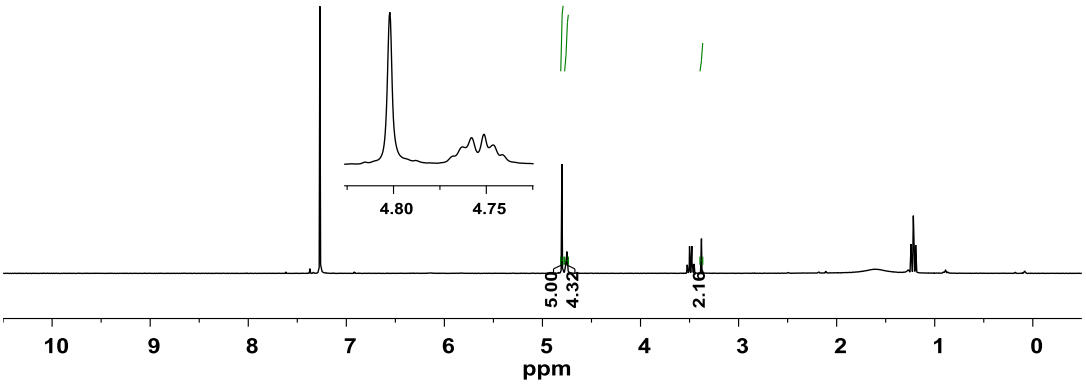

Spectrum 8: 2-osmocenylethanol, 20.

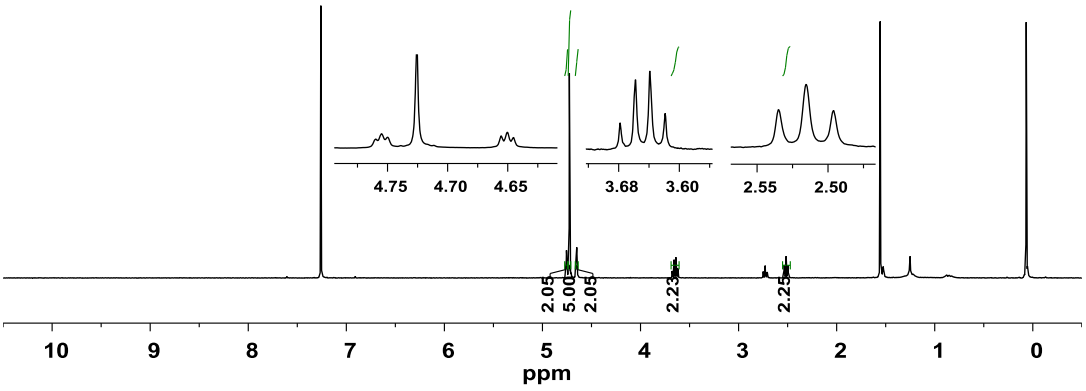

Spectrum 9: Ethyl-3-osmocenylethenoate, 31.

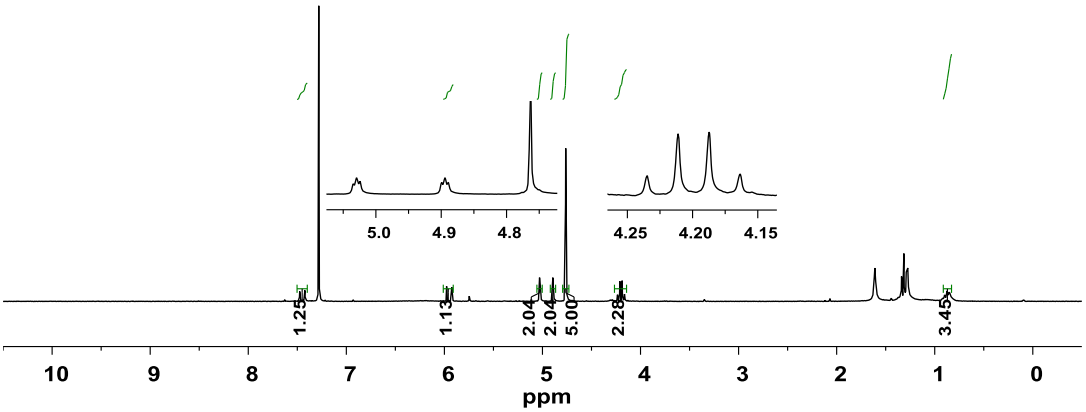

Spectrum 10: Ethyl-3-osmocenylethanoate, 32.

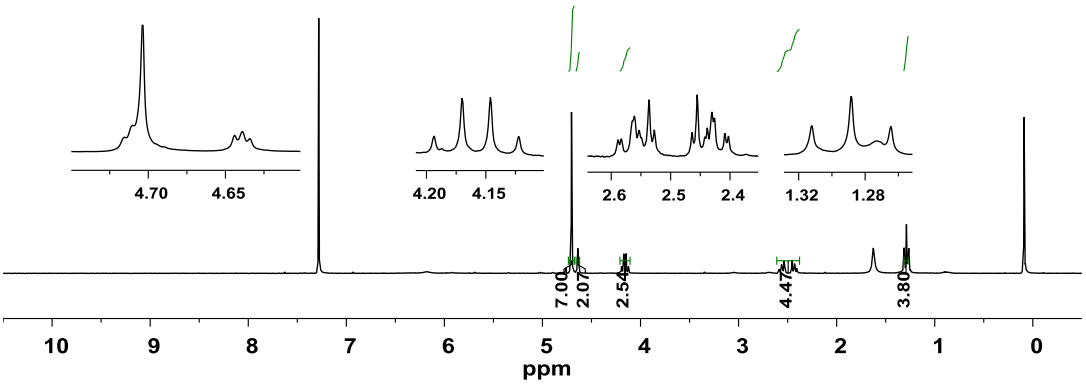

Spectrum 11: 3-osmocenylpropanol, 21.

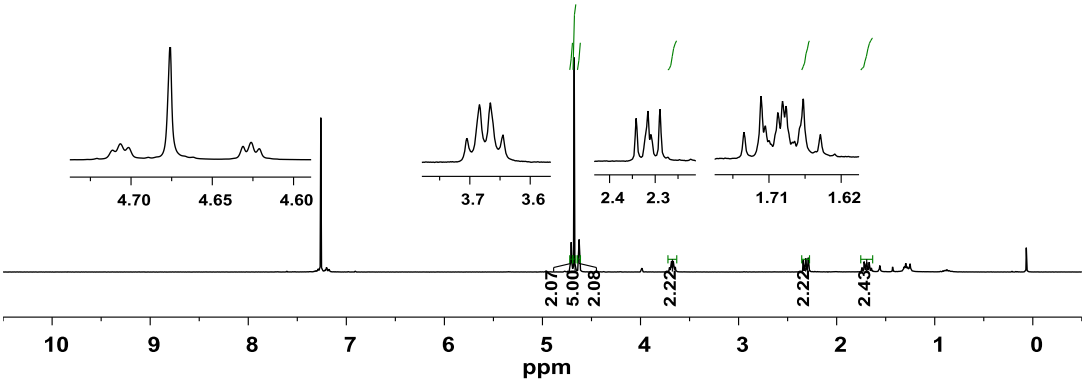

Spectrum 12: 3-osmocenylpropanoic acid, 24.

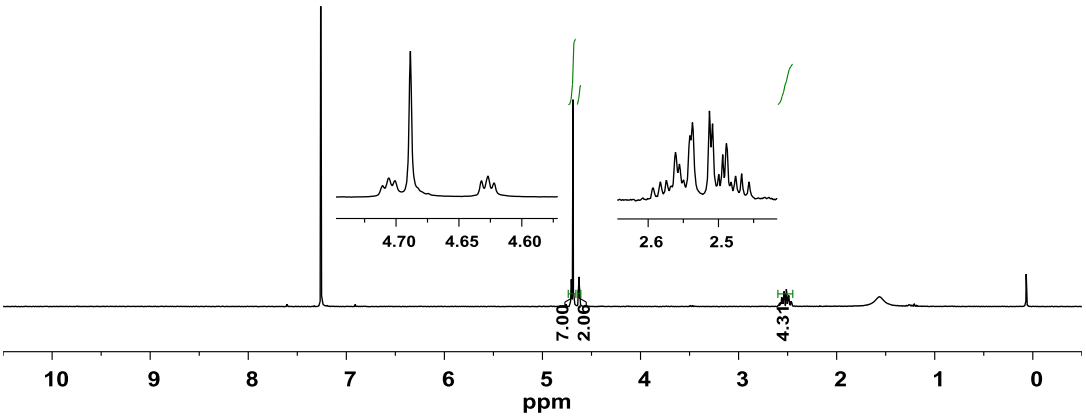

Spectrum 13: 3-osmocenylpropenoic acid, 33.

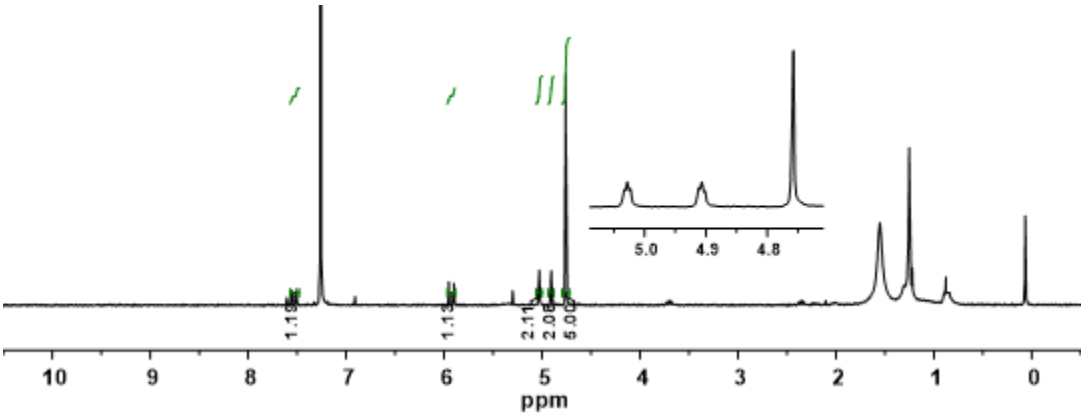

Spectrum 14: 3-carbomethoxypropionic acid, 17.

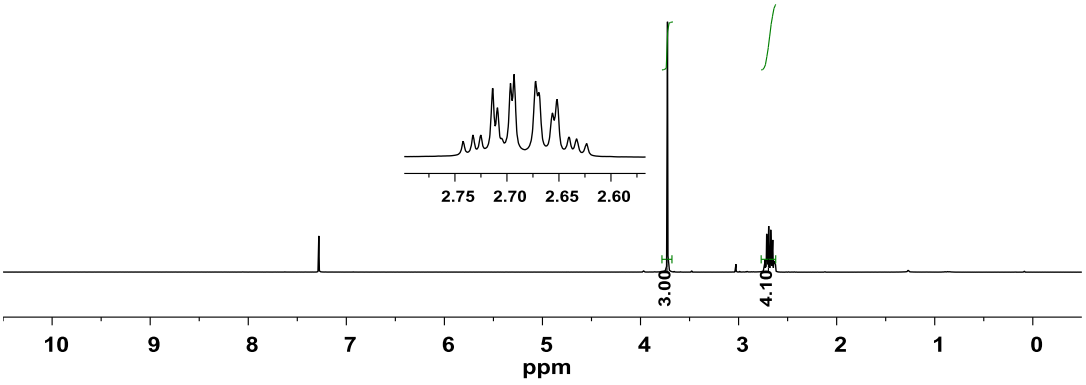

Spectrum 15: 3-carbomethoxypropionyl chloride, 18.

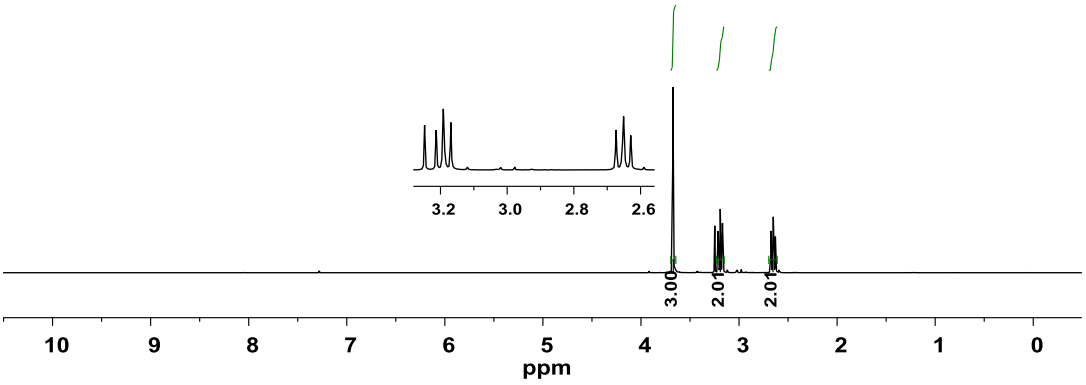

Spectrum 16: Methyl-3-osmocenoylpropanoate, 34.

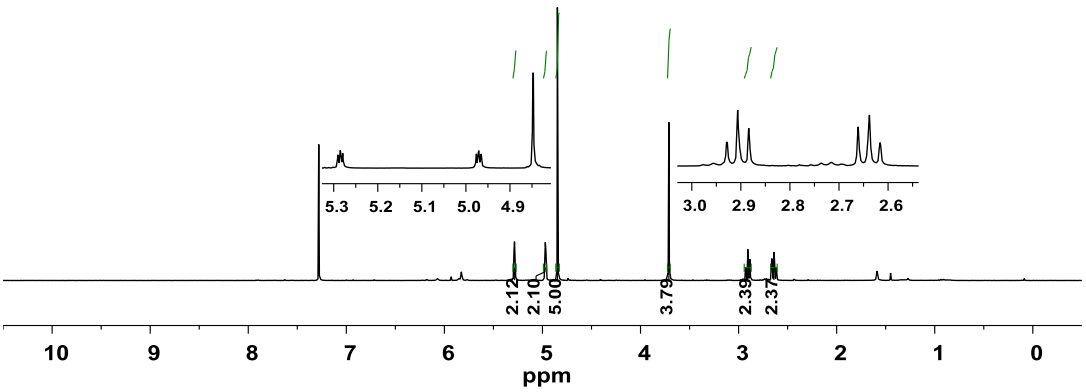

Spectrum 17: 4-osmocenylbutanol, 22.

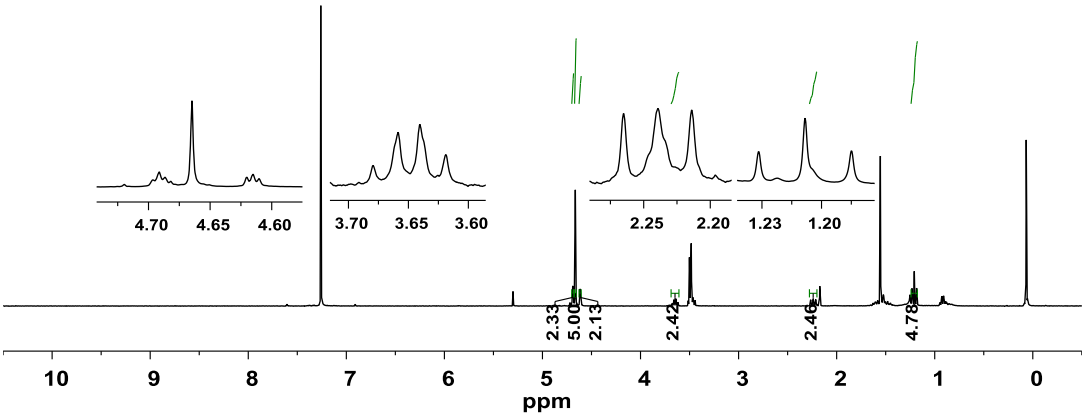

Spectrum 18: Methyl-4-osmocenylbutanoate, 35.

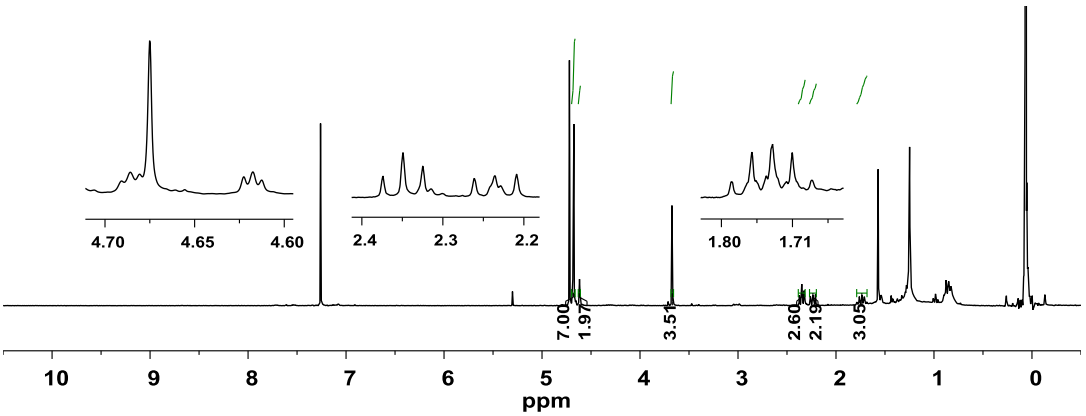

Spectrum 19: 4-osmocenylbutanoic acid, 25.

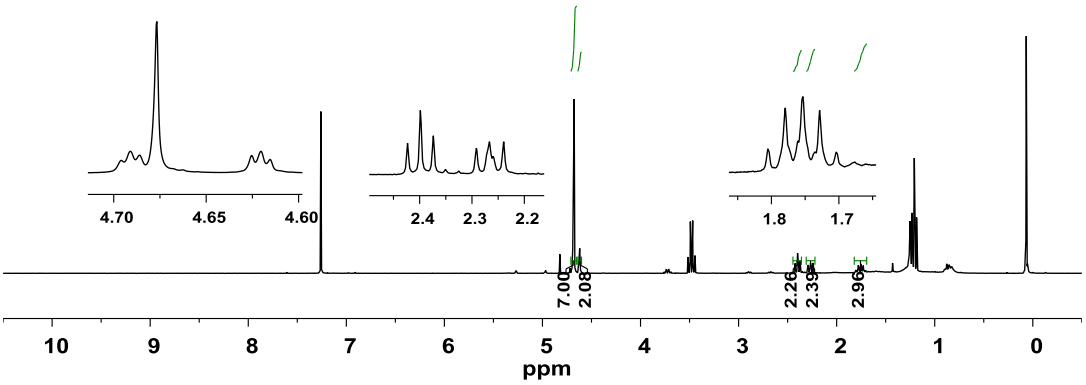

Spectrum 20: N-hydrogen-N,N,-dimethylaminomethylosmocene cation, 28b.

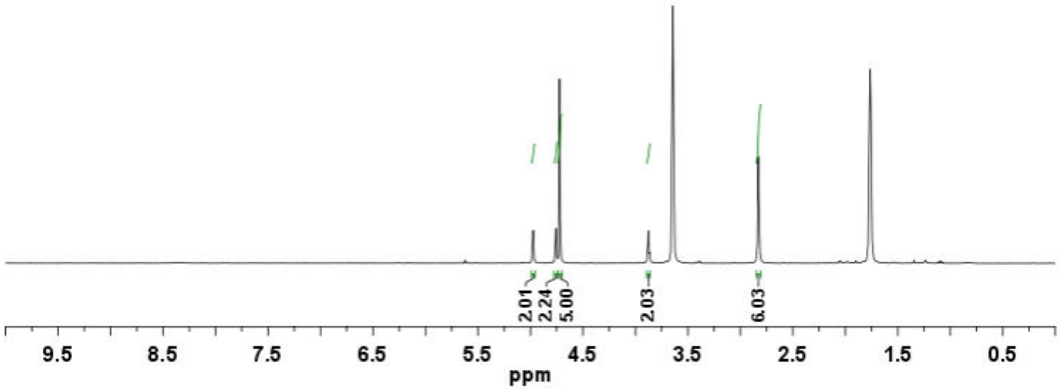

IR Spectra

Spectrum 21: Osmocenecarboxaldehyde, 27.

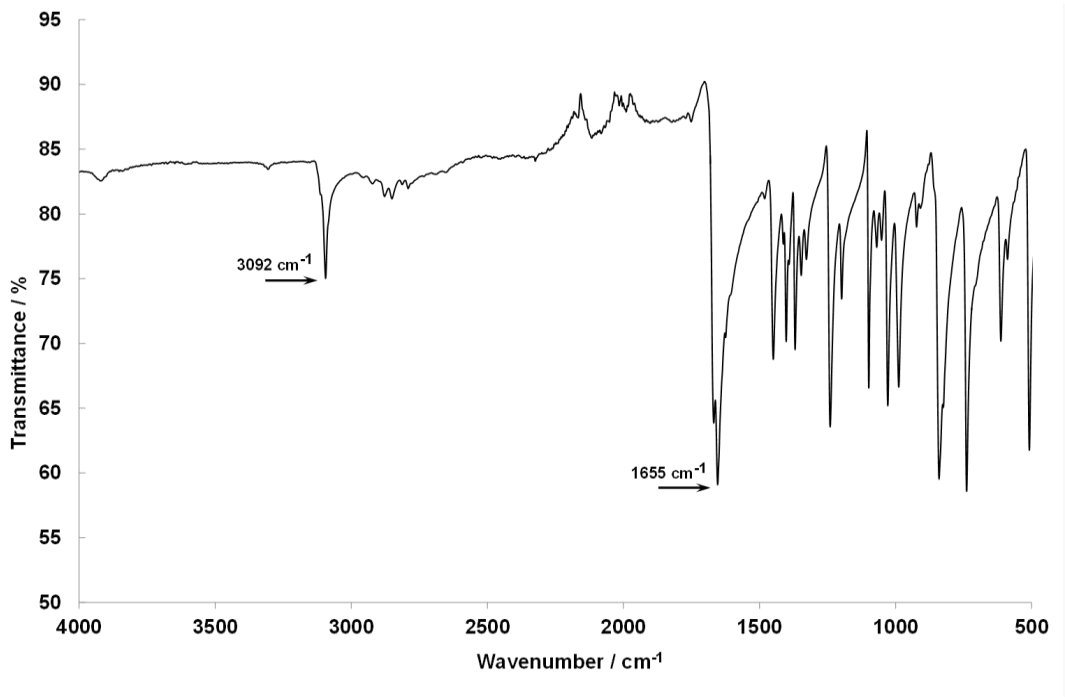

Spectrum 22: Osmocenedicarboxaldehyde, 36.

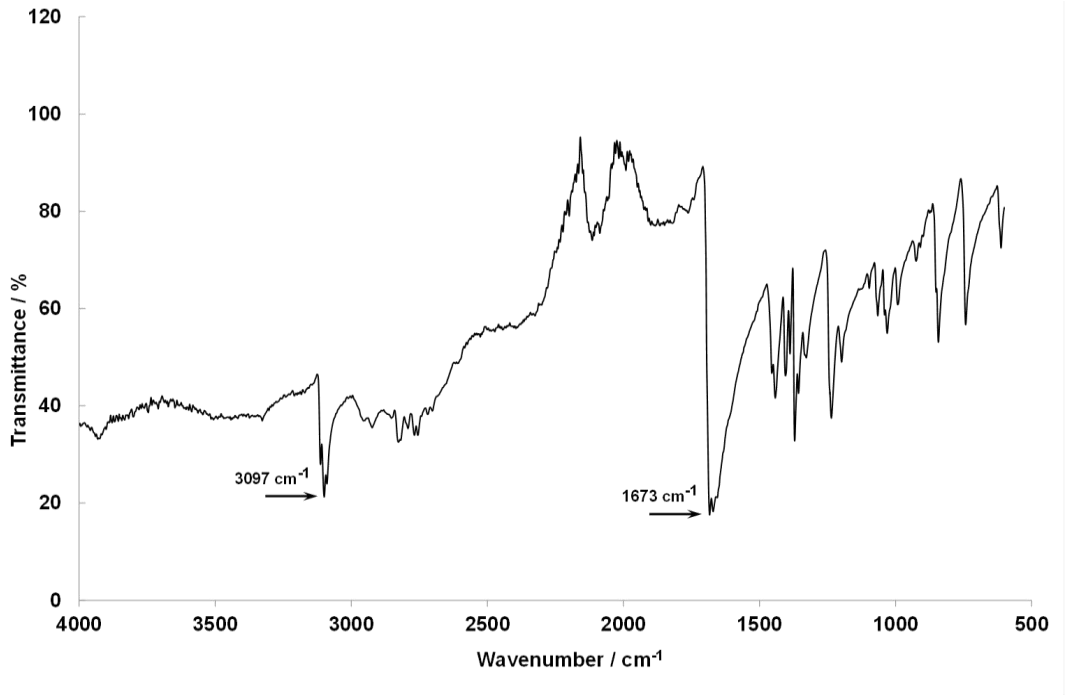

Spectrum 23: Osmocenylmethanol, 19.

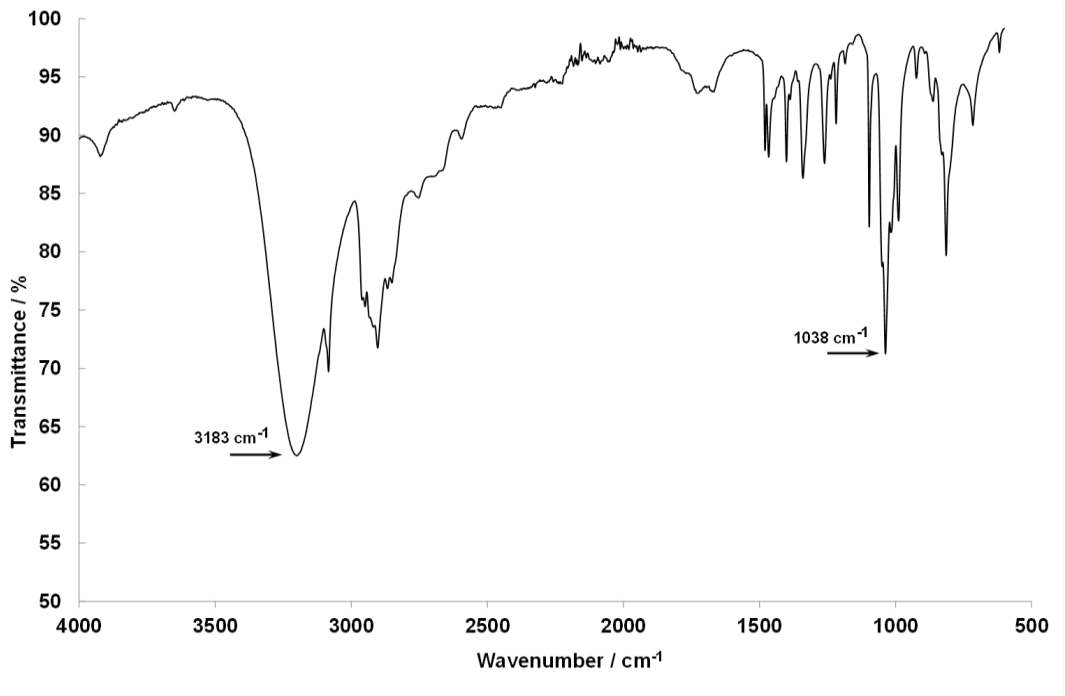

Spectrum 24: N,N-dimethylaminomethyl osmocene, 28.

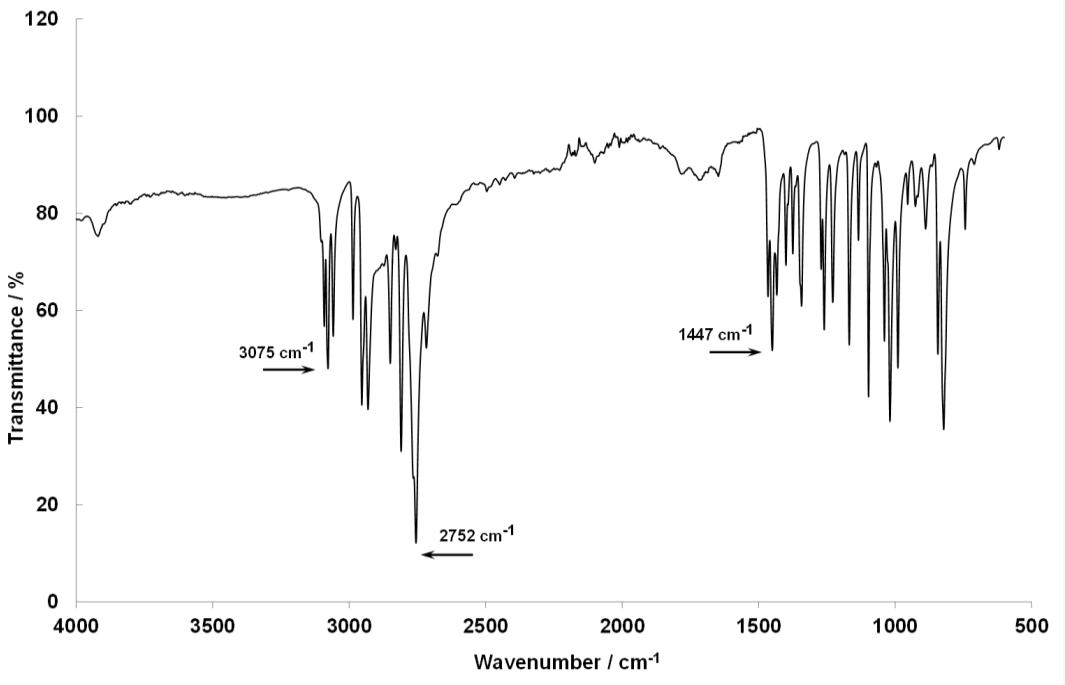

Spectrum 25: N,N,N-trimethylaminomethyl osmocene iodide, 29.

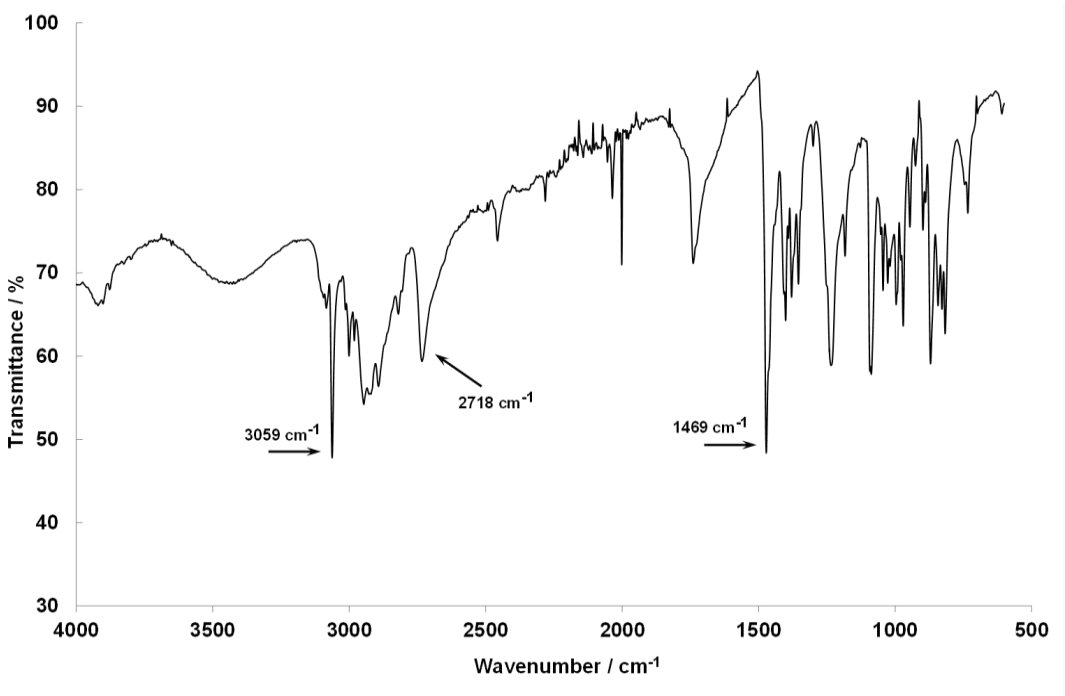

Spectrum 26: 2-osmocenylacetonitrile, 30.

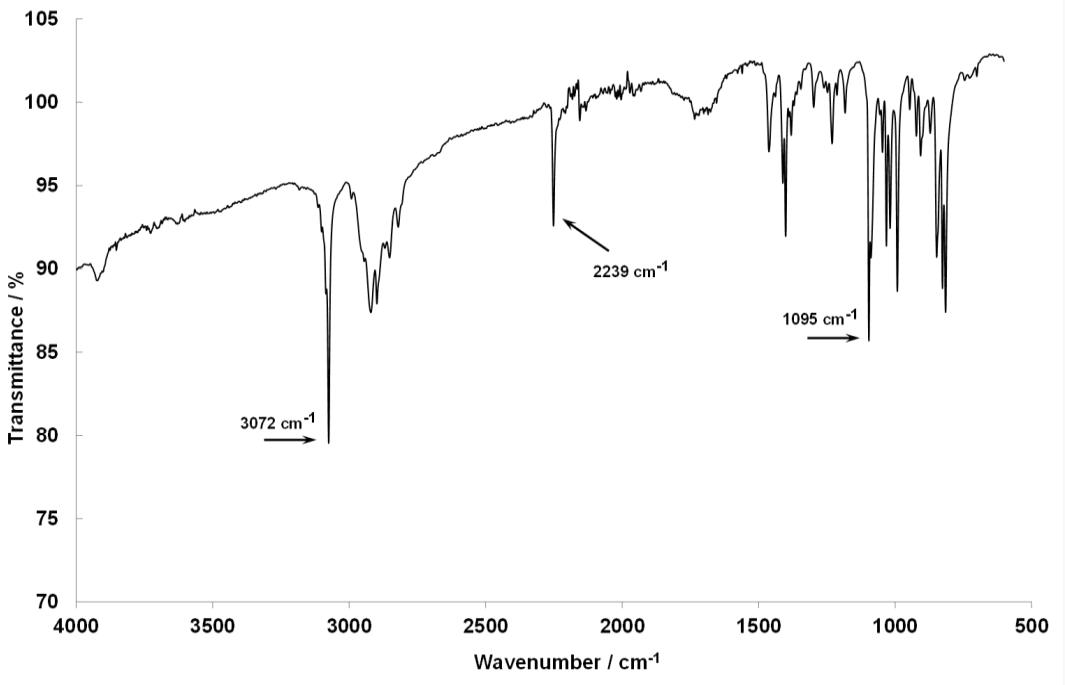

Spectrum 27: 2-osmocenylethanoic acid, 23.

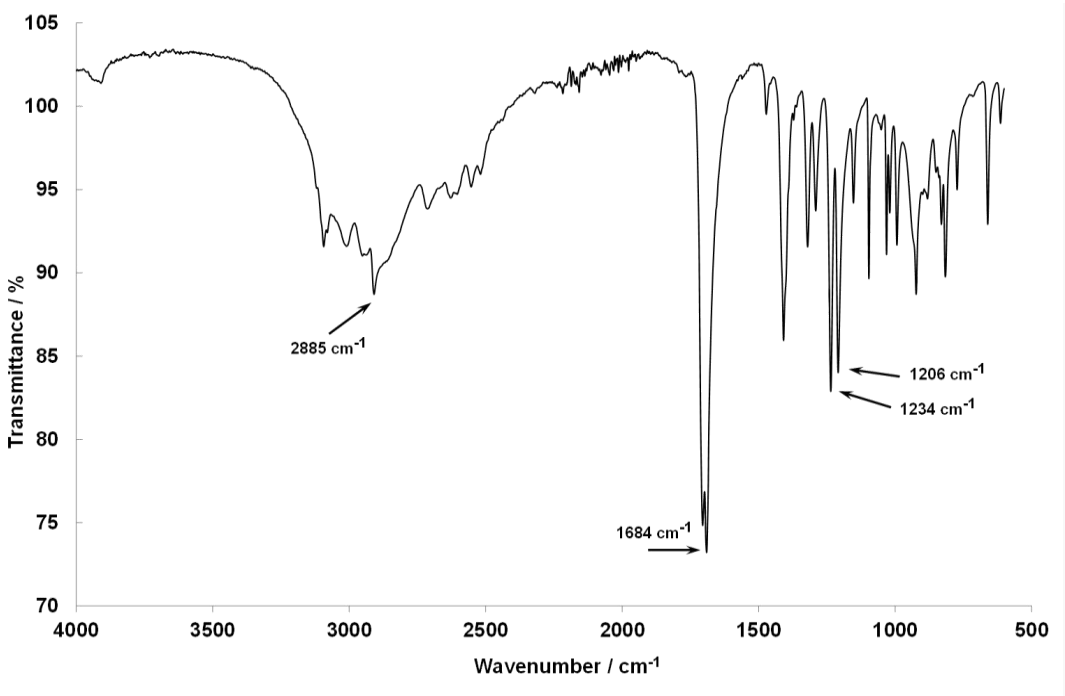

Spectrum 28: 2-osmocenylethanol, 20.

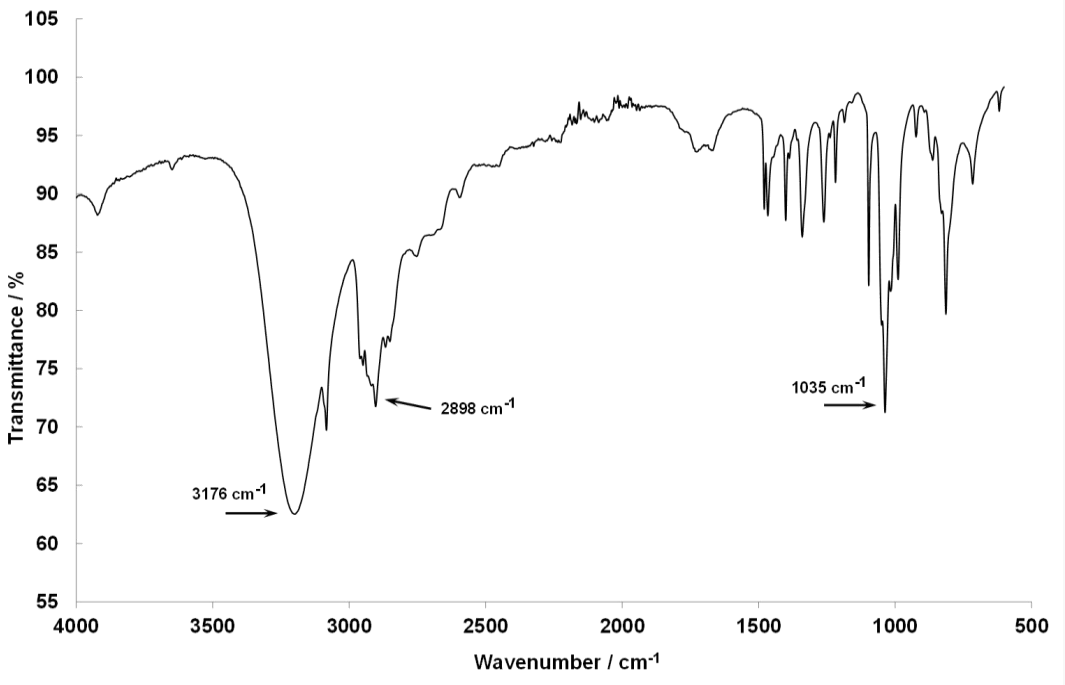

Spectrum 29: Ethyl-3-osmocenylethenoate, 31.

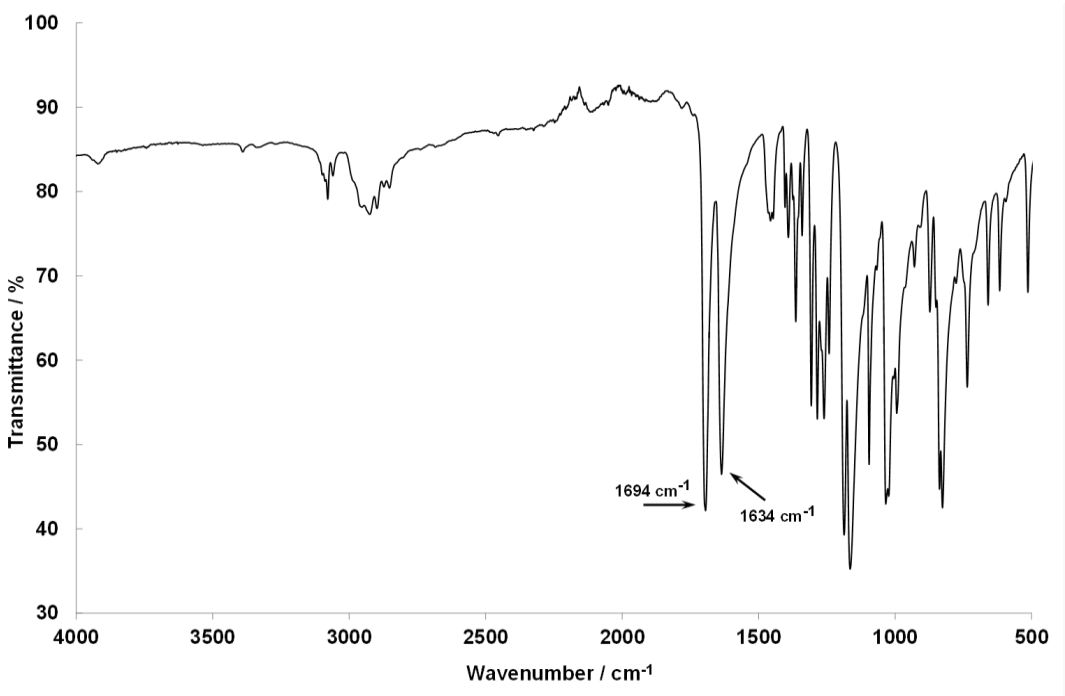

Spectrum 30: Ethyl-3-osmocenylethanoate, 32.

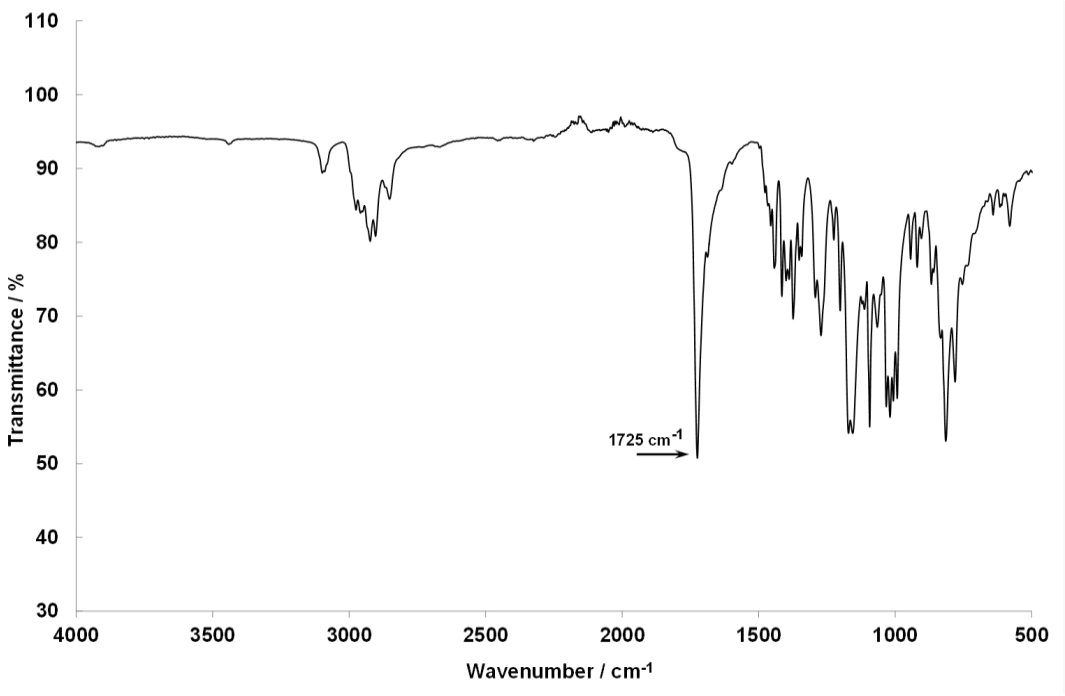

Spectrum 31: 3-osmocenylpropanol, 21.

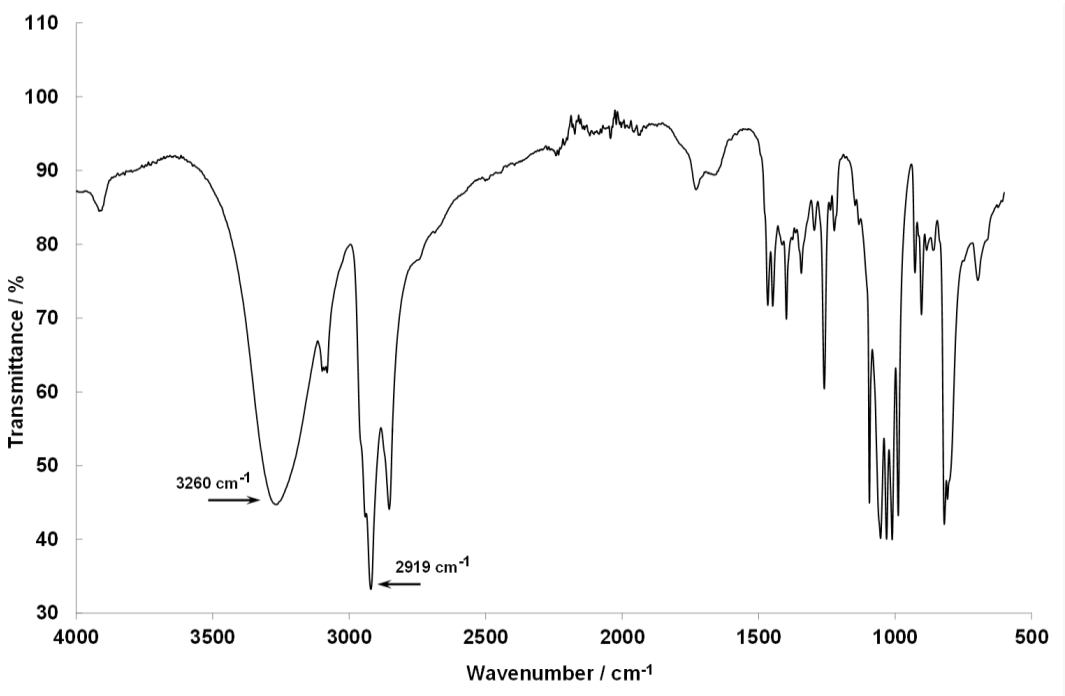

Spectrum 32: 3-osmocenylpropanoic acid, 24.

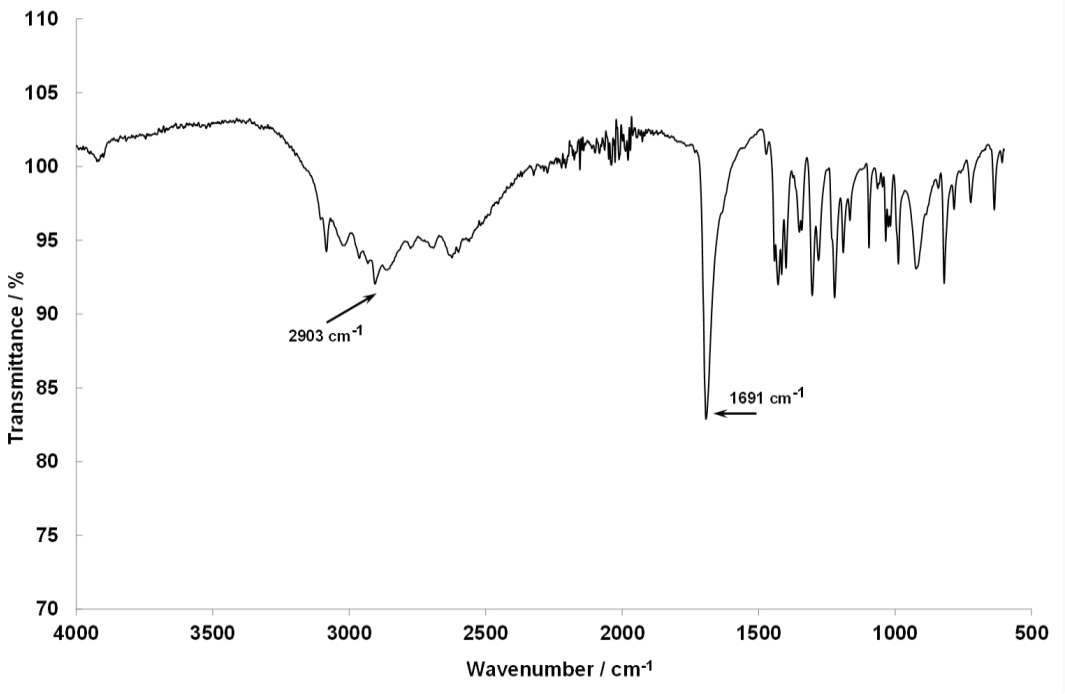

Spectrum 33: 3-osmocenylpropenoic acid, 33.

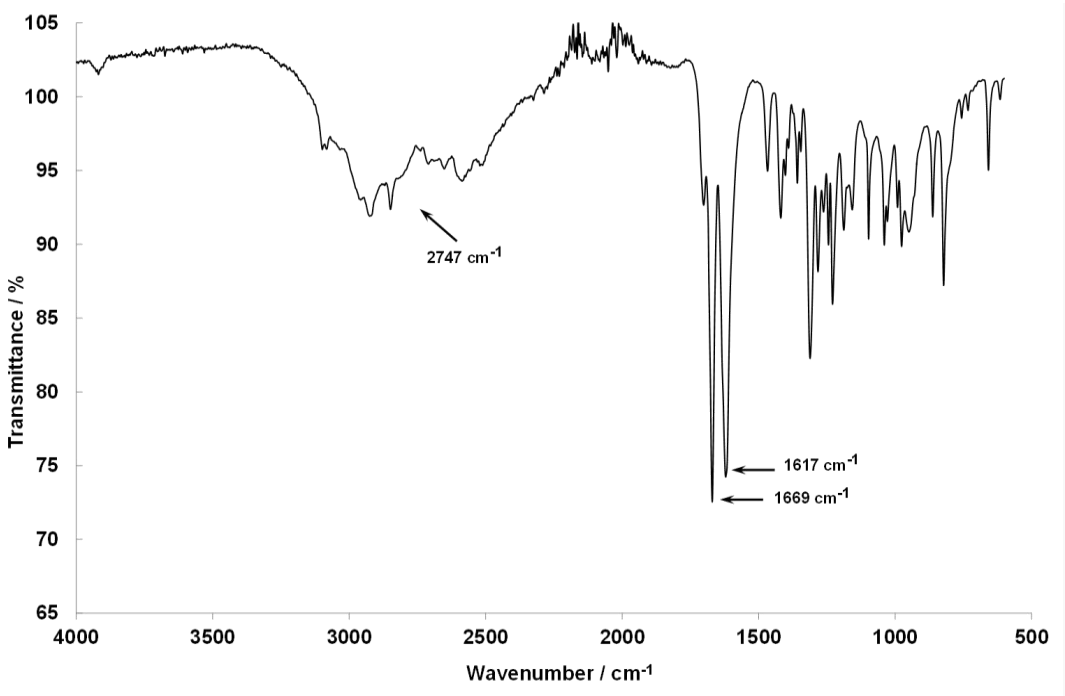

Spectrum 34: 3-carbomethoxypropionic acid, 17.

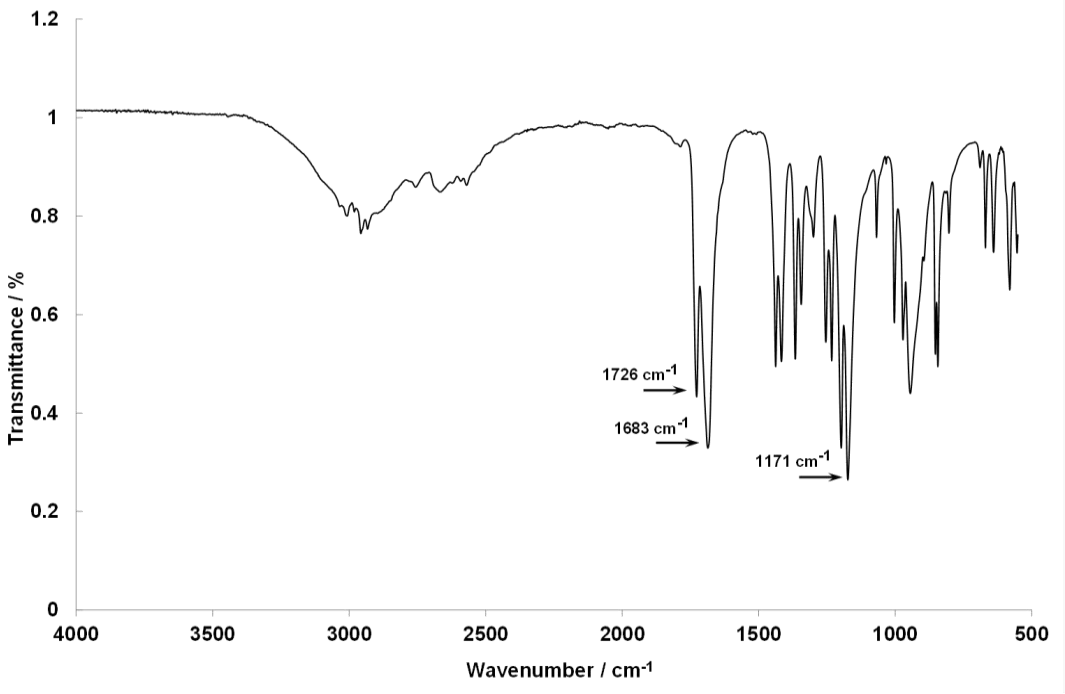

Spectrum 35: 3-carbomethoxypropionyl chloride, 18.

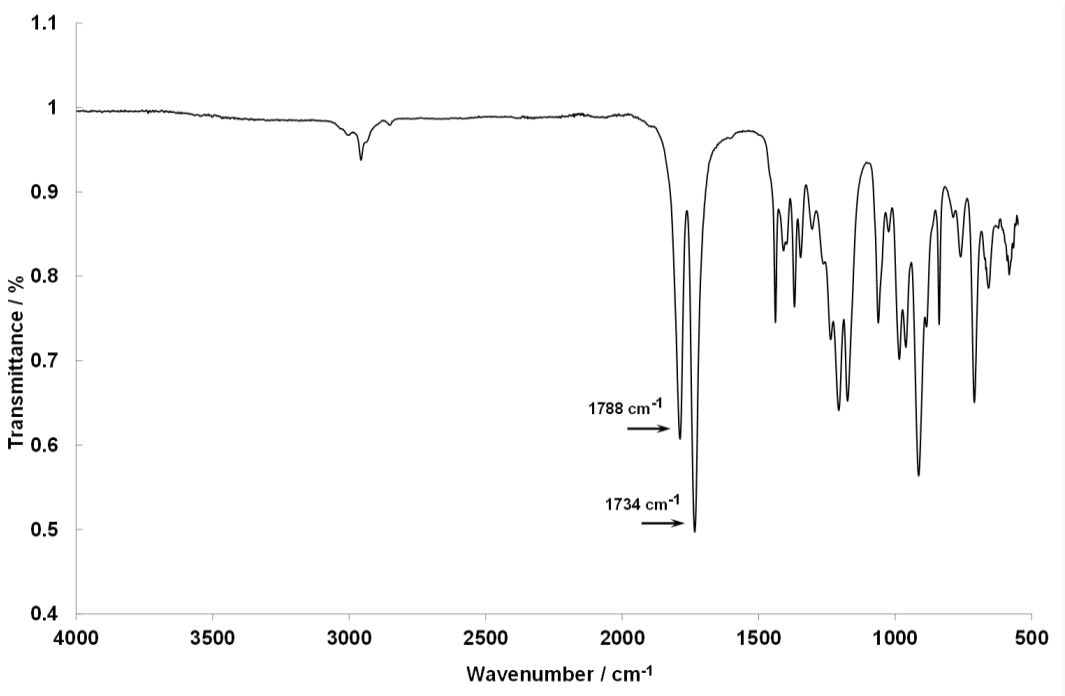

Spectrum 36: Methyl-3-osmocenoyl propanoate, 34.

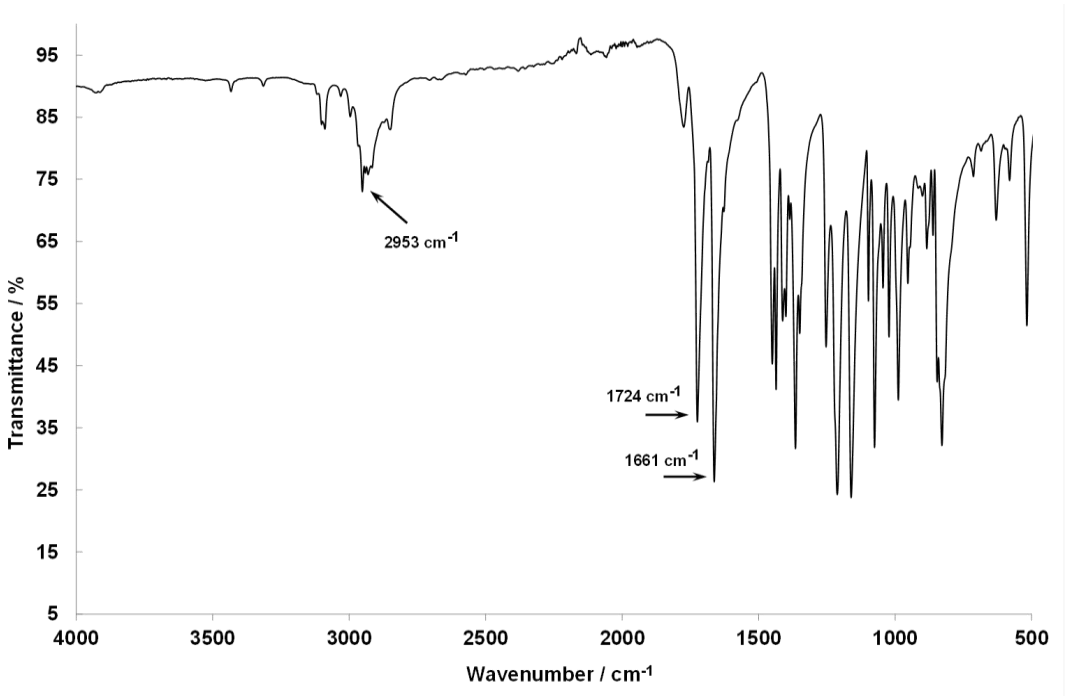

Spectrum 37: 4-osmocenylbutanol, 22.

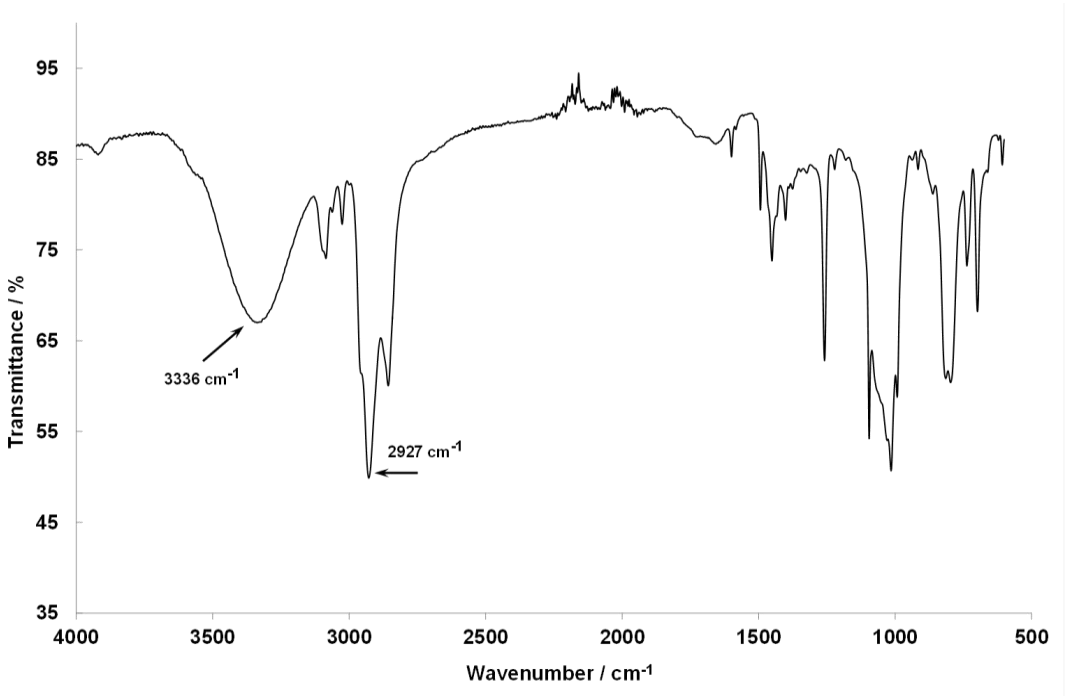

Spectrum 38: Methyl-4-osmocenylbutanoate, 35.

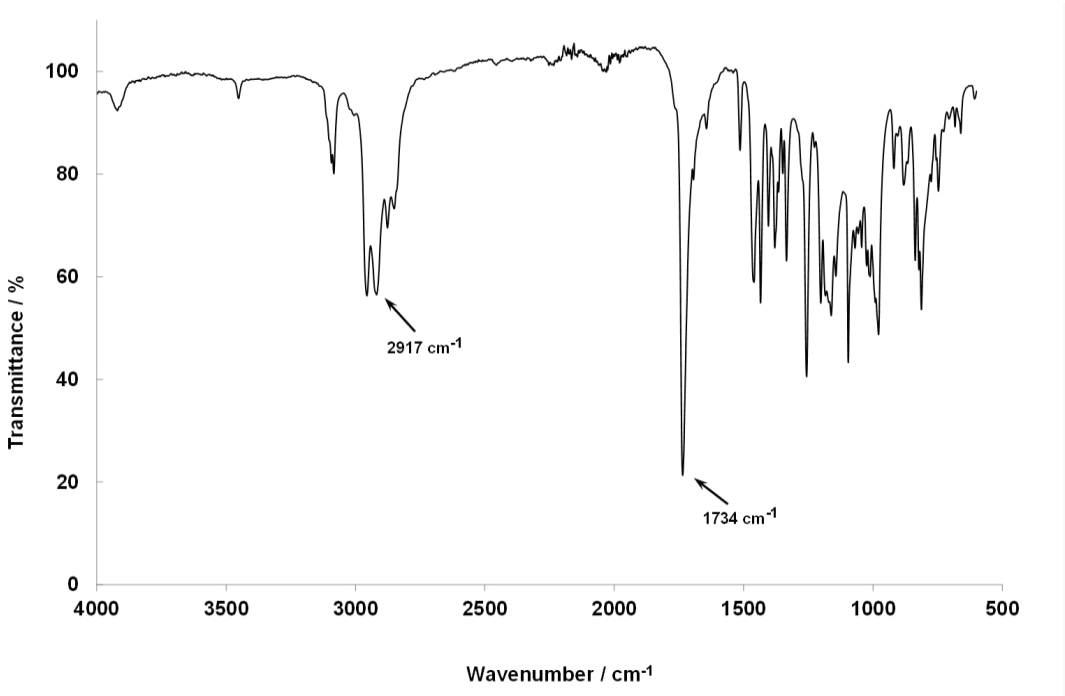

Spectrum 39: 4-osmocenylbutanoic acid, 25.

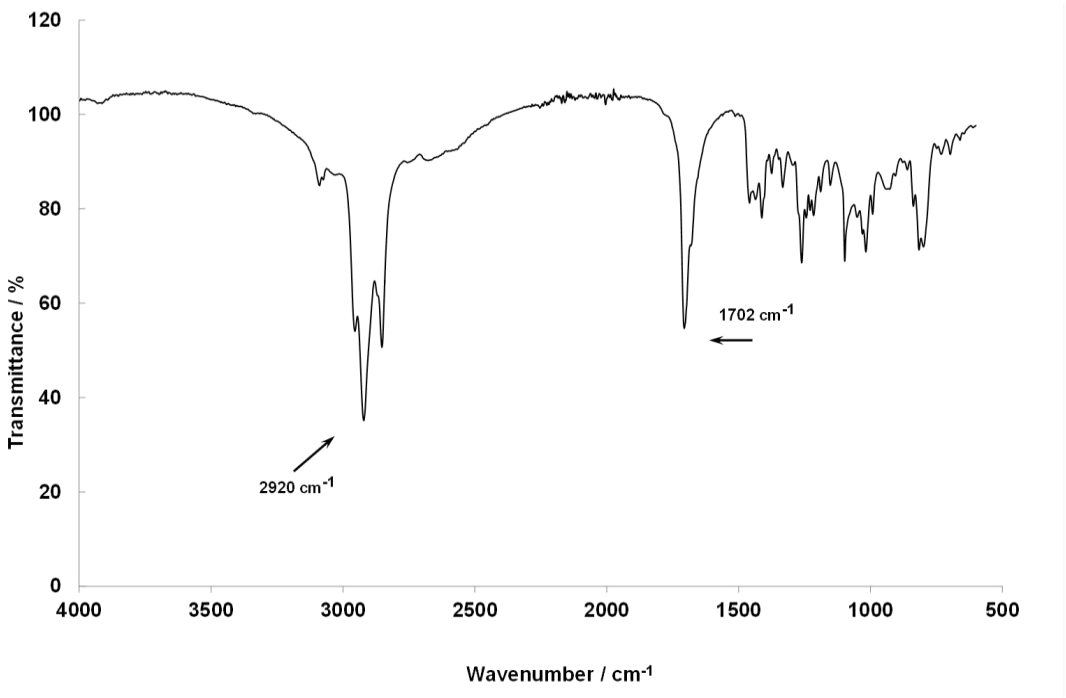

^{13}C NMR Spectra

1-osmocenylmethanol, 19.

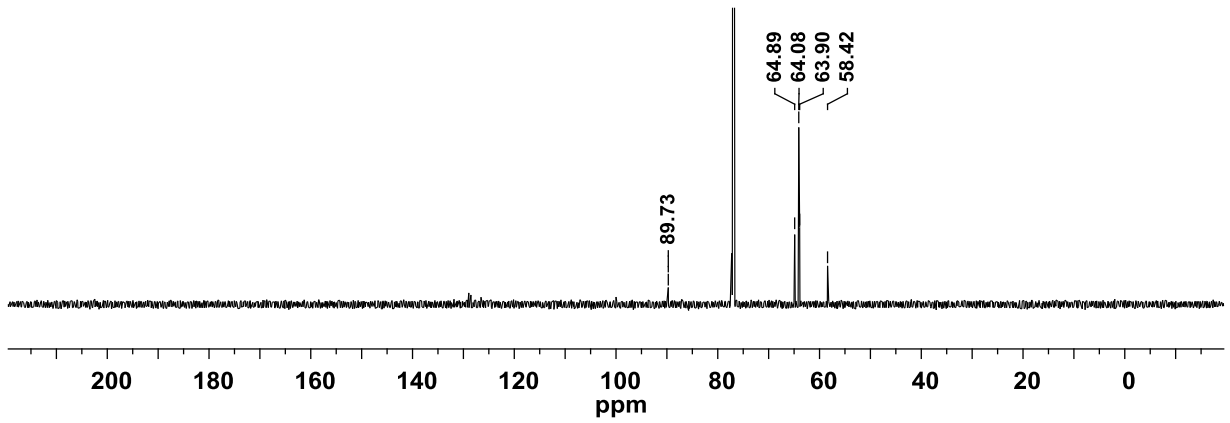

3-osmocenylpropanol, 21.

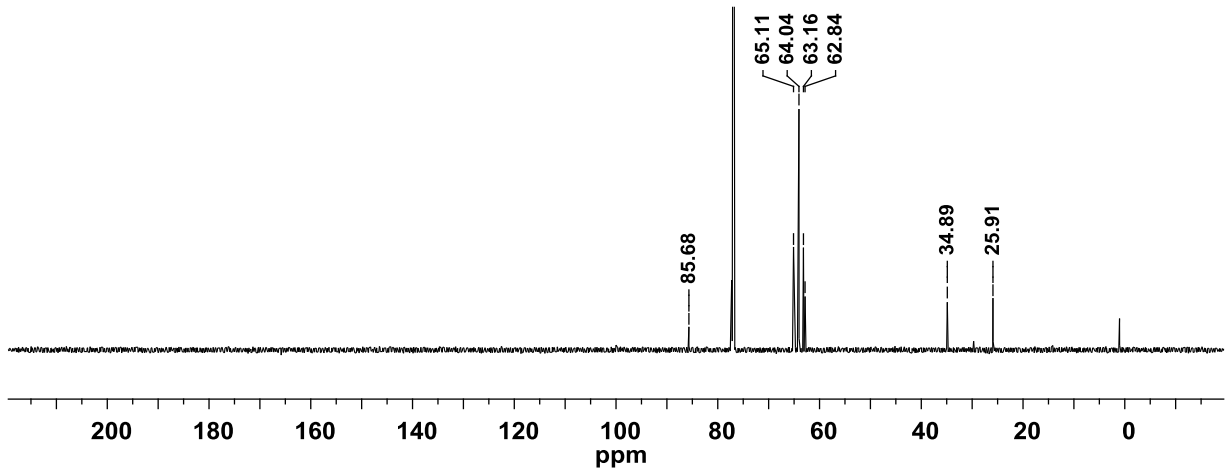

4-osmocenylbutanol, 22.

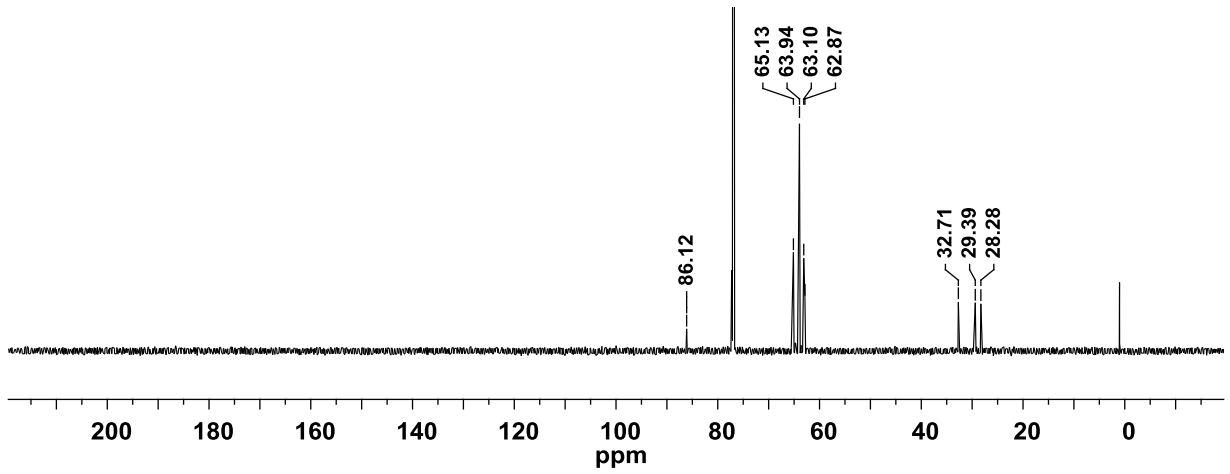

Declaration

I, Maheshini Govender, declare that the dissertation/thesis hereby handed in for the qualification Magister Scientiae in Chemistry at the University of the Free State is my own independent work and that I have not previously submitted the same work for a qualification at/in another university/faculty. I furthermore cede copyright of the thesis in favour of the University of the Free State.

Signed Date

_____ _____